WIND REGIME ANALYSIS AND RESERVE ESTIMATION (CASE STUDY: - KENYA)

Presented By:

MAULIDI BARASA F56/65971/2010

A project submitted to the University of Nairobi in partial fulfilment of the requirements of the degree of Master of Science in Energy Management in the

Department of Mechanical and Manufacturing Engineering,

School of Engineering,

College of Architecture and Engineering

4/5/2013

DECLARATION

I, Maulidi Barasa declare that this thesis is my original work and has not been presented for a degree in other university or any other award.

Maulidi Barasa

College Of Architecture and Engineering School of Engineering,

Department Of Mechanical and Manufacturing Engineering

Signature…… Date……

This thesis is submitted for examination with our approval as the university supervisors:

DR. Alex Aganda

College Of Architecture and Engineering School of Engineering,

Department Of Mechanical and Manufacturing Engineering

Signature…… Date……

Prof. Moses Oduori

College Of Architecture and Engineering School of Engineering,

Department Of Mechanical and Manufacturing Engineering

Signature…… Date……

ACKNOWLEDGMENT

All praises to Allah, the Lord of the world, the most Beneficent and the most merciful for helping me to accomplish this work. To Dr. Alex Aganda, for the help he provided despite his tight schedule. His invaluable technical and editorial advice, suggestions, discussions and guidance were a real support for the completion of this Project. To him, I express my sincere thanks. I would like also to express my thanks to my co-supervisor Prof. Moses Oduori for the useful suggestions on MATLAB/Simulink simulation.

I would like to acknowledge the staff, of the KenGen and Kenya Power. At this stage, there are too many to thank all of them, but I would like to mention Eng. Erastus Kiruga Chief Engineer, Power System Studies and Mr. Onesmus Odhiambo the site in Charge, Ngong Wind Farm who has all been a great support during the past two years. Their input to this project over the years is much appreciated. Very special thanks to my beloved parents Mr. Ramadhan Makokha and Mrs. Beatrice Uside, my brothers Mustafa and Musa my sister Faiza for their patience, understanding and encouragement during the different phases of my work. They spared no effort until this work comes into existence.

ABSTRACT

Kenya is becoming increasingly vulnerable to the low water levels in its major dams caused by recurrent droughts. This has resulted in the deployment of expensive thermal power generation for both standby and base load generation. With a view to addressing this problem, the government has undertaken significant steps in promoting renewable power generation. Wind energy is widely seen as one of the most cost-effective ways to generate electricity among renewables. After the introduction of feed in tariff in 2007 by the government, investors began showing interest in wind energy. Wind energy is projected to surpass 20% of installed capacity by the end of 2015. However, introduction of a significant amount of wind energy into a power system introduces the challenge variability and uncertainty. For correct operation of the power system, it is essential to balance the generation and load. As a result, the time-varying patterns of wind power production has to be taken into account in order to ensure security of supply. The objective of this study is to analyse the wind regime at three site (Ngong, Kinangop and Turkana) and quantify the reserve requirements for Kenya.

In this study, the impacts of large-scale wind power production (exceeding 20% of installed capacity) have been taken into account with the consideration the time varying patterns of wind power production. The first step was to analyse the wind speed data using Windographer software. This was done through a six month monitoring cycle. After which a common set of statistical parameters have been employed to evaluate the site's wind regime. This included the means, the standard deviations and the ranges. In addition to wind speed analysis, Weibull analysis was used to determine the site's wind speed variability. The results of the wind speed analysis was plotted over time to assess the patterns and seasonal trends. The next step, wind speed data was further

converted into wind generation data using appropriate wind farm models designed in the MATLAB/Simulink software. In order to eliminate unnecessary up scaling of wind generation data, an appropriate number of turbines to suit the specified wind farm size. After which, the wind farms output were combined into six possible scenarios based on Kenya's 2015 wind power expectations.

Data validation was done through a comparison was made between the actual to simulated energy data to determine the simulation accuracy. The wind power estimates for 2015 were then plotted both sequentially and chronologically to determine the extent of the variations. Kenya's additional reserve requirement in each scenario was quantified to cover about 99% of the mismatches between hourly demand and supply. Finally, the load following reserve requirement has been determined for different penetration levels. The findings showed no proof of symmetry between the reserve requirements and the wind penetration levels. Therefore, the net system variability does not directly correspond to the reserve size but to the wind generational diversity over within a region.

Table of Contents

List of Figures

List of Tables

List of Acronyms and Abbreviations

$\bar{v}$ - Mean Velocity

A - Area

DFIC - Dr. Fromme International Consulting

DFIG - Doubly Fed Induction Generator

GW - Gigawatts

GWEC - Global wind energy council

IAP - Integrated assessment of the Energy Policy

IPP's - Independent Power Producers.

ITCZ - Inter Tropical Convergence Zone

KenGen - Kenya Electricity Generating Company Limited

KETRACO - Kenya Electricity Transmitting Company

KIPRA - Kenya Institure of Public Policy Research and Analysis

KPLC - Kenya Power and Lightning Limited

kV - Kilovolts

kW - Kilowatts

MATLAB -

MW - Megawatts

NL - Net Load

PV - Photovoltaic

RMSE - Root Mean Square Value

SAEM - Simulated Annealing Expectation Maximization algorithm

SREP - Scaling-up renewable energy program

SWERA - Solar and Wind Energy Resource Assessment

TWh - Terawatt hour

V - Volume

W/m2 - Watt per Meter Square

WTG - Wind Turbine Generator

L - Load

P - Production

W - Wind

f - Frequency

k - Shape Factor

r - Cross Correlation Coefficient

v - Velocity Factor

ρ - Density

σ - Standard Deviation

Chapter 1 INTRODUCTION

1.1 Background

Electricity is a major driving force to the social and economic development of Kenya. Currently, the electricity demand in Kenya is at 1,236 MW against an installed capacity of 1,691 MW. The reserve margin gap between peak demands and available is at 24.5 per cent. This is way beyond the optimum limit of 15 percent. The Kenya electricity generating company limited (KenGen), a state-owned entity, is the primary generator, produces 80% of the electricity, with the independent power plants (IPP's) generating the rest (KenGen, 2011). Sixty five percent (766.88MW) of KenGen's installed capacity comes from Hydro. Currently, the effective capacity under hydro is at 92.95 % (KPLC, 2011/2012).

Kenya's dependency of hydroelectric power has proved to be a problem due to its seasonal nature. Kenya is becoming increasingly vulnerable to weather conditions and the reliability of hydroelectricity as a primary energy source is insecure. Water levels in the major dams feeding the hydropower stations in the region have drastically decreased, culminating in the deployment of expensive thermal power generation for both standby and base load generation (KPLC, 2011/2012). The volatile and unpredictable lofty price of petroleum products used for thermal generation is transferred to the consumer in the form of high utility bills. Petroleum fuel accounts for about 28.57% of the final consumption while electricity while combustible renewable accounts for about 3.11% and 67.65% (DFIC, 2007). Available data shows, Kenya has some of the highest prices throughout the world. The cost of electricity in Kenya is about four times that of South Africa, the country's main competitor in the region, and more than three times that of China (KIPRA, 2009). Kenya continues to miss foreign direct investments partly because of this problem, with considerable penalties on socioeconomic development.

The elevated cost of energy is one of the biggest bottlenecks for the attainment of Kenya Vision 2030. The Kenya Vision 2030 is a long-term development strategy, whose aim is to transform Kenya into a globally competitive and prosperous economy with a high quality of life. It envisages that Kenya will be transformed into a newly industrialized, middle-income country providing high-quality life to all Kenyans in a clean and secure environment. In order to reach an average annual economic growth rate of 10 per cent for the next 18 years as outlined in Kenya Vision 2030, Kenya needs to adopt robust, well thought-out solution for the drought power crisis (KIPRA, 2009).

With a view of addressing the drought-induced crisis, the government has undertaken significant steps in the promotion, development and utilization of renewable-energy resources. The aim is to increase the proportion of renewable contributing in meeting the country's energy demand. There are three main renewable-energy sources currently being exploited in Kenya, i.e. Solar, geothermal and wind energy.

1.2 Solar Energy in Kenya

Solar-energy potential in Kenya is high. Kenya receives daily insolation of 4-6kWh/m2 (GoK, 2011). Solar energy is a virtually inexhaustible resource. Solar-energy is currently under-exploited although it is widely regarded as a plausible option to stimulate rural electrification (KIPRA, 2009). Solar utilization is mainly for photovoltaic systems (PV), drying and water heating. The solar PV systems around the country are primarily for domestic installations with the private sector playing a major role. The solar market in Kenya has been among the greatest and most dynamic per capita among developing countries. Since most rural households will not have their homes connected into the grid in the near future, solar is the largest source of new electrical connections in rural Kenya. The major challenges of using more solar power

include the lack of a satisfactory means of energy storage and concerns about flexibility and economics. Because no power can be produced when the sun is not shining, scientists must develop cost-effective methods of storing solar power in order to supply energy whenever it is needed. The development of effective and efficient storage systems will be one key to the future of our use of direct forms of solar energy.

1.3 Geothermal Energy in Kenya

Geothermal energy is the natural heat from the earth's interior stored in rocks and water within the earth's crust. This energy can be extracted by drilling wells to tap the steam at high pressures, which is then led through pipes to drive electricity. Geothermal resources in Kenya are located within the Rift Valley with an estimated power potential of between 7,000 MW to 10,000 MW spread over 14 prospective sites (SREP, 2011). Kenya has 157 MW of installed geothermal electricity capacity. This accounts to about 9.5 % of the Kenya's installed capacity. However, during the recent droughts in the country, geothermal energy played a critical role as it continued to operate at nearly 100% availability when hydropower stations throughout the country were crippled by the dry spell (Karekezi, 2005). Geothermal is a reliable way to produce energy, it is not affected by climatic variability, and it does not need transported fuels. The government has therefore identified geothermal as the suitable source to supply electricity for base load. The government has plans to increase geothermal power capacity to 576 MW by 2019 (KPLC, 2000). The Government has opened up the industry for private sector participation with the first IPP, OrPower 4, operating in Olkaria III and generating 48 MW. Additionally, IPP's have been licensed to develop Suswa and Longonot geothermal prospects. Kenya Electricity Generating Company (KenGen) has begun the implementation of an

ambitious 280MW project aimed at increasing our geothermal output to 315MW (SREP, 2011).

1.4 Wind Power sources in Kenya

Wind energy is a renewable electricity production from converting the kinetic energy of moving air masses into electricity. When compared to other renewable energy sources, such as solar, wave and geothermal power, wind power is a relatively cheap source of renewable energy. Wind power installations cost 3.5 times less per Watt than PV installations and operate for 12-16 hours at good sites as opposed to 5-6 hours for PV systems (KIPRA, 2009). Therefore, the promotion of renewable energy by a number of governments has led to a strong growth of wind power in the respective countries. Wind energy has experienced rapid growth since the 1990's. The global installed capacity increased by 44 GW in 2012 to 282 GW (GWEC, 2013). Kenya is located within the equatorial region where wind speeds are lower compared to those of higher latitude regions. However, specific parts of Kenya have significant wind resources throughout the year due to the complex topographical features and varying nature of surfaces (Mukabana, 1992). Parts of Nairobi, Rift Valley, Eastern North Eastern and Coast Provinces have wind potential as high as 346 W/m2 (GoK, 2011). Ever since the introduction of feed in tariff in 2007, the wind-power sector has attracted investors set on exploiting the country's huge potential. One-wind generators was installed in Marsabit generating the 200kW wind turbine. It was later decommissioned in 2006, and replaced with two wind turbines of 250kW each at a total cost of Shs.198 million (KPLC, 2011/2012). Feasibility is ongoing for an additional 150 MW capacity of wind generators to the grid (KenGen, 2011).

Ngong wind farm is located 22km southwest of Nairobi, is the only wind farm connected to the grid. (KenGen, 2011). The first phase was commissioned in 1993 as a donation from the Belgian Government. At the time Ngong, was composed of two wind turbines with capacities of 0.15MW and 0.2MW. This summed up to an installed capacity of 0.35MW. The two wind turbines have since been decommissioned. The second phase was commissioned in August 2009 to a capacity of 5.1 MW (KPLC, 2011/2012). The layout of the second phase of Ngong wind farm is as shown in Fig. 1.2. The Ngong wind farm is powered by six Vestas V52 wind turbines producing a total of 5.1MW (0.3% installed capacity) (KenGen, 2011). A feasibility analysis conducted done by KenGen using 14 years data confirmed that the Ngong site was capable of generating up to 14.9 GWh of energy per annum on average from a 5.1MW wind farm (KenGen, 2011). The turbines (doubly fed asynchronous type) have hub heights of 50 meters and rotor diameters of 52 m. The turbines are networked to the Ngong wind substation and control via underground cabling. The Ngong wind farm is directly connected to the wider 66kV distribution network within Nairobi. Wind power varies over time, mainly under the influence of meteorological fluctuations. The variations occur on all time scales: seconds, minutes, hours, days, months, seasons and years. Understanding these variations and their predictability is of key importance for the integration and optimal utilisation of wind in the power system.

In this study, the basic parameters of the project will be assessed (e.g. the number and type of turbines and total installed power) taking into account the wind resource available. Wind speed data will be converted into wind generation data using wind farm models designed in the MATLAB/ Simulink. A comparison between the actual to simulated energy data will be undertaken to validate the model applicability to future scenarios. Six possible wind scenarios

will be considered based on Kenya's 2015 wind power expectations. In order to avoid unnecessary up scaling of wind production data an appropriate number of wind turbine matching a specified wind farm size will be used.

The impact of the wind variability may range from negligible to significant depending on the penetration levels and intermittency of the wind resource. Variations in wind plant output may adversely affect grid reliability and increase the operating costs of the system as a whole. To compensate for these variations, additional generation capacity is needed to provide regulation or set aside as reserves. The time-varying patterns of the site's wind power production has to be taken into consideration while determining the reserve requirement. Consequently, the extra reserve requirement in each site will be quantified both in distinctiveness and additively to cover about 99% of the mismatches between wind and load fluctuations.

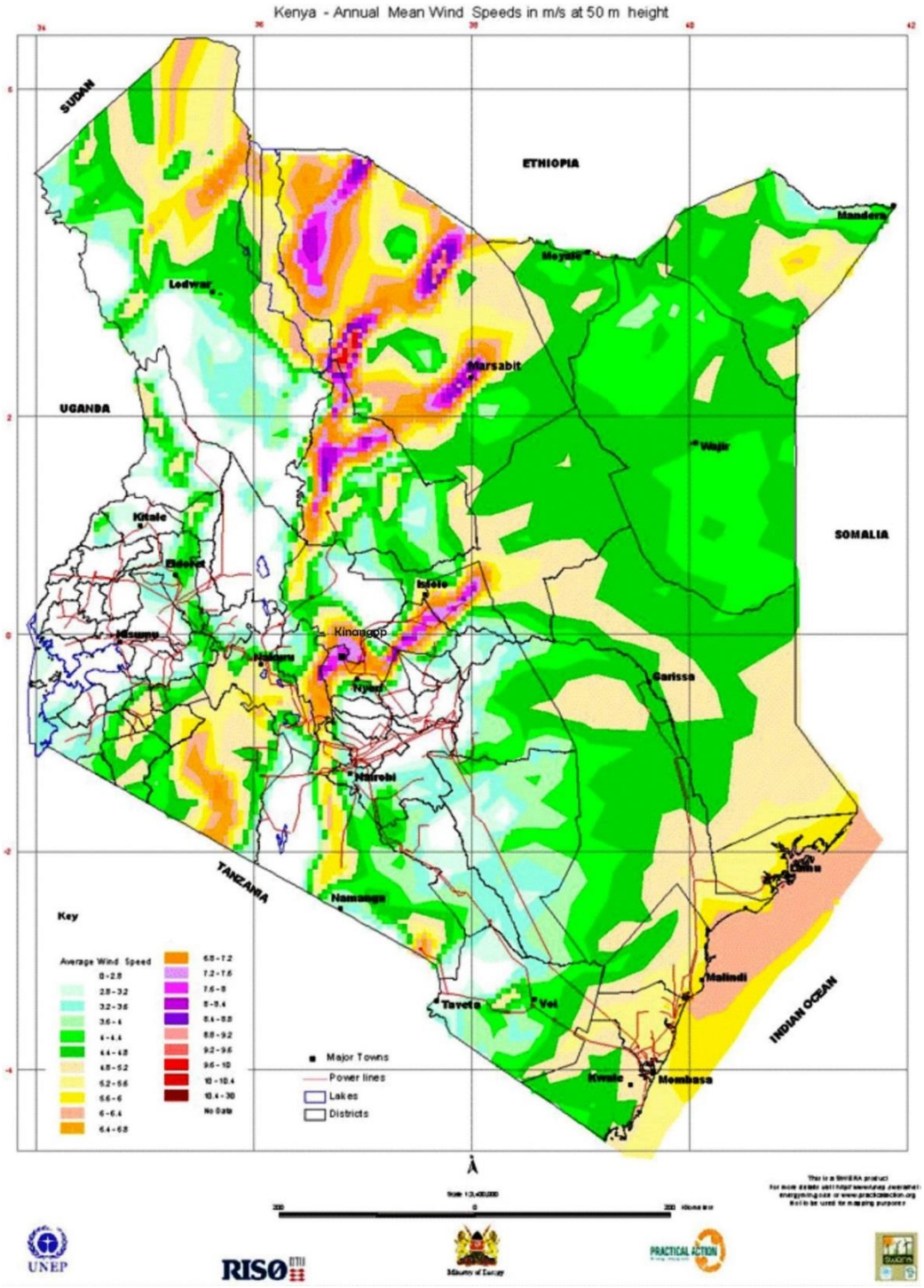

Figure 1.1 Wind Resources in Kenya (SWERA, 2008).

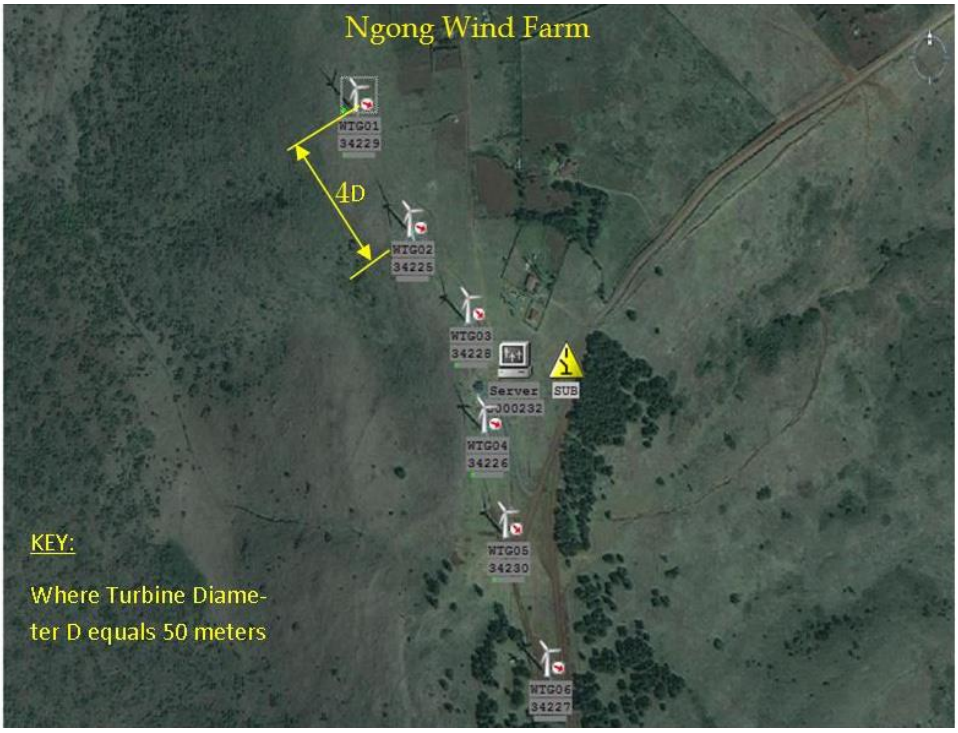

Figure 1.2 Diurnal profile for Turkana from October 2011 to March 2012

1.5 Main Objective:

The main objective of this study is to analyse wind regimes in Kenya and quantify the reserve requirements for different types of regimes, and wind penetration levels. To achieve this, the impact wind variability for three distinct sites will be determined and analysed using statistical methods. These sites are Ngong, Kinangop and Turkana.

Specific Objectives:

1. Analyse and obtain the site-specific characteristics such as mean wind speed, standard deviations, maximums and the minimums for the three sites.
2. Estimate the potential wind power for the sites mentioned using MATLAB/Simulink software.
3. Determine and compare the site's wind variations and Kenya’s load variations.
4. Estimate the net load variations and reserve requirements based on Kenya’s 2015 wind power estimates.

Chapter 2 LITERATURE REVIEW

2.1 Wind power potential and distribution in Kenya and selected sites

Wind power production in a specific region is highly dependent on its average wind speed. Due to the cubic relationship between wind speed and power, even a small variation in the wind speed may result in significant change in power. For example, an increase in the wind speed by 10 percent may enhance the productivity of the turbine by over 33 per cent. Wind is stochastic in nature i.e. Speed and direction of wind at a location vary randomly with time. Accurate estimation of wind potential of a specific region requires rescaling of near surface meteorological from near surface into turbine heights. Two laws are used for this extrapolation, specifically logarithmic law and power exponential law.

The wind regime of a specific region is then modelled for energy production as derived power density by computing for topography, surface roughness and obstacles. Cabello (2010) analysed 9-year wind speed data for the Alicante Spain at a height of 2 meters above the ground and then recycled it to a height of 10 meters using logarithmic law. He concluded that strongest annual averages about 2.1 m/s and weakest annual averages about 1.2 m/s at a height of 10 meters. However, extrapolation to 10 meters heights is still way below the hub heights for wind turbines. The height of 50 meters is considered as the average height of most commercial wind turbine hubs. Therefore, his conclusions would be more appropriate wind power estimation had he considered a height of 50 meters and above. The annual wind speeds are likely to increase if the study heights were to be increased. Archer (2002.) used both logarithmic and power-law relation to extrapolate wind speeds data obtained at 10 meters to 80 meters. Data from 1327 surface stations and 87 soundings in the U.S. for the year 2000 were used. Analysis

was then done to judge the regularity and spatial distribution of U.S. wind power at 80 m. She concluded that the five states with the highest percentage of stations with annual mean 80-m wind speed ≥ 6.9 m/s were Oklahoma, South Dakota, North Dakota, Kansas, and Nebraska. These wind speeds are suitable for the commercial wind turbine with a cut of wind speeds of 4 m/s.

The height of wind power estimation may also affect the diurnal cycle. Lindenberg, (2011-3) demonstrated the wind frequency using the probability distribution function. He concluded that between the heights of 60 to 80m the diurnal cycles strongest on clear summer days. He further established that Europe experiences high nocturnal wind speeds due to reduced download transfer moments. Then again, at a height of 33m above the ground the diurnal cycle was still strong with maximum around noon followed by decreasing wind speeds in the afternoon. This was due to thermal circulation with strong mixing of the near surface boundary.

A comprehensive review of wind regimes of Europe and Kenya will enable us to understand the applicability of different studies undertaken on reserve requirement. Model calculations show that surface (10 m above ground level) wind speeds across the majority of Europe are less than 4 m/s. None the less, the annual mean greater than 4 m/s occur across 13.5% of the Europe's land surface area. There is also a significant drop off in surface area between the wind speed bands, 3.5 to 4 m/s and 4 to 5.5 m/s (Eerens, et al., 2008). The Nordic region for example exhibits seasonal variations with averages ranging from 22 to 34 percent of nominal capacity. Wind production in winter usually exceeds that of summer. Wind power production is 110-140 percent of average in winter month and 60-80 percent in the summer months (Holtinen, 2004). In the UK, winter months (December to February) account for about 33 percent of annual electricity while summer months account for about 17 percent (Sinden, 2005). Conversely, the

seasonal trends in wind speeds exhibited in Kenya correspond to that of rainfall; high wind speeds are exhibited during dry seasons while low wind speeds during wet seasons. The strong meridional flows that occur during the transition period of the rainy seasons and the stable stratification is marked by a decline in moisture content due to the winds travelling long distances over land (often relatively parallel to the coastline) and to the north-south orientation of the Kenyan highlands.

The rainy seasons coincide with the periods of the year when the Inter-Tropical Convergence Zone (ITCZ) is passing over this part of the continent. Most parts of Kenya experience two rainy seasons and two dry seasons (Mukabana, 1992). The former is commonly known as the "Long Rains" (March-July). Showers and thundershowers are widespread during long rains, especially in the afternoons and at night. The wind speeds are lower in most parts of the country. The latter is known as the "Short Rains (Late October-mid December). Unlike the long Rains, north-south oscillations are rare during the short rains. Heavy storms are likely to occur during the season, and more so, during the rainfall peak month of November. However, the wind speeds are still low in most parts of the country (Mukabana, 1992). The two dry periods that occur over most parts of Kenya, run from mid-December to late February and June to late September. The speeds are high during dry seasons is brought inland by North-easterly and South-easterly monsoon winds (Mukabana, 1992). These monsoon winds have a direct effect on the different regions of the country. For instance, higher speeds between April and September are characteristic of the south-easterly monsoon winds while the lower speeds from December to March and May to August are characteristic of the north-easterly Monsoon (Okeyo, 1987).

Apart from seasonal variations in rainfall, Kenya has naturally occurring features that influence the wind speeds within certain regions. Mukabana (1992) showed how the local features (Lake Victoria, the Indian Ocean, orography, Turkana-Marsabit corridor, etc.) played some major role in the generation and control of the local mesoscale circulations in the absence of the large-scale forcing. An example is the channelling effect known as the Turkana Jetstream. The Turkana Jetstream is triggered off by the orientation of the terrain that forms a corridor in this locality between the Kenyan Highlands to the south and the Ethiopian Highlands to the north. The Turkana Jetstream is ultimately responsible for the consistent winds found on the South Eastern shores of Lake Turkana. The strong winds exist throughout this channel with speeds decreasing where the channel is wider (Asnani & Kinuthia, 1979). Oludhe (2008) assessed the diurnal wind power potential for Marsabit taking into account the mesoscale winds associated with topographical features. Data was analysed to obtain the magnitude and duration of winds for each scale of motion. He concluded that the Marsabit region had the high wind power potential of more than 1000Wm/2 with strong diurnal and seasonal variability.

Another example is the meridional wind maxima could be the southerly monsoon winds, which flows at the Kenyan coast and is reputed to have a core over the town of Garissa. Southern regions of the country and especially in the coast province are directly affected by the monsoon winds that blow over the Indian Ocean (Mukabana, 1992).

Mukabana (1992) determined the influence of the large-scale flow on the diurnal weather patterns over Kenya using a three-dimensional limited-area model, the Regional Atmospheric Modeling System. He assessed the scale-interaction between the large-scale monsoonal flow and the local mesoscale circulations that are generated and controlled by local features like Lake Victoria and the Indian Ocean, orographic barriers, the Turkana-Marsabit corridor, and

the overall resultant effect on the diurnal weather patterns over Kenya. He concluded that the diurnal weather patterns for the coastal region, the eastern slopes of the Kenyan highlands, and the Lake Victoria region with the region in the Turkana-Marsabit corridor were related to the scale-interactions between the local circulations. Like the sea/land breeze and the lake/land breeze circulations, upslope/ downslope drainage winds with the prevailing southeast monsoon wind current. The intense precipitation over the Kenyan highlands is brought about by a strong convergence between the lake-breeze, coupled with upslope winds from the lowlands, with the large-scale southeast monsoon currents during the afternoon period. The intense convective precipitation rates over the highlands continued to drift westwards to the Lake Victoria Basin. Hence, the eastern parts of Lake Victoria received convective rainfall generated over the Kenyan highlands and this advances westwards to the Lake Basin by the South-easterly monsoon winds.

Arthur (2011) used six-year data collected from twelve different stations to study the hourly wind speed. The data covers the six-year period between January 1995 and December 2000; measurements were taken for every hour of everyday at 10 meters above the ground. He then selected one site due to its wind potential, geographic location and socioeconomic potential. The measured data were then analysed in WindPRO/ WAsP simulation software to determine wind speed at different heights; optimize the system for different hub heights. He then concluded that the data collected from three sites with valid explicitly, Voi, Marsabit and Wajir have the top three annual average wind speeds of 8.9, 7.8 and 7.4 m/s respectively. Marsbit had a wind speed range of 14.53 m/s. Saoke (2011), analysed the wind speeds characteristics in Juja, Kenya using short-term (three months) data of daily wind speeds at 13 m and 20 m heights. Using the calculated shear exponent, an extrapolation of the speeds was done to higher

heights of up to 150m. The wind shear exponent and the roughness parameter for the selected site at Juja were found to be 0.16 and 0.048 m respectively. He then concluded that the wind speed frequency distribution at the 20 m was determined and the mean wind speed found to be 5.04 m/s with a standard deviation of 2.59. While the maximum wind speed obtained at the 150 m height was 8.4 m/s during the month of October. The wind potential was modelled using the Weibull probability function and power density of Juja site was found to be 131.35 W/m2.

2.2 Wind power estimation

Wind power production is normally simulated using system models or analytical methods. Analytical method, wind speed data in time series format is used together with system variables (Ackermann, 2005). System models have been successfully used for defining the distribution of wind in a region, over a given period. Successful analysis of wind velocity and its distribution at a prospective site is necessary for the assessment of the energy potential. The distribution describes the amount of time on a particular site that the wind speed is between different levels. Wind turbines installed at two sites with the same average wind speed may yield entirely different energy output due to differences in the velocity distribution. The quantification of the impacts of wind resource integration into the grid requires a wind generation model with the appropriate level of detail for representing the uncertainty in the wind speed and its impacts on the wind power output.

There are two main approaches for wind power modelling namely: Deterministic and Probabilistic. Probabilistic approach is based on the site's wind speed. Probabilistic approach is preferred by many researchers because it can be used in almost all sites and for all types of wind turbines (Ackermann, 2005). However, this approach fails to represent the characteristic for the wind farm during nominal operation characterized by small deviations in grid quantities

from the nominal values and the occurrence of wind speed changes. Probabilistic model is widely used to evaluate the expected energy produced by each unit in the resource mix over a specified period and determine the expected system production costs, the expected emissions, the reliability indices, and other variable effects over the specified study period. The probabilistic simulation is used in long-term planning studies to investigate factors such as the optimal resource mix determination to serve the forecasted load (Maisonneuve & Gross, 2011).

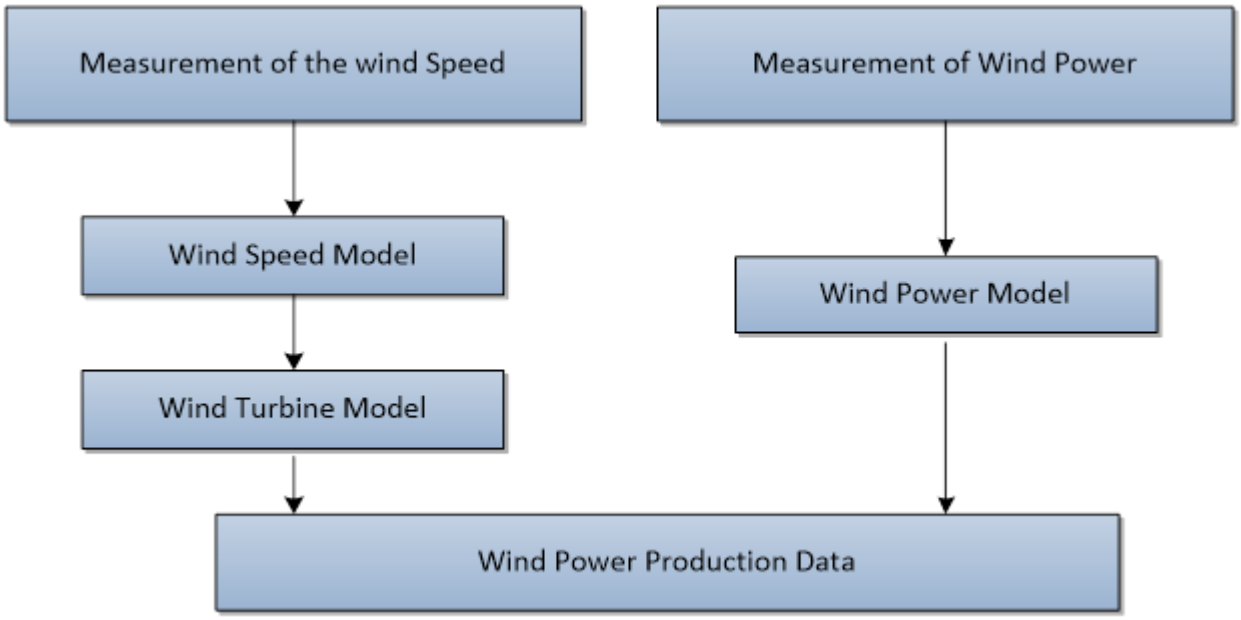

Figure 2.1 Wind Power Simulation Process

The assessment of impacts of wind variations on the power system needs critical understanding of wind distribution. The Weibull distribution is the most common probability density function used in the wind data analysis. The Weibull distribution is used to represent probability distributions of many natural phenomena (Lun & Lam, 2000). The Weibull distribution is described by two parameters, the scale and shape values. The shape parameter describes the

shape of the curve, while the scale parameter describes amplitude. These parameters are manipulated to provide a Weibull distribution fit for almost any given wind speed data. If the confidence level of a Weibull distribution is low, meaning the Weibull distribution is not an accurate representation of the data; other probability density functions such as Rayleigh's distribution can be used to express the wind behaviour.

Besides the shape and scale parameters, the Weibull can be used to determine the wind speed range in a specified site. Waewsak (2011) analysed the statistical wind data obtained from measurements for the 12-month period of January to December 2008 at Thasala district in Nakhon Si Thammarat province, southern Thailand. He analysed statistical wind data set using Weibull distributions in order to investigate the Weibull shape and scale parameters. The Weibull parameters obtained from WAsP 9.0 analysis as well as from the probability density function and cumulative distribution function of graphical methods was compared and the mean bias error between the methods was determined. He concluded that the monthly Weibull shape parameter was in the range of 1.1-2.8, while the monthly Weibull scale parameter was in the range of 2.27-5.94 m/s corresponding to monthly mean wind speeds in the range of 2.2-9.4 m/s. The mean wind speeds at 20 m, 30 m, and 40 m determined by WAsP 9.0 from the observational data were in the range of 2.4-7.8 m/s, 2.7-8.3 m/s, and 3.1-8.8 m/s respectively. Arthur (2011) analysed the Data for the three locations; Voi, Marsabit and Wajir using Windorgrapher software to determine the details about the diurnal cycles and Weibull distribution curves. He then concluded that Wajir generated smooth and promising monthly average speed curve. The representation of the diurnal cycle of wind speeds in Marsabit shows a range between the highest speeds and lowest is approximately 1.8 m/s. The effect of low wind speed below the cut off the wind is more severe than stormy events above cut out speeds.

Sinden (2005) demonstrated how low wind speeds > 4m/s can cause a majority of hours with no generation (zero) while the high wind speed causes less hours of no generation about 1% of the incidents. Sinden (2005) reported that the impact of low wind speed could be less severe during peak hours.

In general, for a fixed set of data and underlying statistical model, the method of maximum likelihood is used for selecting values of the model parameters that produce a distribution that gives the observed data the greatest probability (i.e., the shape factor and velocity factor). Maximum-likelihood estimation gives a unified approach to estimating experimental wind data. Ahmad (1995) computed using maximum likelihood method, the modified maximum likelihood method and the graphical method. The three methods were compared to their performance. He concluded that root mean square values (RMSE) values show that the modified maximum likelihood method performed better than the low root mean square error in frequency distribution format. Maximum likelihood has the limitation of a low root mean square error while the least square method is less accurate and its accuracy is affected by the bin size in the cumulative distribution format. The least squares regression was carried out in its cumulative frequency distribution and not on its actual wind speed data. This way, all the points are given equal weightage although some of the bins may have a larger number of data points than others. The maximum likelihood method curve fit seems reasonable, but it resulted in a substantial under prediction of wind power density (Waewsak, Chancham, Landry, & Gagnon, 2011).

Deterministic approach, the turbine model designed by use the maximum value of the production is used for transforming wind speed data into power production data (Ackermann, 2005). This approach is based on wind power curve as stated in the data sheet for the wind

turbine. Alternatively, it can be based on actual turbine parameters (system variables) designed to produce the same power duration curve. Sinden (2005) used a hypothetical wind turbine model to convert wind speed to wind power production. Wind speed measurement collected from the sites was used to generate a hypothetical model of all wind turbines located in the UK. One major drawback to the use of hypothetical model is the fact that the model accuracy depends on the system variables used in the wind farm. Papavasiliou (2011) uses a power curve that has been superimposed on the data sample of the two wind integration (penetration) levels. The power curve used in the study resembled that of a typical wind generator, although it is smoother due to the geographical diversity of the wind sites.

Some researchers opt for the actual wind production data for analysis. Holtinen (2004) uses a single point measurement of actual data up-scaled to represent wind power production of a larger area. The wind production data has been rescaled to a specified wind penetration level. However, up-scaling approach has the limitation of up scaling the wind variation. Up scaling also neglects the small deviations in grid quantities resulting to erroneous representation of wind power characteristic over a region. In order to depict the grid quantities in individual sites, Holtinen relies on the correlation between different sites with distance. However, the distance correlation assumes equal site distribution over a region as opposed to concentration of sites over regions with favourable wind regimes. This often results to the linearity of the smoothing effect in a region. Halamay (2010) used unadjusted wind power data from wind farms (1600MW) within the Bonneville Power Administration representing up to 14 percent. He then rescaled the wind power data to desired penetration levels based on different scenarios. He uses historical data as baseline data adding a coaction term to cater for growth.

Maisonneuve (2011) determined the need in the planning domain through the development of a computationally efficient probabilistic production simulation approach with the capability to quantify the variable effects of systems of varying levels of wind penetration with the uncertainty in the variability/intermittent effects of wind generation at multiple sites together with the other sources of uncertainty explicitly represented. The simulation approach is based on the identification of the prevailing wind regimes in the regions where wind resources are located and the judicious application of conditional probability concepts in incorporating the wind regime representation. The regimes-based approach effectively captures both the seasonal and the diurnal variations of renewable resources and their correlation with the load seasonal and diurnal changes.

2.3 Wind Variability Estimation

The additional reserve requirement and cost in balancing the system on different timescales are primarily due to fluctuations in the power output generated from the wind. The impact of wind variability in the power system depends on the size and the inherent flexibility of the power system (Ackermann, 2005). Wind variability has to be taken into account to reap the maximum benefits of wind power. The variability of wind has been widely studied. Recently also measured large-scale wind power production data have identified that wind variability in a region reduces due to "smoothing" effect of geographical spread and timescale. Smoothing effect is quantified using statistical parameters such as production (P) and fluctuation (ΔP) time series i.e. the maximum variation of production (extreme ramp rates), the probability distribution of the variations and the standard deviation (σ). The precise smoothing effect of the geographical distribution depends very much on local wind regime and on the total size of the geographical area. Holtinen (2004) studied the statistical parameters of large-scale wind

production to establish the smoothing effects. She established that the relative standard deviation of uncorrelated time series reduces due to geographic spread and number of turbines. The smoothing effect of wind power production from larger areas is due to the low correlation of production from different sites. She further demonstrates how zero and peak are common for an individual turbine; as the number of turbines increases in a region the number of zeros and peak reduces.

Ideally, to maximise the smoothing effect, the number of wind turbines within a wind farm needs to be very large and the wind speeds occurring in different parts of the system should be as uncorrelated as possible. Holtinen also concludes that it never reaches total calm all over the Nordic region. However, her conclusion less applicable to Kenya's 2015 wind power estimates since she tends to overlook the site-specific characteristics and the wind farm concentration in areas with favourable wind regimes. The siting of wind power plants in Kenya is primarily governed by the characteristics of the local wind regime, which varies both geographically and temporally. Consequently, the net system variability may not smooth out linearly due to concentration of wind farms on the northern and coastal regions of the country.

2.3.1 Short term variability

Wind variability can be divided into two distinct timescales i.e. Short term and long variability. Short-term variability, the consequence of turbulence or transient events includes inter-hour variability and intra-hour variability. Inter-hour variability, which covers timescales of seconds to minutes, is the sub-hourly differences between scheduled energy and forecasted demand. These differences are usually met by load-following units that can ramp output quickly to balance supply and demand. Intra-hourly variability covers several hours; determined using the

average dispatch capacity that is made available for intra-hour load following. Halamay (2010) calculated the reserve requirement using forecasted renewable resources (wind, solar & wave) and load. Regulation requirement was calculated using 10 minutes difference between the actual and forecasted values. The same was repeated in the hourly timeframe to calculate the imbalance requirement. This approach is more accurate because of different timeframes; however, analysis of variability for different renewables at the same time could result in errors since there is no correlation. Due to data limitations and the fact that short-term variability is quite small and hardly affects the system, Inter-hour variability will not be considered this study.

The maximum wind power fluctuations experienced in the power system are reduced due to turbine smoothing effect. The smoothing effect of a specified area has an upper limit. There will be a saturation for variation; that is, where an increase in the number of turbines will not decrease the (relative) variations in the total wind power production of the area. Beyond the point of saturation, the smoothing effect can be increased only if the area covered becomes larger. Holtinen (2004) carried out time series analysis of load forecast errors and wind power variations. In order to assess the additional resources to manage the balance between generation and demand in the hourly horizon, 4σ confidence level covered about 99% of the mismatches. The Load forecast was dropped by half of load variability. She concluded that the smoothing effect of a specified region has an upper limit i.e. a point where an increase in the number of turbines in a region will not increase the relative variation. Wang (2005) quantified the average variations in large-scale wind plant in the Midwest of the US. He concluded that the average hourly variations reduce from 7.0 to 5.2 percent as standard deviation reduces from

10.7% to 7.9 percent when wind turbine numbers increase from 14 to 250. This shows that hourly variation increases as the number of turbines in a wind farm increase.

Load Following reserve refers to spinning and non-spinning capacity required to meet within-hour shifts of average energy due to variations of actual load and generation from forecast load and generation (Ackermann, 2005). Spinning reserve is used by system operators to compensate for unpredictable imbalances between load and generation caused by sudden outages of generating units, errors in load forecasting or unexpected deviations by generating units from their production schedules. Non-spinning reserve is connected to the system but can be accessed after a short delay after the generator powers up. These reserves usually are ready to generate within ten minutes (Miguel, Ortega, & S.Kirschen, 2008).

The maximum step changes experienced in the power system depends on the penetration levels and power system's flexibility. This phenomenon has been extensively studied throughout Europe. Holtinen (2004), reported that the maximum hourly step changes are inside ± 20 percent of installed capacity per country. Hourly variations are between 91 to 94 percent of the time between 5 percent of installed capacity and 99 percent of the time $\pm$ 10 percent of capacity. Brandberg (2005) investigated how the market reacts to 4000MW of wind power in Sweden. He used hourly step changes to estimate wind forecast errors: the difference between the production the hour prior to the hour of operation and hour of operation. He concluded that a regulating power of 2680MW was required. Holtinen (2004) studied the impact hourly step changes on large-scale wind production in the Nordic electricity system. She concluded that the increase in reserve requirement would be about 0.33 TWh/annum at 10 percent penetration level and 1.15 TWh/annum at 15 percent penetration level. Axelsson (2005) determined the increase in reserve requirements in Sweden for different penetration levels and timescales. He

concluded that the hourly variations increase from 20MW (0.5 percent installed capacity) to 80MW (1.0 percent installed capacity) as wind power penetration increased from 4000MW to 8000MW. This shows that reserve requirement corresponds to step changes and increases with penetration levels.

2.3.2 Long-term Variability

Long-term variations of wind power relevant for integration in the power system include the seasonal and inter-annual variations, caused by climatic effects. Monthly and Seasonal Variations are important for electricity traders that have to deal with electricity forward contracts, where wind power volume has an influence on price. They are also important for power system planning. However, it appears that for both electricity trading and system planning purposes, these deviations, resulting from annual statistics of wind power produced, can be sufficiently hedged. Inter-annual variations are relevant for long-term system planning, rather than daily power system operation. Various studies have been undertaken to determine the impacts long-term variability in a power system. Sinden (2005) studied the characterization of the UK wind resources and relationship to demand using 34 years, hourly wind speed data recorded from 66 onshore sites. He concluded that wind power availability in the UK varies at a rate of 7.4 percent per annum. Wind power availability corresponds to wind speed availability. These are not particularly important for the daily operation and management of the grid, but plays a role in strategic power system planning. Different studies have shown that wind power in a region experiences seasonal effects. Sons (2005) analysed hourly wind speed data from 2001-2003 to estimate the level of aggregated wind power production has some seasonal effects with higher averages in winter than in summer. Soens concludes that large-scale wind integration in Belgium does not require a substantial increase in balancing reserves,

even if wind power is evenly spread across the country. However, one serious weakness of the study is that the impacts of meteorological forecasts in reserve management have been overlooked. Assuming that the entire region around the study site has a normal distribution could result to less accurate results. This is one serious weakness considering the fact that different wind regions have different distributions. Cabello (2010) studied the wind characterization in Alicante Spain based on data of station distributed over the study area. He demonstrated the fact that that both Bimodial and Trimodial frequency distribution were observed in Alicante Spain. Calif (2005) categorized wind speed fluctuations into distinct classes to estimate the probability of a distribution to belong to a class. Wind speed probability distribution function was classified using Dirichlet distribution mixtures. SAEM (Simulated Annealing Expectation Maximization algorithm) algorithm was used to give a distinction between the classes of wind speed distribution. He concluded that 90% of wind speed sequences are symmetrical monomodal is modelled by a Gaussian probability distribution function; 9% of wind speed sequences are dissymmetrical monomodal probability distribution function modelled by a Gram-Charlier function while the remainder is bimodal probability distribution function.

Wind regimes-based approach described in the project is an effective methodology for capturing both the seasonal and the diurnal variability of wind resources at a specific site. For the realistic emulation of the actual system operations, the simulation has to capture the seasonality effects, as well as changes in the resource mix and resource characteristics, the new policy and legislative initiatives, the investment decisions, and the maintenance schedule of the resources (Maisonneuve & Gross, 2011). Sinden (2005) analyses both long-term and seasonal variability. Long-term analysis of wind variability requires the express the hourly wind power

output as a percentage of rated capacity to allow for variability analysis. This makes it easier to fit data for long time fames in a single diagram. Sinden presents electricity demand by percentile rank from 1 hour to 8760 hours. His approach makes it easier to summarize several hour data into a single point. However, this method of analysis makes it difficult to establish the trend and the variability. Holtinen (2004) analyses the wind production and corresponding electricity demand arranged chronologically and by duration from 1 hour to 8760 hours. Her approach makes it easier to establish both the trends and variability from a single plot. For example, it is easier to depict the seasonal trends for an entire year using long time steps (approximately 500 hours) as opposed to short time steps. This suggests that two separate data sets have to be plotted to establish the variability in short periods and trends over long periods.

2.4 Load analysis

Generally, a power system is operated so that the generation portfolio satisfies the load demand using the transmission and distribution network. The loads vary, and their statistical distributions and the correlation between them must be modelled (Boehme, 2006). The changes in demand may be represented by load curves or by load duration curves. Load curve is crucial to power system analysis because the demand for power is traditionally described by a load duration curve. The load curve is a graphical summary of the relationship between of varying load with respect to chronological time. A load duration curve in contrast illustrates the variation of a certain load in a downward form such that the greatest load (peak load) is plotted in the left while the smallest one in the right. As seen later in the study both load curves and load duration curves can be represented in a single plot. Thus, the load curve will be viewed with respect to time while load duration curve independent of time.

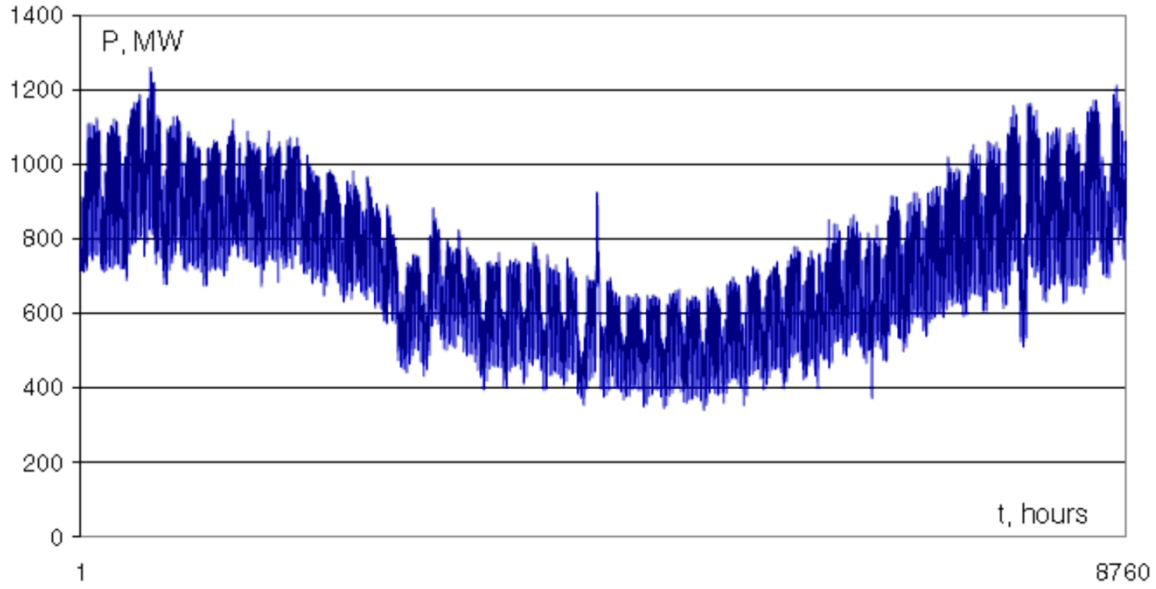

Figure 2.2 Annual electric load curve (Liik, 2005).

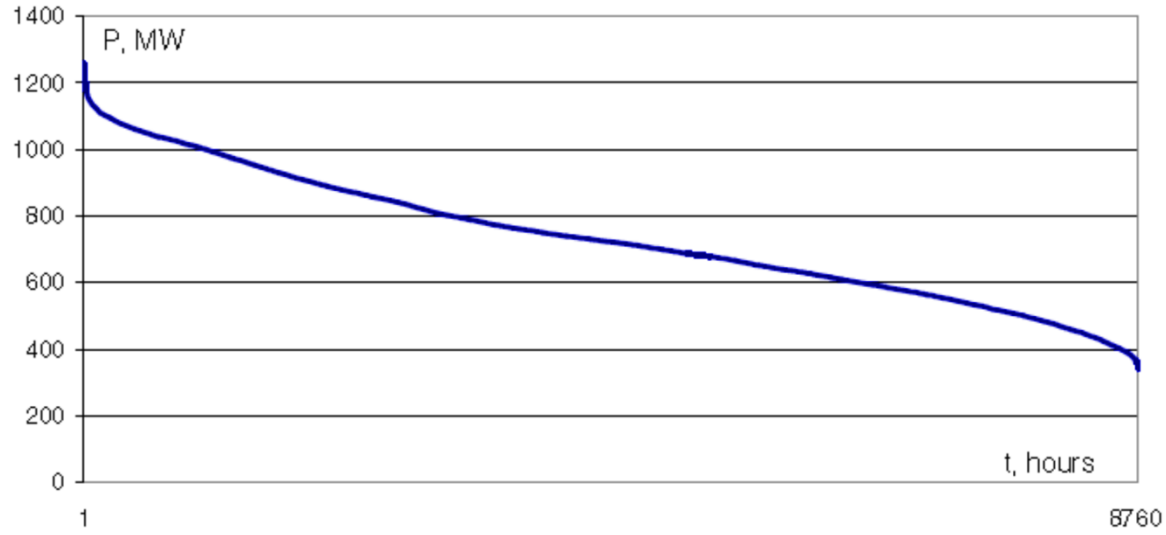

Figure 2.3 Annual load duration curve (Liik, 2005).

Electricity demand is traditionally divided in three load periods from the longest to the shortest: base load, shoulder and peak demand. A common modelling approach to integrate renewable

with the screening curve methodology is to use the net load duration curve; derived by subtracting hourly wind power output from hourly load. Wind is thus modelled as a negative load (Brun, 2009). The examples of the load curve and curve for one year are shown in Fig. 2.2 and Fig. 2.3.

The load duration curve (seen in Fig. 2.3) provides a useful summary of a year's worth of hourly fluctuations in electricity demand; the area under the load duration curve represents the energy demanded by the system. The height of each slice is a measure of capacity, and the width of each slice is a measure of the utilization rate or capacity factor. The product of the two is a measure of electrical energy (e.g. kWh). It is more convenient to deal with load duration curve than the load curve. The load duration curve illustrates the behavior of the electricity market, for example, the likelihood of peaking plant to be required for service, and the impact that this might have on price. A load-duration curve is a useful tool for comparing the impacts of different renewable portfolios on the grid. Liik (2005) demonstrated that generating capacity planning could use also load duration curves determined for shorter periods than a year, as separate curves for winter, spring-autumn and summer. Either the actual load level (MW) is represented as the percentage of the peak load over the course of the year (Pu). The latter, a normalized form of load duration curves is used for the modelling of electricity demand for the generation optimization model. The load-duration curve for a particular system makes it easy to see, for example, that the total system load exceeds 90% of peak load in 200 hours out of the year, or that in 50% of the year, the load is at or above some level of capacity in MW. In general, a flatter load-duration curve is better for grid operation, allowing dispatchable generation to run at a higher capacity factor over the entire year and requiring less

peaking reserves. The easiest system to operate, for example, would be one with a load-duration curve that is a horizontal line indicating the demand is entirely constant for the whole year.

A fundamental characteristic addressed by power system operation and planning is the diurnal and seasonal variations in system load. It is axiomatic that system loads have daily peaks and valleys and that those extremes vary with season and between years. The installed generation must be capable of serving the load at all times. In wind integration studies, load curve can be used to establish the seasonal variations in electricity demand. Liik (2005) derives the seasonal and diurnal variations of load from the annual consumption. Three seasons (winter, intermediate, summer) and differentiates day and night in each season splitting a year so into six time divisions. The user of the model can determine the lengths of the seasons and day/night in each season. The load in each time division is calculated by dividing the energy consumption in that interval by the length of the interval (number of hours in it). As a result, six average load levels will represent the annual load curve. To account the peaks of electric load, a special coefficient is used. It shows the amount by which installed capacity exceeds the average load in the time division of maximum demand. He concludes that the Estonian power system, the base-load forms about 35%, intermediate load about 40% and peak-load about 25% of the maximum load. Boehme (2006) demonstrated the use of power flow solutions with hourly time steps over a year or more to produce load duration curves for system components. He concluded that load duration curves give a much more comprehensive picture of the system compared to single, seasonal figures. Furthermore, statistical analyses and detailed investigations of phenomena can easily be performed.

The effect of additional reserve requirements for the power system is estimated by combining the standard deviation of load and wind variations. However, what the system sees is net load

(load minus wind power production). The net load duration curve is obtained by deducting the hourly wind generation from the load demand for the corresponding hour. If load and wind power production are uncorrelated, the net load variation is a simple root mean square (RMS) combination of the load and wind power variation. The larger the area in question and the larger the inherent load fluctuation in the system the larger the amount of wind power that can be incorporated into the system without increasing variations. The reserve requirement can be expressed as three times the standard deviation (4σ covers 99% of the variations of a Gaussian distribution). Examples of net load duration curves for different wind penetration levels of wind power in the U.S. from 10% to 30 % of peak demand are shown in the Fig. 2.4. The gap between the reference the load curve and any of the net load curves highlights the significant number of hours that net load is lesser than that of load. At the right hand side, a more pronounced downward tail for any of the net load duration curves than for the load duration curve can be explained by a high availability of wind during periods of low demand. On the contrary, a similar upward tail between net load curves and reference load curve at the left hand side is due to a low percentage of wind power during periods of high demand.

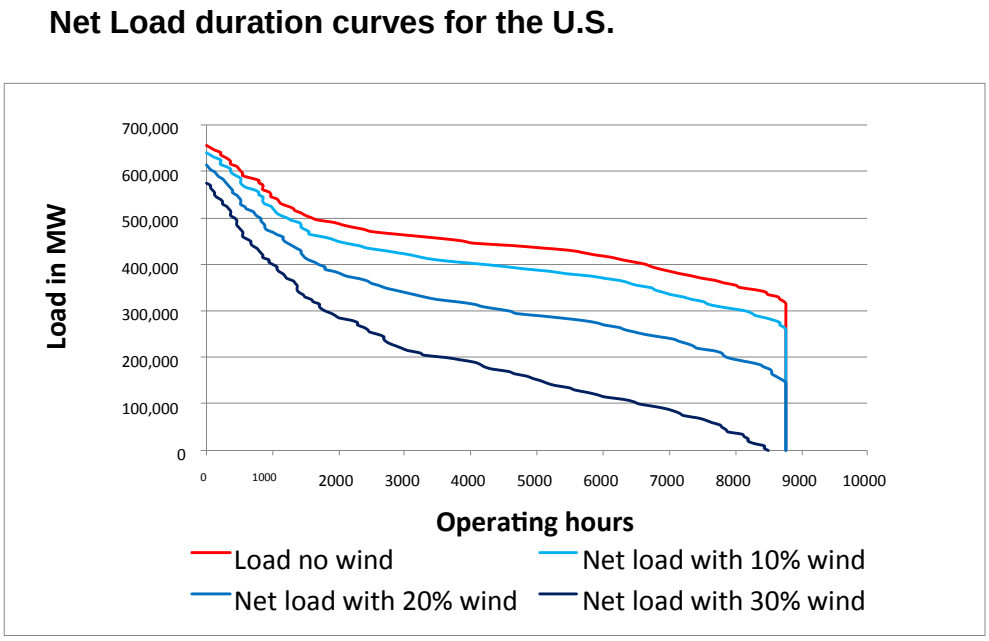

Figure 2.4 Annual Net load duration curves (Brun, 2009)

Studies have shown that the distribution of changes in net load flattens and broadens when large-scale wind is added to the system. Halamay (2010) analyzed the reserve requirements for the Pacific Northwest of the U.S. including wind, solar, and ocean wave energy specifically, using actual load and wind power data, and solar and ocean power data generated from resourcemeasurements. The load was compared with net load the variability added by wind to the net load increases the reserve requirements. Consequently, the net loads were calculated using the sum of the forecasts for each component: load, wind, wave, and solar. He concluded that the decremental reserve required for the load alone was 379.3 MW while for the load minus 15% wind it is 447.3 MW, and for the load minus 5% wind, 5% solar, and 5% wave, it is 412.1 MW. The implication is that high renewables penetrations will likely increase the ramp requirements for many hours of the year. Boehme (2006) analysed long-term statistical data for both demand and onshore wind turbine output in Scotland, and generally applicable in north

Western Europe. He concluded that they show some similarities in behaviour: Demand and generation in winter are higher than in summer, and around midday, they are higher than at midnight. Despite this resemblance, it is possible that the combined wind farm output across an area as large as Scotland will be well below 10% of the rated capacity while demand is above 90% of the annual peak.

Chapter 3 METHODOLOGY

3.1 Ngong Wind Farm Survey

Site survey was carried out at the Ngong wind farm, currently the only wind farm connected to the Kenyan grid. The site survey lasted from January to March 2012. The main task was to establish the performance of individual turbines based on their wind speed characteristic and further validate the MATLAB simulations. The turbine wind speeds was measure at the hub height 52 meters. Twelve-month period was considered sufficient to determine seasonal variations at the site i.e. the wind speed characteristics for both the wet and dry seasons. However, due to several data limitations, wind speeds was recorded for only six months (October 2011 to March 2012).

The simulation of wind speed was performed using Windographer software (see section 3.2) and the computation of site variability was done use of Weibull Analysis. The Maximum Likelihood Method and Least square Method methods for determining k and c are outlined in section 4.4. The wind farm model (used to convert wind speed data into to simulated power output) was implemented in MATLAB/Simulink software as described in section 3.4 to 3.6. After which, the actual and simulated turbine outputs were compared to establish the applicability of MATLAB/Simulink simulation. The wind farm input parameters were based on the Vestas V52 turbine nameplate details. The turbine Wind Turbine Modelling parameters are as describe in section 4.2. Subsequently, necessary adjustments were made to the turbine input parameters to reduce the error margin between the simulated and actual data. The functionality of the anemometers (installed in each of the turbine) requires power; hence, no data can be recorded during power failure (blackout). Therefore, data was assessed to establish

the link between the turbine failures and zeros (or gaps) in the wind speed data. All these gaps as results of turbine failure were then filled using Windographer software. This eliminated all traces of power failure in the data and improved simulation accuracy.

Figure 3.1 Maintenance work at the Ngong Wind Farm

Figure 3.2 Control and switching centre at the Ngong Wind Farm

3.2 Data

The data required to achieve the study objectives was obtained as follows:-

1. Wind speed data for Ngong was obtained directly from the KenGen turbines at a hub height of 50 meters in excel format. This data covered a period from October 2011 to March 2012 with a sample time of one hour.
2. The wind speeds data for Kinangop and Lake Turkana was sourced from the Ministry of Energy at a height of 40 meters in .row format. This data was later converted to excel

format. This data covered a period from April 2011 to September 2011 with a sample time of one hour.

3. Historical load data were sourced from KPLC load database in excel format. This data covers a period from June 2008 to November 2008 with a sample time of 30 minutes.
4. All the load and wind data obtained at a sample time of shorter than an hour was then averaged to obtain the hourly data.
5. The measured height of the wind speed data for Kinangop and Turkana (sensor height, 40 meters) used in this research does not correspond to the hub height of Vestas V52 wind turbine (50 meters). Therefore, a height transformation must be applied to the wind speed time-series from the measurement height to the turbine hub height.

The relationship between wind speed and height was determined by the function shown in equation 3.1.

$$V_{50} = V_{height} \times \left(\frac{50}{height}\right)^{\frac{1}{7}} \tag{3.1}$$

Where V_{50} is the wind speed in meters/ second, height is the height in meters of the data-collection station (either 40 or 50 meters) and 1/7 is the power factor used to convert wind speed from one height to another (Milligan 2003).

3.3 Wind Regime Analysis

The wind speed data (time series format) was fed into Windographer to estimate the wind probability function, the diurnal range and the monthly statistics for Ngong, Kinangop and Turkana. The wind speed at a height of 50 m above ground level covers a six-month period running from October 2011 to March 2012. Statistical wind data set was analysed using Weibull distributions in order to investigate the Weibull shape and scale parameters. The Weibull shape and scale parameters, k and c, corresponding to the wind speed distributions were then obtained from the maximum likelihood algorithm for Weibull fitting. The findings are as discussed in chapter 6.

3.4 Simulation work flow

The wind power simulation workflow used in this study is as described below;-

1. Wind speed data were imported from an excel file into the MATLAB workspace using the Import Wizard. The Import Wizard lets you select the data to import when analysing a portion of an Excel worksheet or specific columns or rows in a MATLAB array. A time plot for the wind speed was then created to gain insight into the data features before commencing the simulation.
2. The workspace model imports the correct data subset to the DFIG wind farm model.
3. Simulation was then run on Phasor mode. A Phasor model allows the transient stability study with long simulation times (<100 time steps). In the wind, farm model shown in figure 3.1 the simulation has a run time of 3171 hours; this corresponds to the study period from October 2011 to March 2012.

4. After the simulation was complete, the wind generation data also in time series format were then loaded to a scope while it is also tapped from the file block in excel file format. The generation data was then exported to an excel file for further analysis.

The chronological presentation of hourly wind generation and electricity demand is sorted by in descending order. Total duration of every load level over a period is calculated. Wind generation and Load Duration Curve; the function of wind generation and load level depending on its duration is produced. Both wind generation and load duration curves are then normalized to determine the Normalized Generation and Load Duration Curve. The normalized function of wind generation and load level for its duration is produced.

3.5 MATLAB/Simulink Wind Farm Model

The Aggregate wind farm Model was designed and implemented using different electrical components shown in Fig. 3.3. The wind farm is composed of a specific number of turbines depending on the wind capacity each rated at 0.85MW. The wind farm is connected to a 25 kV network, via 25 km line 120 kV/25 kV transformer. The 25 kV network is further connected to the 120 kV network through a 30 km 25 kV line and a 120/25 kV transformer. All the network parameters were set to a frequency of 50Hz to comply with the Kenya's grid specifications.

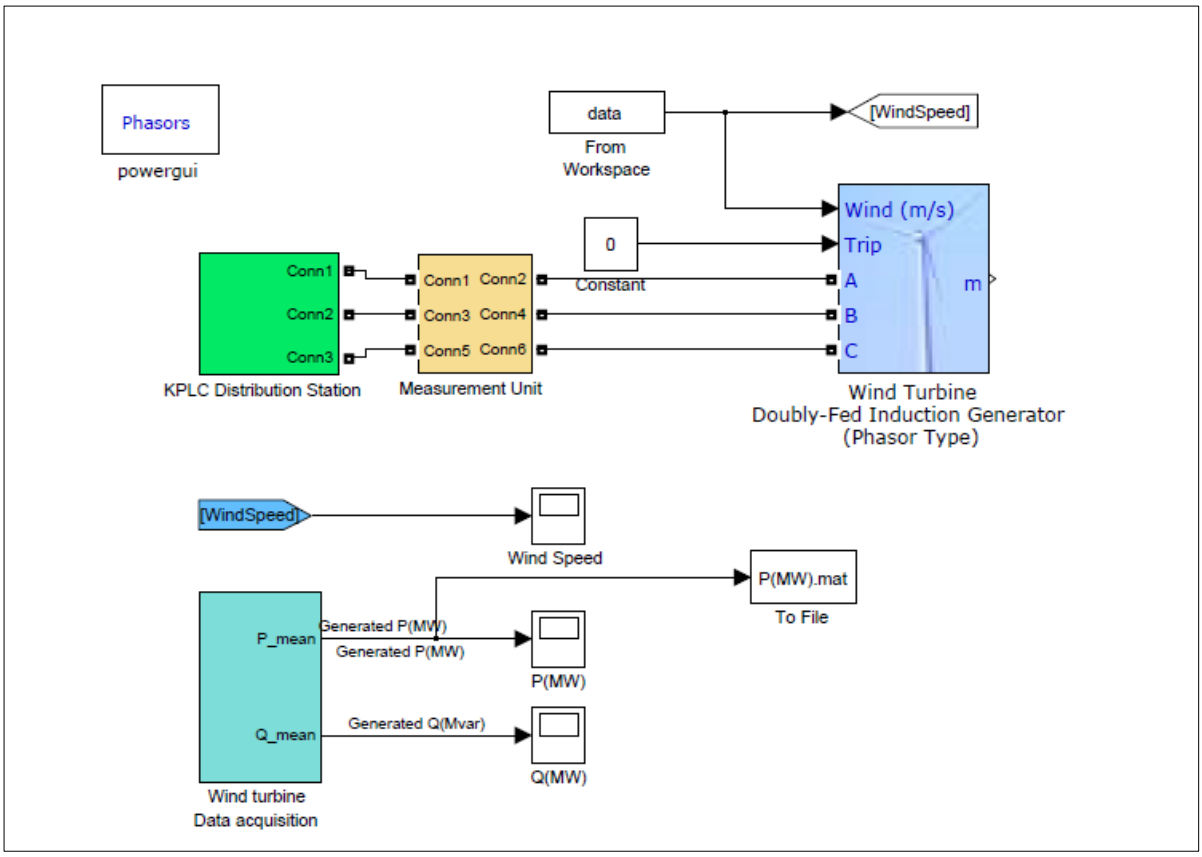

Figure 3.3 MATLAB/Simulink wind farm model layout

3.6 Simulation assumptions

This study made the following simulation assumptions;-

1. Vestas turbine use Opti-speed concept, a term that refers to their technical variance between the fixed speed and variable speed wind turbine. This concept is based on speed or torque control by use of variable impedance at the rotor of the induction machine. The benefit of the Opti-speed concept is the simplicity of a fixed wind turbine, but at the same time having the possibility of flicker regulation and load minimization especially at high wind speed. However, this concept was overlooked in the MATLAB simulation.

2. The concept of full aggregation (which assumes that all wind speeds and mechanical speeds are almost the same) has been applied in this study. Aggregation makes it possible to represent the entire wind farm using only one turbine model hence reducing data requirement and computational time.

The model takes into account one aggregate generating capacity based on the number of wind turbines. In reality, turbines located close to each other are affected by the same wind blowing through. However, for the purpose of this study, the correlation coefficient of wind between turbines is assumed negligible and the aggregate capacity of the wind farm is used.

3.7 Study scenarios

This study therefore determines site specific the reserve requirements for different types of regimes based on futuristic scenarios. The estimated wind penetration level in each scenario was selected based on Kenya's 2015 wind power expectations. Wind penetration level refers to the fraction of energy produced by wind in comparison to the installed capacity. Since there is no generally acceptable maximum wind penetration level, 0.374 Pu was chosen as the maximum penetration level. Some of the scenarios have single sites while others multiple sites. The scenarios with multiple wind sites are chosen to analyse the effects of geographical spread of the power system. The different scenarios analysed in this study are as described below;-

Scenario 1: Load only

Scenario 2: Ngong wind farm (phase I (1 &2) and II) 0.024 Pu

Scenario 3: Ngong (phase I (1 &2) and II) combined with Kinangop 0.083 Pu

Scenario 4: Ngong (phase I (1 &2) and II) combined with Turkana 0.316 Pu

Scenario 5: Ngong (phase I (1 &2) and II) combined with Kinangop and Turkana 0.374 Pu

Scenario 6: Ngong wind farm up-scaled up to 0.374 Pu

3.8 Estimation of hourly variations and load following requirements

In order to determine the impact of wind variability on operational reserve this study was undertaken on the control area basis. This refers to a state in which wind output is not matched one on one by a change in another generating unit in the opposite direction: the total aggregation that has to be balanced.

The procedure for determining hourly variations and the net load following requirement is as described below;-

1. Data from the Normalized wind generation and Load Duration Curve was used to determine the load and wind variations. The difference between wind and load generations of two consecutive hours was used to determine the hourly load and wind variations as expressed in equation 3.2 & 3.3. Load variation and wind variation results were stored in excel format for further analysis.

$$\Delta P = P(h+1) - P(h) \tag{3.2}$$

$$\Delta L = L(h+1) - L(h)$$

(3.3)

Where (h) is represents the current hourly and $(h+1)$ represents the following hour.

2. The net hourly variations in each of the scenarios are determined by subtracting the wind variations from the load variation as shown in equation 3.4. The net load in this case is defined as the system demand requirement to be met by wind generation alone i.e. wind power is seen as a negative consumption. The Net Load variation results were stored in excel format for further analysis.

$$\Delta NL_i = NL_i - NL_{i-1} = (L_i - P_i) - (L_{i-1} - P_{i-1}) = \Delta L_i - \Delta P_i$$

(3.4)

Where NL denotes the net load (MW), L the load (MW) and P the wind production and i is the hour (from 2 to 3170).

3. The standard deviation σ for the hourly variations was then determined as shown equation 3.5.

$$\sigma = \sqrt{\frac{\sum_{i=1}^{n}(x_i - \mu)^2}{n}}$$

(3.5)

4. The standard deviations for two wind farms were then combined to determine the overall wind power forecast error σ_{W12} as shown in equation 3.6 (Doherty, July 2005).

$$\sigma_{W12} = \sqrt{\sigma_{W1}^2 + \sigma_{W2}^2 + 2r_{12}\sigma_{W1}\sigma_{W2}} \tag{3.6}$$

Where cross-correlation r_{12} is measure of how well two time series follow each other. Cross-correlation $r_{12,}$ gets near max value 1 if the vicissitudes within the two time series occur simultaneously, zero (o) if the vicissitudes do not follow each other and -1 value if there is tendency of increasing on one side while decreasing at the other side.

$$r_{12} = \frac{\frac{1}{n}\sum_{i=1}^{n}(W_1 - \mu_{W1})(W_2 - \mu_{W2})}{\sigma_{W1}\sigma_{W2}} \tag{3.7}$$

5. The standard deviation of net variations σ_{NL} was then determined by a simple square root sum of the standard deviations of load σ_L and wind power σ_W (The equivalent value of overall wind power forecast error σ_{W12}) as shown in equation 3.8.

$$\sigma_{NL_{n+1}} = \sqrt{\sigma_L^2 + \sigma_{W_n}^2} \tag{3.8}$$

6. The increase in the variations was then determined as shown in equation 3.9.

$$I = 4\left\{\left(\sqrt{\sigma_L^2 + \sigma_W^2}\right) - \sigma_L\right\}$$

(3.9)

7. The increase in variation for scenarios with more than two wind farms (e.g. Scenario 5), the assumption is additional wind capacity will result to additional variation of the system a result of the nth wind farm was calculated using equation 3.10 below.

$$I_n = 4^n\{(\sigma_{NL1} - \sigma_L)(\sigma_{NL2} - \sigma_{\sigma NL1}) \dots \dots \dots (\sigma_{NLn} - \sigma_{NL-1})\}$$

(3.10)

8. Depending on the scenario, the load time series was then multiplied by the increments I *or* I_n to determine the net load time series.
9. The frequencies net load variations for the different scenarios was determined and plotted using Microsoft Excel.
10. The maximum upward and downward net load variations were determined using the tails of their respective distributions. Step 8 was then repeated for the load time series.
11. The maximum net load variation for the different scenarios was then compared to the maximum load variations to estimate the load following reserve requirements in each scenario.
12. The load following requirements at different penetration levels was plotted in Microsoft Excel. The findings are discussed in the next chapter.

Chapter 4 WIND ANALYSIS AND MODELLING

4.1 Analysis of Wind Speed characteristics using Weibull Distribution

A proper analysis of statistical wind data is a very important step when performing a wind resource assessment, which supports a wind energy feasibility. The performance of wind turbine generators (WTG) on a particular site can be determined by the wind speed characteristics and the corresponding WTG power curve. Wind energy production is high during the high-load periods, the wind resources can displace one or more peaking and, typically, expensive controllable units. On the other hand, if the wind energy production is significant during the low-load periods, the system operators need to lower the output of the base loaded and non-flexible units. As the shape of the daily wind power production depends directly on the diurnal wind speed pattern, the wind speed model must reflect this characteristic. The diurnal wind-farm power production pattern directly influences the scheduling of the controllable resources. Multiple daily patterns may occur throughout a year depending on the site wind characteristics (Maisonneuve & Gross, 2011).

The Weibull distribution is a mathematical expression that provides a good approximation to many measured wind speed distributions. Despite claims by several researchers, that Weibull does not fit well when the wind regimes present bimodality (Cabello & Orza, 2010) , the Weibull distribution technique is still widely accepted and used in the wind energy industry as the preferred method for describing wind speed variations at a given site. The Weibull distribution density is as shown by equation 4.1 (Biswas, February 2010).

$$f(v) = \frac{k}{c}\left(\frac{v}{c}\right)^{k-1} \exp\left\{\left(\frac{v}{c}\right)^{k}\right\} \tag{4.1}$$

Where c is the scale parameter, in the units of the speed and k is the shape parameters are:

$$c = \frac{\bar{v}}{\Gamma\left(1 + \frac{1}{k}\right)}$$

, (4.2)

$$k = \left[\frac{\sigma}{\bar{v}}\right]^{-1.086} \quad (1 \leq k \leq 10$$

(4.3)

Where the mean wind speed $\bar{v}$ and the variance σ^2 are:

$$\bar{v} = \frac{1}{N-1}\sum_{i=1}^{N} v_i$$

(4.4)

$$\sigma^2 = \frac{1}{N-1}\sum_{i=1}^{N} (v_i - \bar{v})^2$$

(4.5)

Here, Γ is the gamma function. The k and c are important in describing in describing the wind power potential in a specific site. The Weibull k value is the unit-less shape factor that reflects the breadth of the distribution. Lower values of k values correspond to broad distributions where the wind speed tends to vary widely, while higher k values correspond to tighter distributions where the wind speed tends to stay within a narrower range. For a typical

commercial turbine like the Vestas V52 850kW (Currently installed by KenGen at the Ngong wind farm) the two extreme values of the shape can have a large difference in wind power.

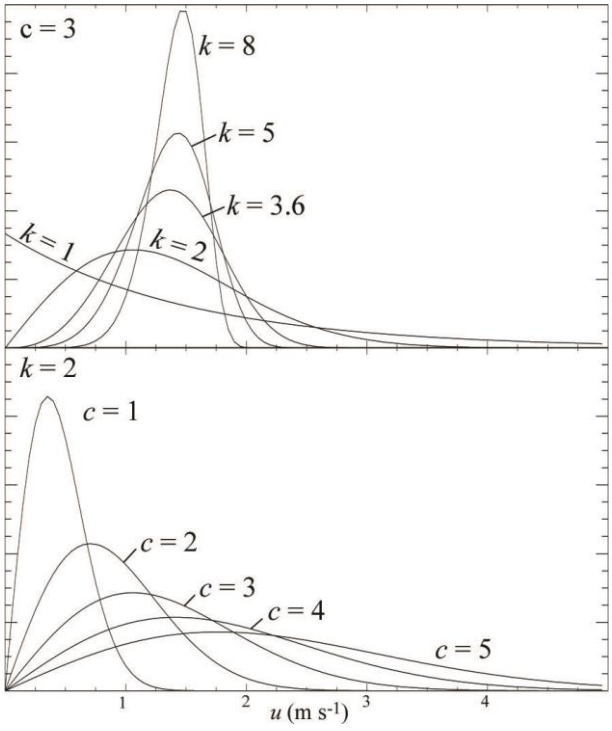

Figure 4.1 Examples of Weibull distributions for varying values of the shape parameter k and scale parameter c

The parameter k is key in the analysis of wind potential in a specific site. As its name suggests, the shape parameter controls the form of the distribution, ranging from exponential (k = 1), to Rayleigh (k = 2), to an approximation of a Gaussian (k = 3.6), to more skewed distributions of higher values of k. For k equals three, the Weibull distribution looks like a bell-shaped function, thus winds blow all the time at a constant speed (Archer & Jacobson, 2002.). When the k surpasses three, the wind distribution approaches the normal distribution, often referred to as a Gaussian distribution. Under this situation, the relatively stable wind speeds provide ideal conditions for wind turbine operation. If a wind regime has a value of k lesser that the two then it is regarded as a weak regime. Any wind regime with the value of k lower than 1.5 can pose

a serious challenge to wind integration because of its high variability. However mixing different wind regimes with different value of k will reduce variability, increase predictability and reduce zero outs. Besides the shape parameter k, the influence of the scale parameter c should also be taken to account. The scale parameter c describes how much the distribution is stretched the distribution is along the horizontal axis. The scale parameter c is directly related to the mean wind speed for a given value of the shape parameter k. The higher the value of c is the higher the mean wind speeds are.

When analysing Weibull distribution for experimental data, we have to estimate the Weibull parameters k and c. The common methods for determining k and c are Maximum Likelihood Method and Least square Method. Other methods not described here include; Graphical method, Standard deviation method, Moment method and Energy pattern factor method

4.1.2 Maximum Likelihood Method

The method of maximum likelihood (the term first used by Fisher, 1922a) is a general method of estimating parameters k and c in for experimental data. To estimate the parameters c and k using maximum-likelihood, an initial guess of $\hat{k}$ = 2 is used for solving the following equation for the estimation $\hat{k}$. Once the value of $\hat{k}$ is found, the value of $\hat{c}$ is determined by the equation 2.6.

$$\hat{c} = \left[\frac{1}{2N}\sum_{i=1}^{N} v_i^{\hat{k}}\right]^{\frac{1}{\hat{k}}} \tag{4.6}$$

This equation for $\hat{c}$ is seen to be a generalization of the equation for k = 2 for the Rayleigh distribution to the general k for the Weibull distribution (if we substitute $\hat{k}$ = 2 in this equation we get equation 2.7.

$$\hat{k} = \frac{\sum_{i=1}^{N} v_i^k inv_i}{\sum_{i=1}^{N} v_i^k} - \frac{1}{N}\sum_{i=1}^{N} inv_i$$

(4.7)

4.2 Wind Turbine Modelling

The purpose of the wind turbine is to covert wind speed into an electric power output. The performance of a wind turbine depends on the wind speed, which varies with time and depends on regional weather patterns and type of landscape. Relationship between wind speed υ (m/s) through a sweeping area A (m) of wind turbine and wind energy per unit time or wind power P (W) is as follows;

$$P = \frac{1}{2} C_p \rho A V^3$$

(4.8)

Where ρ represents the air density (kg/m3).

From this relationship, it can be seen that the relationship between wind speed and power is nonlinear, cubic. Any error in wind speed forecast will actually give a large (cubic) error in wind power. In addition, for entire wind farm, this relation is more complex as different turbines in the farm use multiple wind directions and speed to achieve optimal power output of

wind farms. The power coefficient C_p gives the fraction of the kinetic energy that is converted into mechanical energy by the wind turbine. It is a function of the tip speed ratio (λ) and depends on the blade pitch angle for pitch-controlled turbines. The tip speed ratio may be defined as the ratio of turbine blade linear speed and the wind speed as follows;

$$\lambda = \frac{R\omega}{V} \tag{4.9}$$

Substituting (4.8) in (4.9), we have:

$$P = \frac{1}{2} C_p(\lambda) \rho A \left(\frac{R}{\lambda}\right)^3 \omega^3 \tag{4.10}$$

As seen in the previous chapter, simulations of Doubly Fed Induction Generators (DFIG) wind farms was performed in MATLAB/Simulink. The turbine model was developed to represent a wind farm for converting wind speed into power. The six basic model elements include aerodynamic system; Mechanical system (turbine rotor, shafts, gearbox and the generator rotor); generator drive (generator and power electronic converters, if any): pitch control and protection system of the wind turbine.

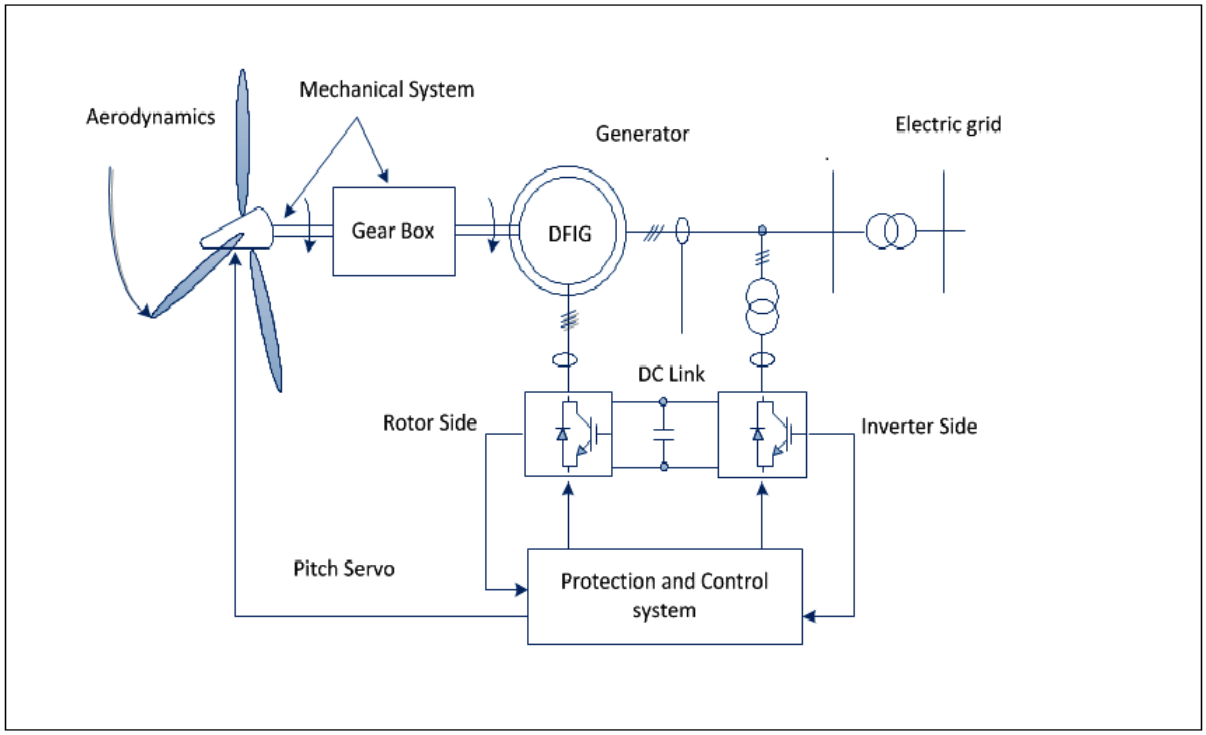

Figure 4.2 Wind Turbine Control

4.2.1 Aerodynamic system

The aerodynamic system of a wind turbine is the turbine rotor (i.e. the blades of the wind turbine). The turbine rotor reduces the wind speed and at the same time transforms the absorbed kinetic energy of the air into mechanical power. In this study, various topological aspects that influence the performance of the aerodynamic model have been neglected. Therefore, the mechanical power output calculated based on the blade radius and the measured hourly wind speed data (blade tip speed). The aerodynamic system is a lumped mass one, i.e. it does not model the double mass phenomenon. The turbine pitch controlled is controllable. The control signal for the pitch angle (β) comes from the DFIG control block. The coefficient C_p is calculated through a look-up table and the output of the wind turbine block is the torque on the

induction generator axis. The pitch angle β is only varied to limit the over-speed of the generator.

4.2.2 Mechanical system

The wind turbine is connected through a gearbox to the generator, which in turn is connected directly to the power system. The gearbox transmits torque and revolutions from the rotor to the generator. The main gearbox consists of a planetary gearbox combined with a two-stage parallel shaft gearbox, and a tooth coupling transmits the torque and the rotary motion of the planetary stage to the two-stage parallel shaft gearbox. The main shaft of the rotor is mounted into a hollow shaft (input shaft) of the gearbox, and a shrink disc transmits the torque. As the main shaft is supported by two main bearings, only pure torque is transmitted to the gearbox. Two torque arms support the gearbox and torque and oscillation are absorbed by pre-tensioned oscillation dampers, which are located between the torque arms of the gearbox and the main frame. Finally, the torque is transmitted from the high-speed shaft to the generator by a flexible composite coupling, which is located immediately after a 3-caliber disc brake. The 3-caliber disc brake is mounted directly on the high-speed shaft. The values of the induction generator parameters are default.

4.2.3 Induction generator

An important part of the turbine is the induction generator. It converts the mechanical energy from the gearbox to electrical energy. The generator is connected to the grid, which transfers the electrical energy to the consumer. The generator is coupled to the grid with the stator and the rotor is supplied from a converter via a slip ring. The generator can be coupled in star or delta connection. The generator is coupled in star mode if the total power is low (equivalent to a small generator); in the case of high total power the generator is coupled in delta mode. The

advantage of the star coupling is that the speed range is increased and the losses in the generator and converter are reduced. The values of the induction generator parameters are reported in Appendix 2.

4.2.4 Pitch Control System

The goal of the protection system is to protect the wind turbine from damage caused by the high currents that can occur when the terminal voltage drops because of a short circuit in the grid. The pitch angle controller is active only in high wind speeds. In such circumstances, the rotor speed can no longer be controlled by increasing the generated power, as this would lead to overloading the generator and/or the converter. Therefore, the blade pitch angle is changed in order to limit the aerodynamic efficiency of the rotor. This prevents the rotor speed from becoming too high, which would result in mechanical damage. The optimal pitch angle is approximately zero below the nominal wind speed. The DFIG has an AC-DC-AC converter system consisting of two control sub-systems (two semiconductor power converters, one on the rotor side and one on the grid side), as illustrated in Fig. 5.1. The stator side is connected directly to the 50Hz grid while the rotor side is fed at variable frequency through an AC/DC/AC converter.

The AC-DC-AC converter system is used for controlling both the active and reactive power flows independent of rotor speed. The DFIG wind turbine configuration consists of an induction machine (vector control) based on a double-axis theory of electric motors. The rotor-side converter vector control system makes use of the aligned to stator magnetic flux vector coordinate system, while the grid-side converter regulation system employs the grid voltage vector. The Grid Side Converter is modelled using a universal bridge model with IGBT’s (Insulated-Gate Bipolar Transistors) connected to the IG (Induction Generators) terminals

through a series RL filter. The control of the Grid Side Converter aims at keeping the DC-link capacitor voltage constant at nominal value. The DC-link consists principally of electrolyte capacitors and a bus-bar, which connects the grid inverter to the rotor inverter. The converter maximum power is half the IG rated power. The nominal DC-link capacitor voltage is 1200V. The rotor side converter is modelled using a universal bridge model with IGBTs connected to the IG rotor windings. The values of the protection system parameters are reported in Appendix 2.

4.2.5 Network Model

In order to take into account specific site characteristic like variability, wind turbine models have been combined to develop a stochastic model of an aggregate wind farm. Aggregate wind farm models are very suitable for simultaneous simulation of a large number of wind turbines, making it possible to estimate efficiently the impact of a large wind farm on the power quality. Aggregation adequately represents the characteristics of the wind farm during normal operations characterized by small deviations of the grid quantities from nominal values and wind variations. The main advantages aggregation is the fast computation, reduced memory requirements and the ease of use, either for variable or constant speed models. This is more accurate than up scaling which neglects small deviations in grid quantities. The layout for a large wind farm is as shown in appendix 2.

Chapter 5 RESULTS AND DISCUSSION

5.1 Simulation validation

The simulated data were validated at the site using direct comparison actual wind production data at the Ngong wind farm. Simulation was done on MATLAB/Simulink at the current wind penetration levels. This was later on followed by a simulation of Ngong phase 2 and 3 to determine the impacts of Kenya's 2015 wind power expectations. The wind farm model input parameters were based on the Vestas V52 turbine. The MATLAB / Simulink software uses an aggregated wind turbine model representing an entire wind farm. All aspects wind farm aspects including disturbances have been considered in the aggregated model.

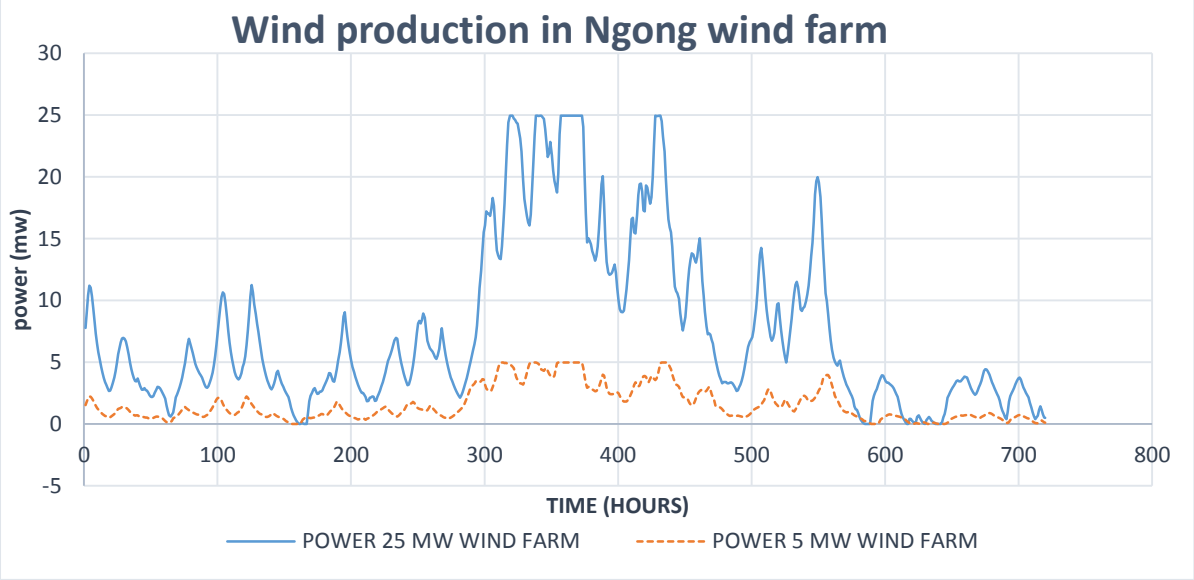

Figure 5.1 Wind production data for Ngong based on 2011/12 and 2015 expectations

The results show a similar pattern for 5MW and 25MW wind farm, peak and zero-outs coincide. However, the up-scaled 25MW wind farm appears to be slightly smoother compared to the wind farm. As seen in Fig. 5.1 unlike up scaling the smoothing effect is considered. The

peaks and zeros coincide since the same data has been used in both cases. Since the measured data from KenGen was available in kWh, The Wind production data shown in Fig. 5.1 was further converted into energy by multiplying with the number of hours. The monthly power out was classified into the high wind seasons running from December to February and low wind months running from March to September. The Nominal Turbine output is a hypothetical scenario in which the turbine produces peak power for the entire month. The simulated production is a product of the average simulated power kW and the actual number of hours the turbines has been running. The actual number of hours are hypothetical assumptions that wind turbines will be running for the entire month while as Simulation time depends on data availability. The actual hours caters for zeros and gaps in the data caused by instrumentation error or when the turbines are shut down during maintenance or when wind speeds speed were lower than the cut-off wind speeds. The same hour simulation output is the product of the average simulated power kW and the actual hours in a month. Therefore, the same hour power out can produce a positive or negative error depending on whether the value of actual data surpasses or below the simulated data. The simulation time were as follows; June for 107 hours, July for 744 hours, August for 276 hours, October for 347 hours, November for 720 hours, December for 744 hours, January for 744 hours and February 696 hours. Conversely, the actual time determined from the grid ok hours were as follows; June for 697 hours, July for 722 hours, August for 740 hours, October for 710 hours, November for 664 hours, December for 724 hours, January for 715 hours and February for 662 hours. Comparing the two time sets the error time consequence to missing data was as follows; June for 590 hours, July for 22 hours, August for 464 hours, October for 363 hours, November for 56 hours, December for 2 hours, January for 29 hours and February for 34 hours.

Fig. 5.2 to 5.5 shows the annual energy outputs for turbines 1, 2, 4 and 6 respectively. As seen from both figures no turbine reaches its peak in any of the turbines from June 2011 to February 2012. When the peak production and actual production are compared in all the turbines, the actual production exceeds 1/2 the peak production during the high wind speed months and its 2/3 the peak during the low wind speed months. Furthermore, when the simulated production and actual production are compared in all the turbines, the simulated total production is slightly lower compared to the actual total production during the low wind months but has the same shape (follows the same trend). On the contrary high simulation accuracy during the month of December, January and February can be attributed to the fact that low amount of data that was missing during these months while the low simulation accuracy during the month June, August and October can be attributed to the large amount of data missing, resulting in underestimation of energy. When we consider the energy output for turbine 1 the same hour simulation output compares well with the actual output in most of the months following a similar trend. However, June and October have the least simulation accuracy due to the difference between their Simulation time and Actual hours. This shows that the reliability of the wind turbine will also have an impact to the simulation accuracy. Ultimately, MATLAB simulation is more reliable. The real and simulated output from the turbines compared well for several months. This shows data availability has great influence to simulation accuracy. Turbines 2 and 4 show similar trends in the energy outputs when compared to Turbine 1. However, Turbine 5 appears to be slightly different. The simulation output is slightly lower than the actual output in all the months except for February. In summary the validity of the MATLAB/Simulink simulation is depends to data availability.

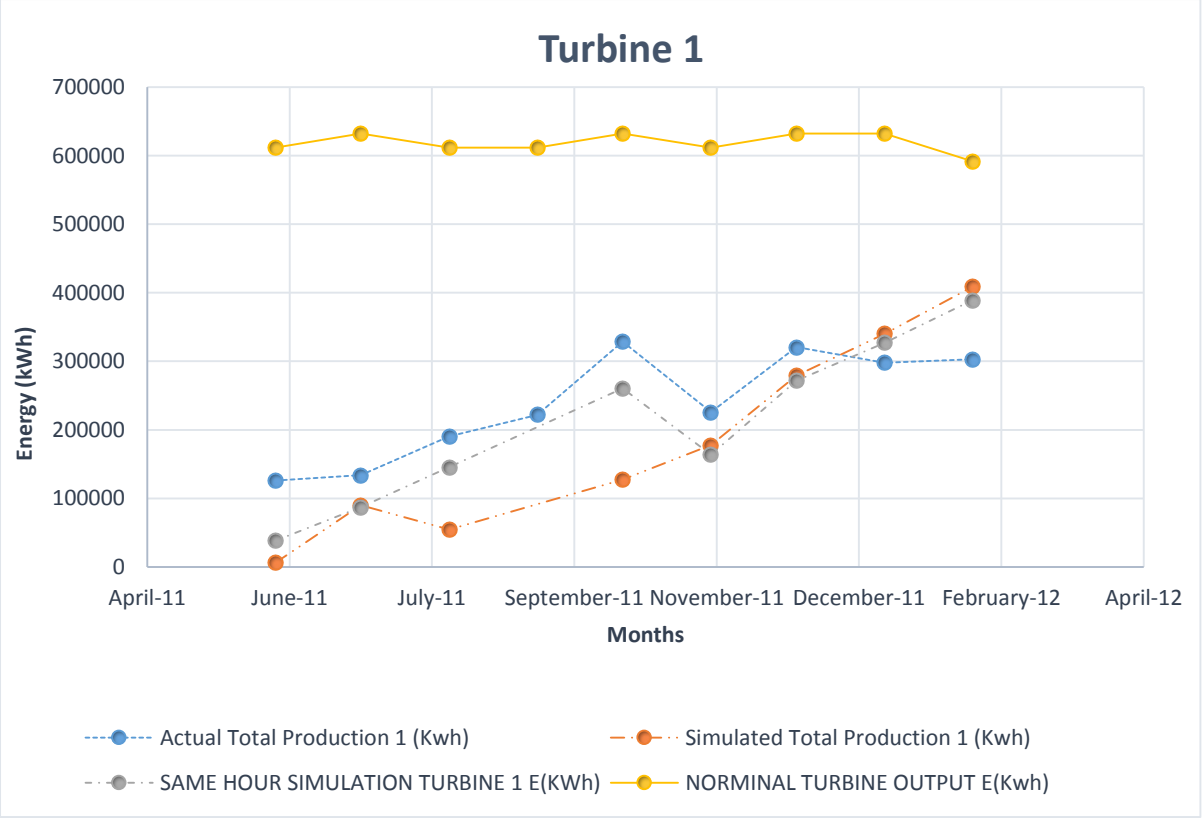

Figure 5.2 Turbine 1 Energy Output from June 2011 to February 2012

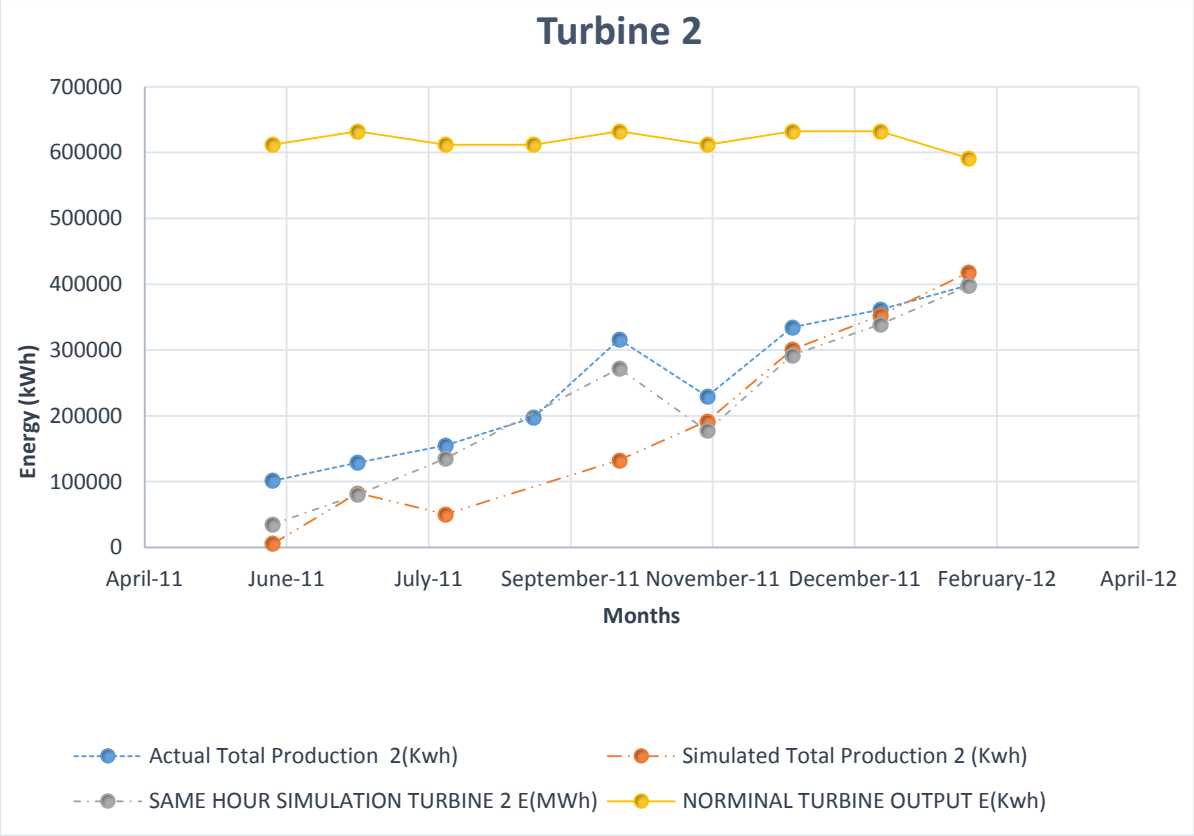

Figure 5.3 Turbine 2 Energy Output from June 2011 to February 2012

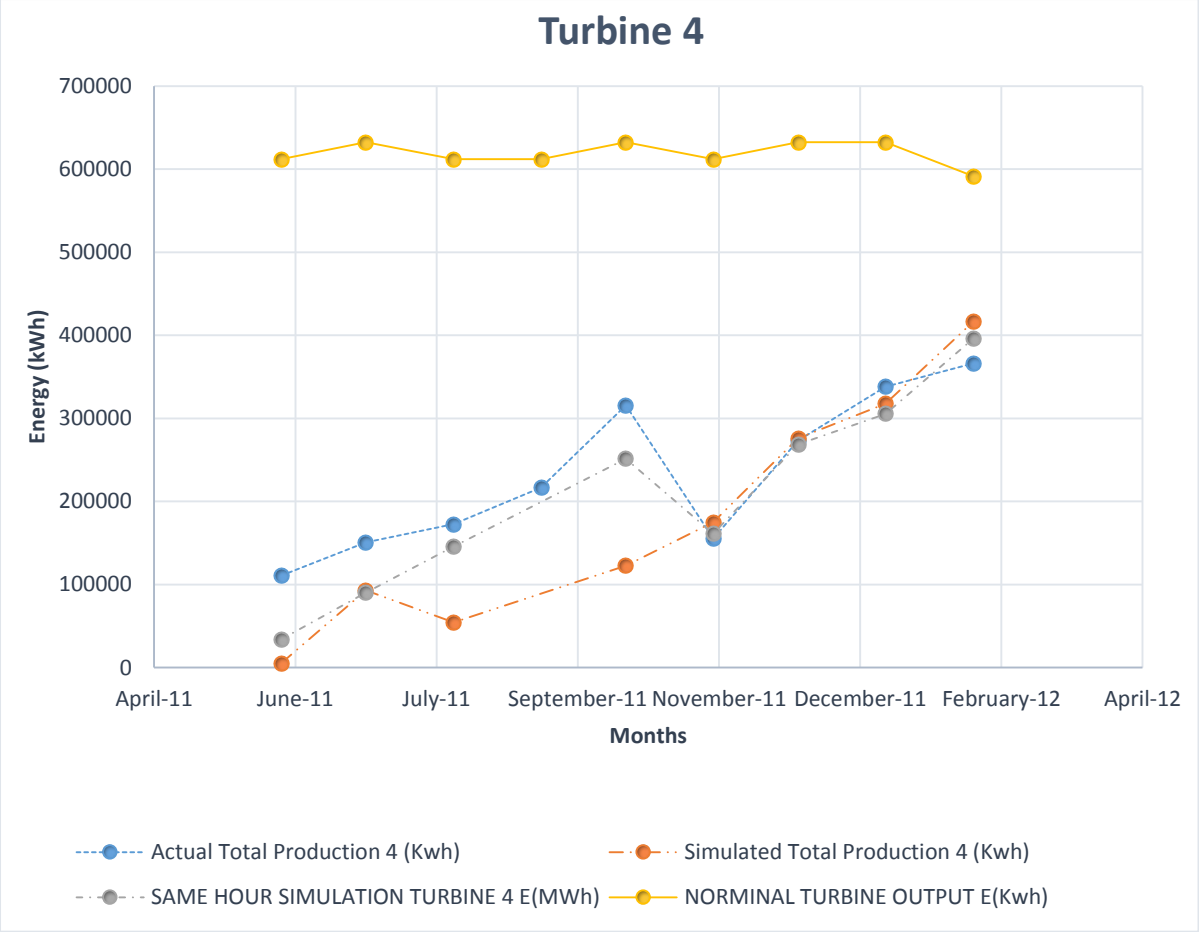

Figure 5.4 Turbine 4 Energy Output from June 2011 to February 2012

5.1 Wind Regime

Wind analysis of the three sites was done with the use of Windographer software. The three sites are Ngong, Kinangop and Turkana. The data (time series format) were sorted out to minimize errors due to instrumentation failure; all zeros and gaps. Excel spreadsheet was used to generate the respective wind power profiles. Figures 5.5 to 5.7 show the wind speeds for Ngong, Kinangop and Turkana sites for the duration of October 2011 to March 2012. As seen on the plots, the wind speeds are stochastic in nature and highly unpredictable. The general wind speed pattern in the three sites is predominantly random. Clearly, Ngong depicts more

zeros with no spikes; Kinangop depicts fewer spikes with no zeros, and Turkana depicts more spikes but with no zeros.

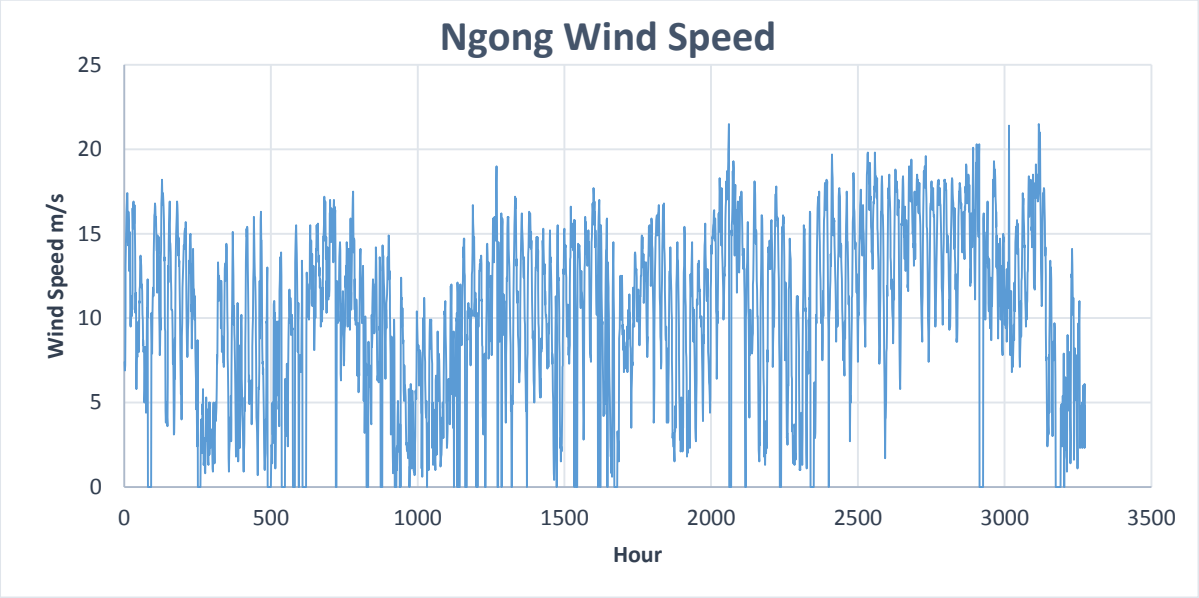

Figure 5.5 Wind speeds from Ngong from October 2011 to March 2012

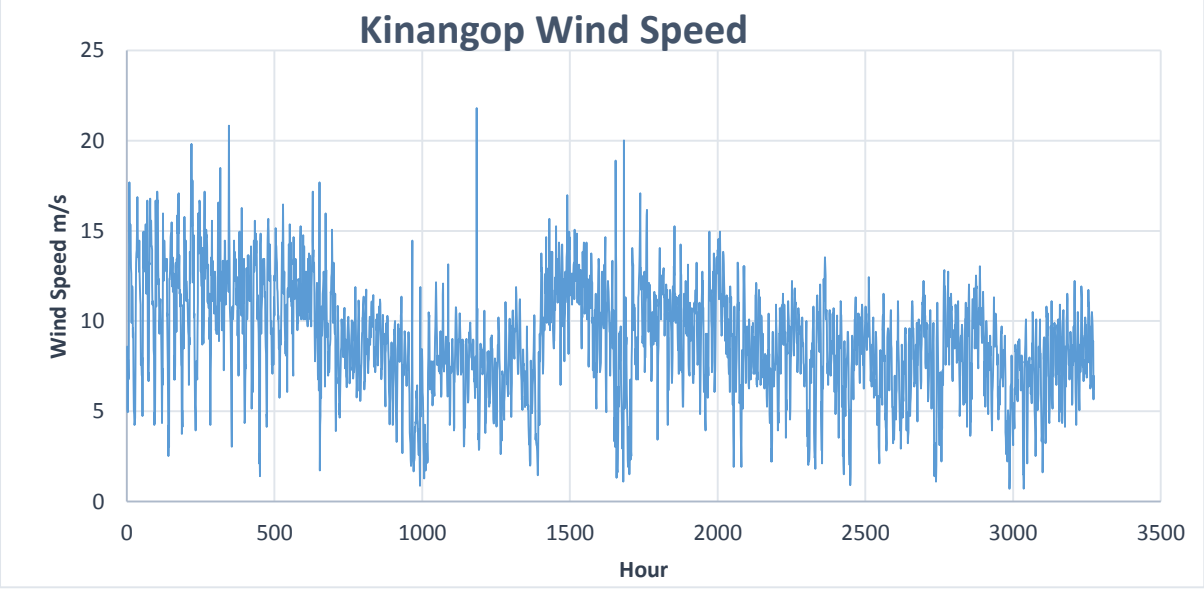

Figure 5.6 Wind speeds from Kinangop from October 2011 to March 2012

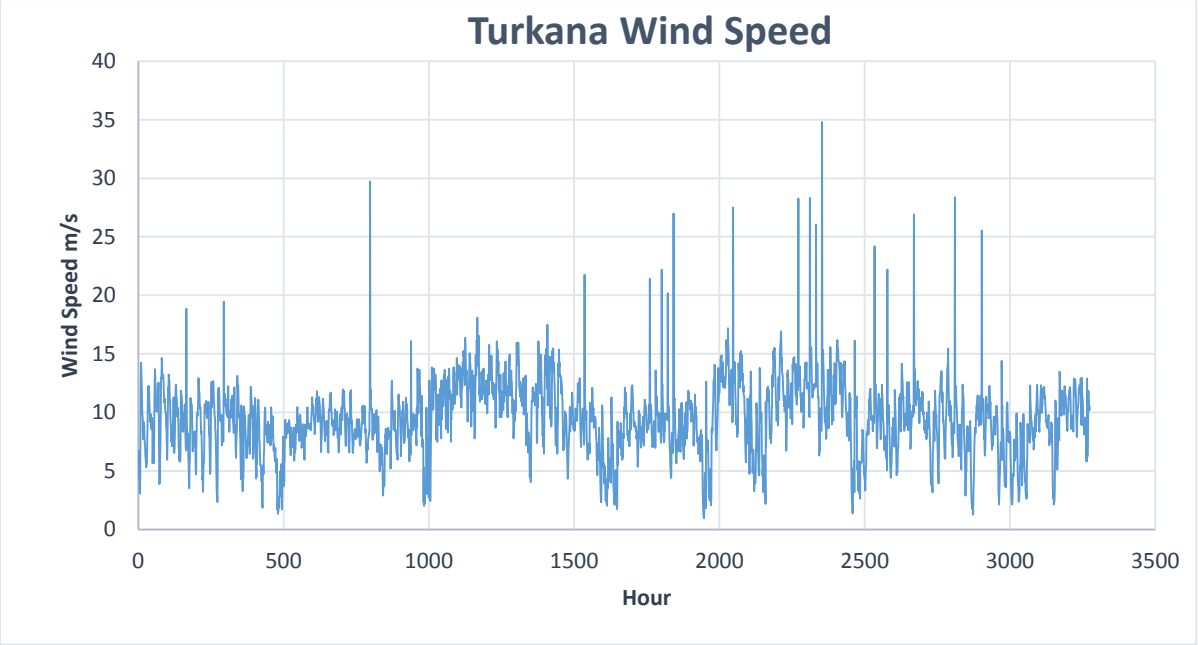

Figure 5.7 Wind speeds from Turkana from October 2011 to March 2012

5.2 Diurnal Average Wind Speed

Figures 5.8 to 5.10 show the diurnal averages for Ngong, Kinangop and Turkana from October 2011 to March 2012. December to February recorded high wind speeds. Their daily averages are between 6 and 15 m/s. October, November and March recorded low wind speeds with averages between 3 and 11 m/s. Clearly, Ngong exhibits seasonal effects in wind speeds described in section 2.1: high wind speeds correspond to dry seasons while low wind speeds wet seasons. On the contrary, Kinangop and Turkana exhibited no seasonal effects. The daily averages for Kinangop are between 6 and 10 m/s and 9 and 12 m/s respectively for the entire period.

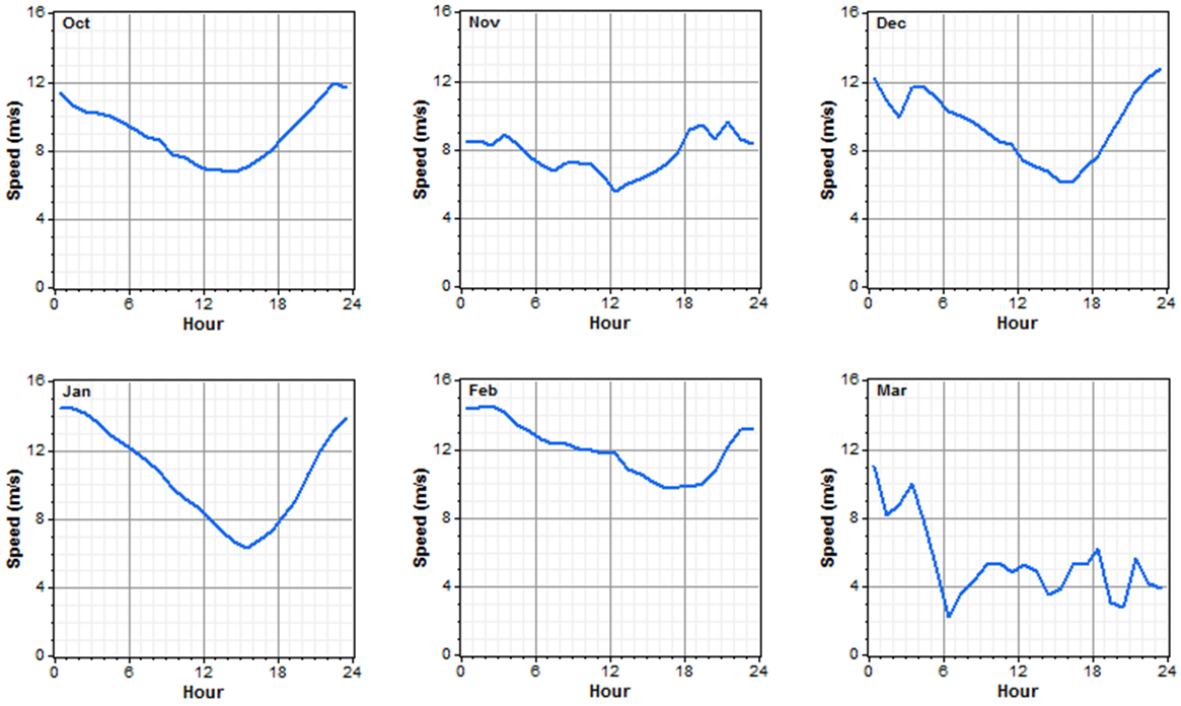

Figure 5.8 Diurnal profile for Ngong from October 2011 to March 2012

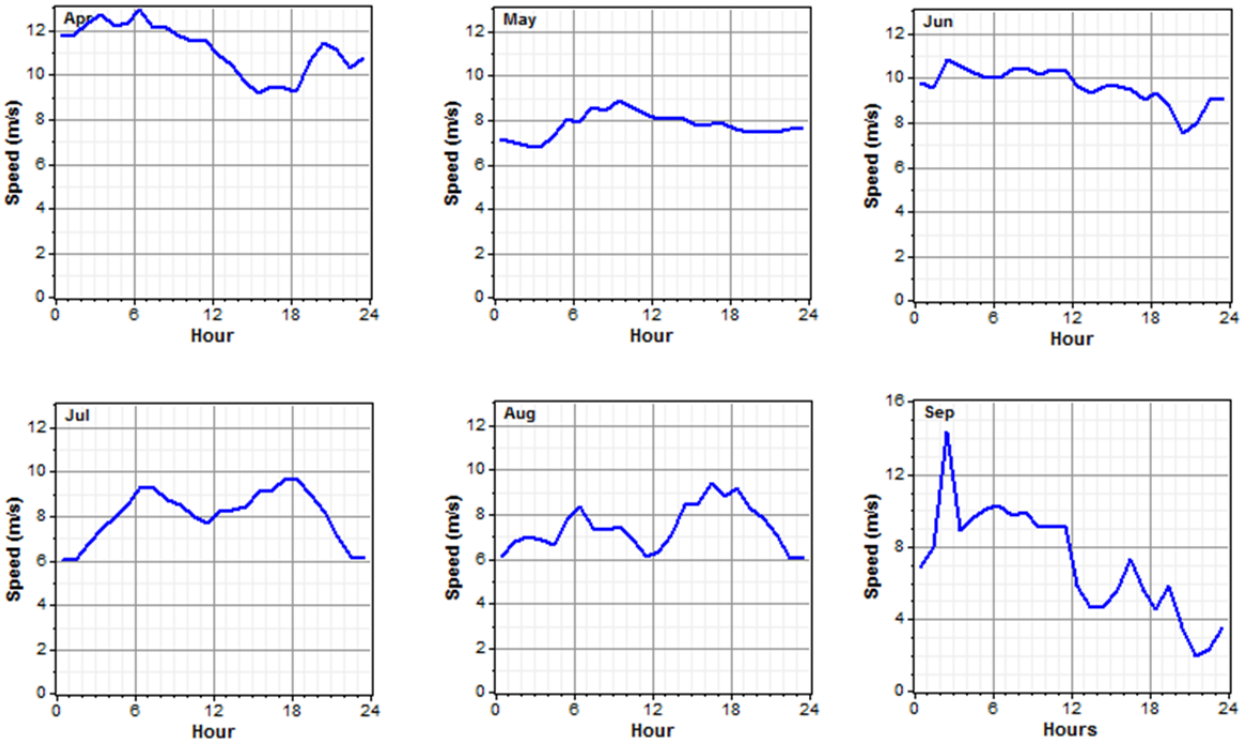

Figure 5.9 Diurnal profile for Kinangop from October 2011 to March 2012

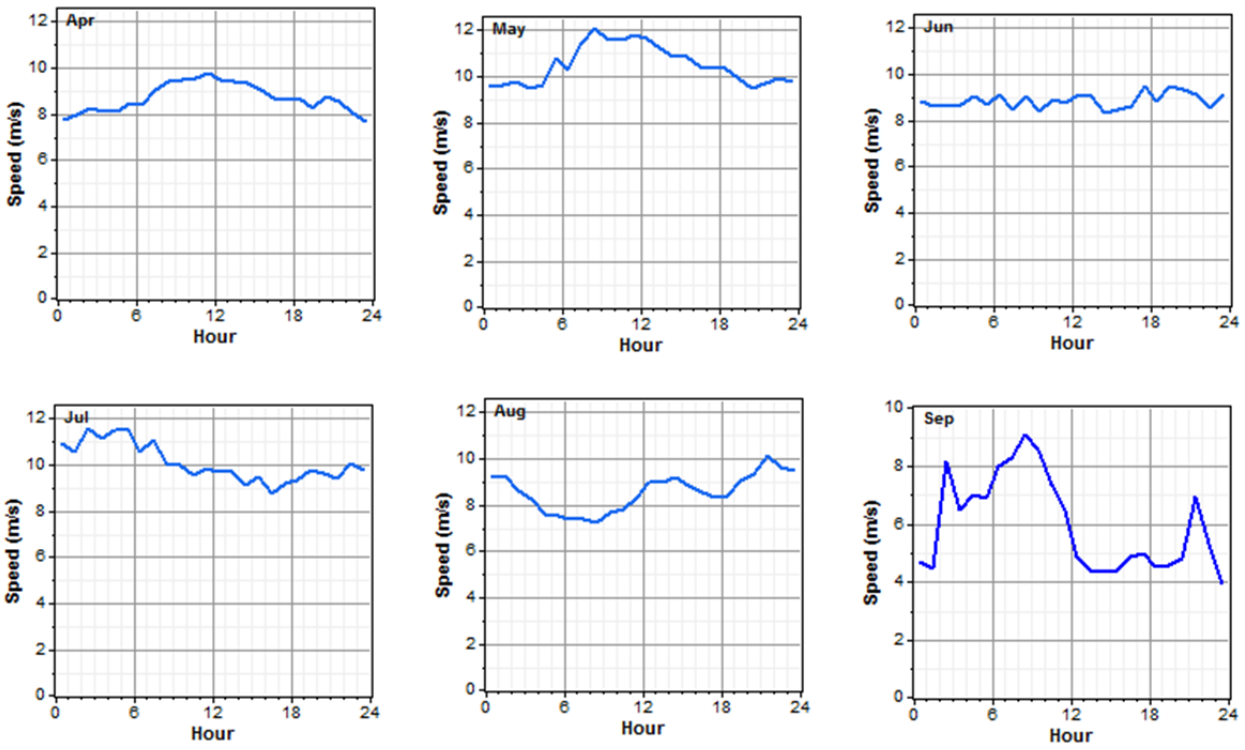

Figure 5.10 Diurnal profile for Turkana from October 2011 to March 2012

5.3 Monthly Variations

Figure 5.11 shows the statistics for Ngong from October 2011 to March 2012. The mean monthly wind speeds for Ngong are higher in January and February ranging between averages of 4 to 17 m/s and lower in October to December ranging between averages of 2 to 14 m/s.

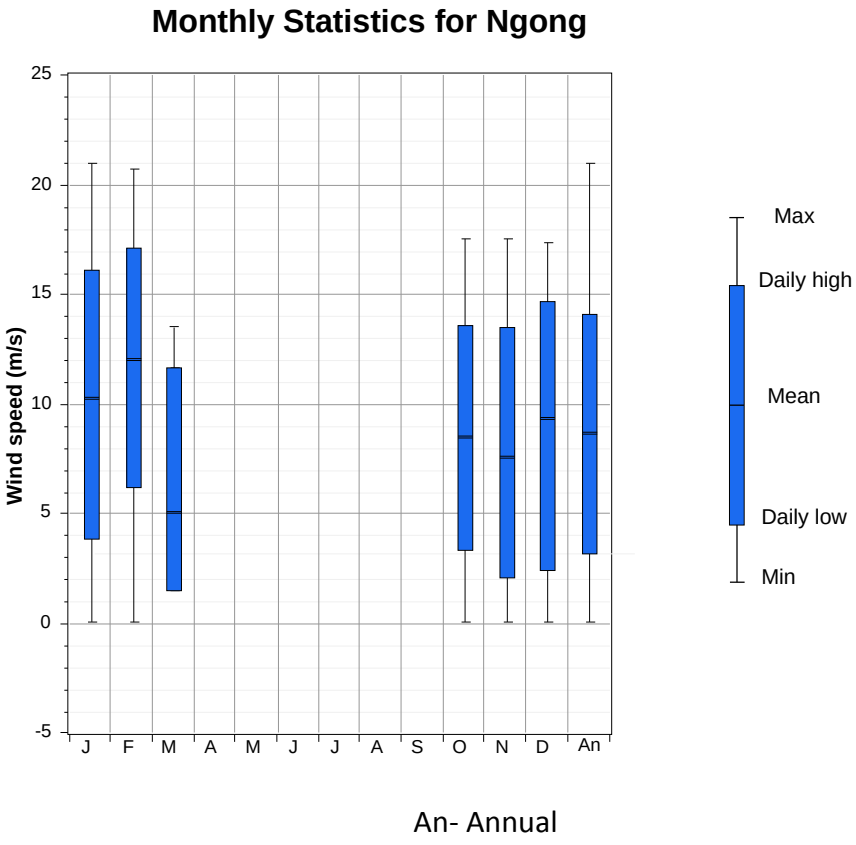

Figure 5.11 Monthly average wind speeds for Ngong from October 2011 to March 2012

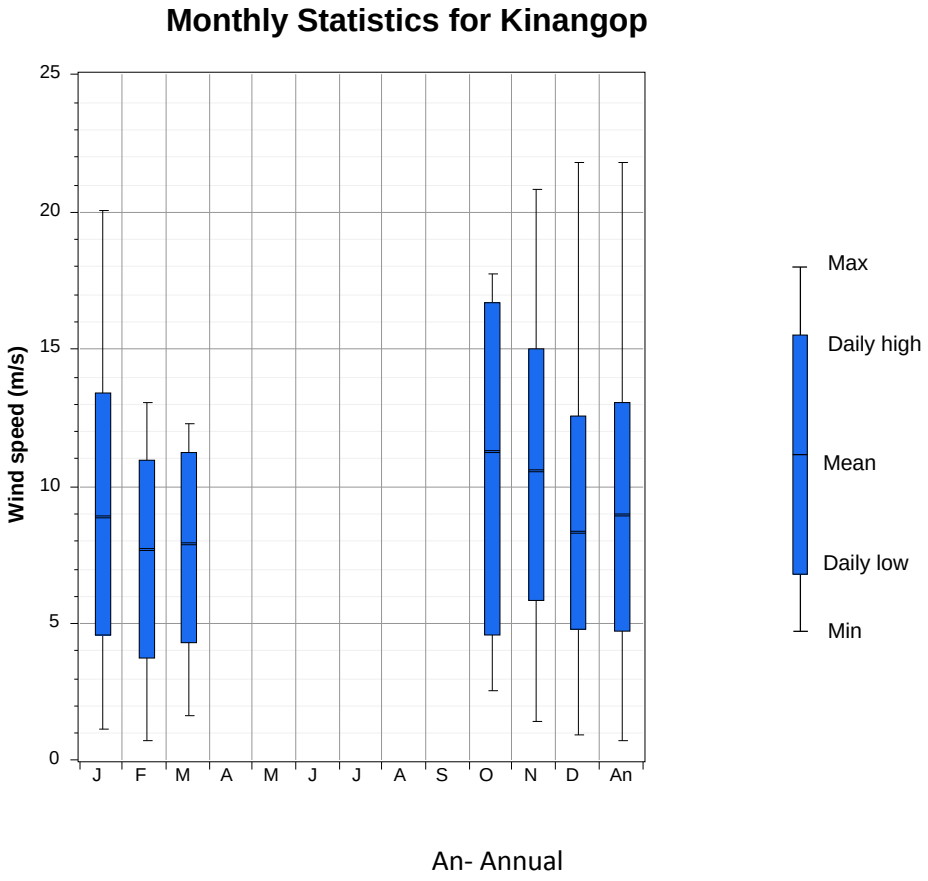

Figure 5.12 Monthly average wind speeds for Kinangop from October 2011 to March 2012

Figure 5.12 and 5.13 shows the monthly statistics for Kinangop and Turkana during from October 2011 to March 2012. Kinangop, apart from October where wind speeds ranges between 4 and 17 m/s, the rest of the month range between 4 and 15 m/s. Neglecting the spikes and zeros i.e. max and min, Turkana records the least wind speeds ranges between 6 and 15 m/s for most of the month. Daily high exceeds 15 m/s during the month of January. There is no evidence that the wind speeds in Kinangop, and Turkana do not relate to the rainy seasons. Unlike Kinangop and Turkana, Ngong experiences seasonal variations in its monthly wind speeds. As it can be seen, the wind speeds do not seem to follow any simple pattern. Therefore,

Statistical analysis of the sites wind regime will pave way for variability studies. The next sections introduce the probabilistic function that can describe its frequency of occurrence against bins of speeds ranges.

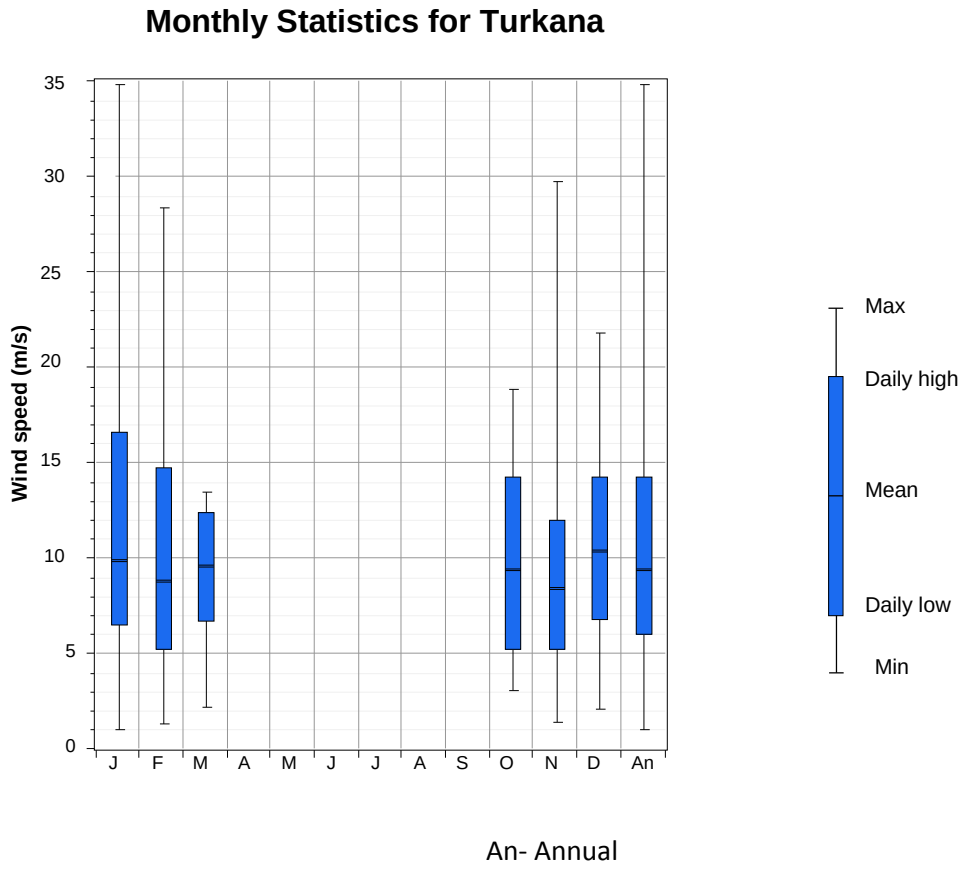

Figure 5.13 Monthly average wind speeds for Turkana from October 2011 to March 2012

5.4 The Weibull Distribution

The Weibull distribution parameters for this study have been generated using Windographer Software. Figure 5.14 shows the Weibull distribution function based on the maximum likelihood algorithm for Ngong from October 2011 to March 2012. The Weibull shape parameter k, describes the wind variability and the scale parameter c is the velocity factor. The Weibull fit for Ngong shows a leftward skew due to the high number of zeros. The shape parameters k and the speed parameters c at 50 m for Ngong are 1.67 and 9.44 m/s respectively. Despite a high mean wind speed of 11.5 m/s, the value of k is low due to the elevated standard deviation value at 6.92 m/s. The average wind speeds at Ngong range from zero to 23 m/s. This shows that Ngong has high variability. The hourly variations for Ngong exhibited can be attributed to channelling effects of wind due to the hills around Ngong.

Despite this, Ngong is still an ideal site for wind power production because of the high average wind speed. Higher wind speeds in Ngong compensate for the occasional zero outs in Ngong, especially when the wind farm size is larger Fig. 5.15 shows the Weibull distribution function based on the maximum likelihood algorithm for Kinangop from October 2011 to March 2012. The maximum likelihood Weibull fits properly because Kinangop has a near-normal distribution around the average wind speed of 8.846m/s. The value of k and c at 50 m for Kinangop are quite high at 3.36 and 9.96 m/s respectively with a low standard deviation of 2.997 m/s. Clearly, Kinangop is an ideal site for wind turbine operation because of its lower variability. However, Ngong still has the potential to produce more power per turbine because the elevated average wind speeds.

Figure 5.16 shows the Weibull distribution function based on the maximum likelihood algorithm for Turkana from October 2011 to March 2012. Turkana exhibits the highest variability of the three sites. The maximum Likelihood Weibull does not fit properly because of the high wind speed range of 3 to 35 m/s and lower values of k and c at 0.84 and 9.33m/s respectively. Despite this, Turkana is still an ideal site for wind power production because of its high average wind speeds of 9.43m/s.

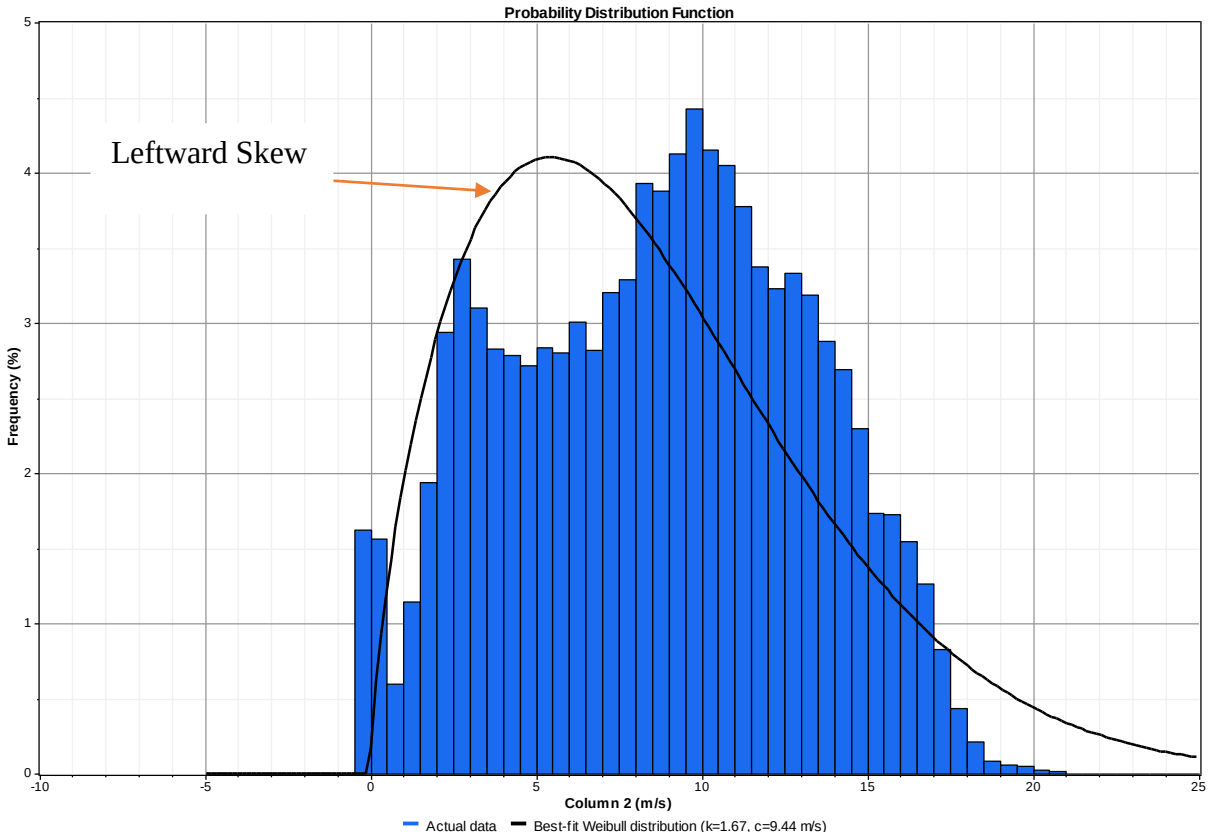

Figure 5.14 Probability Distribution for Ngong from October 2011 to March 2012.

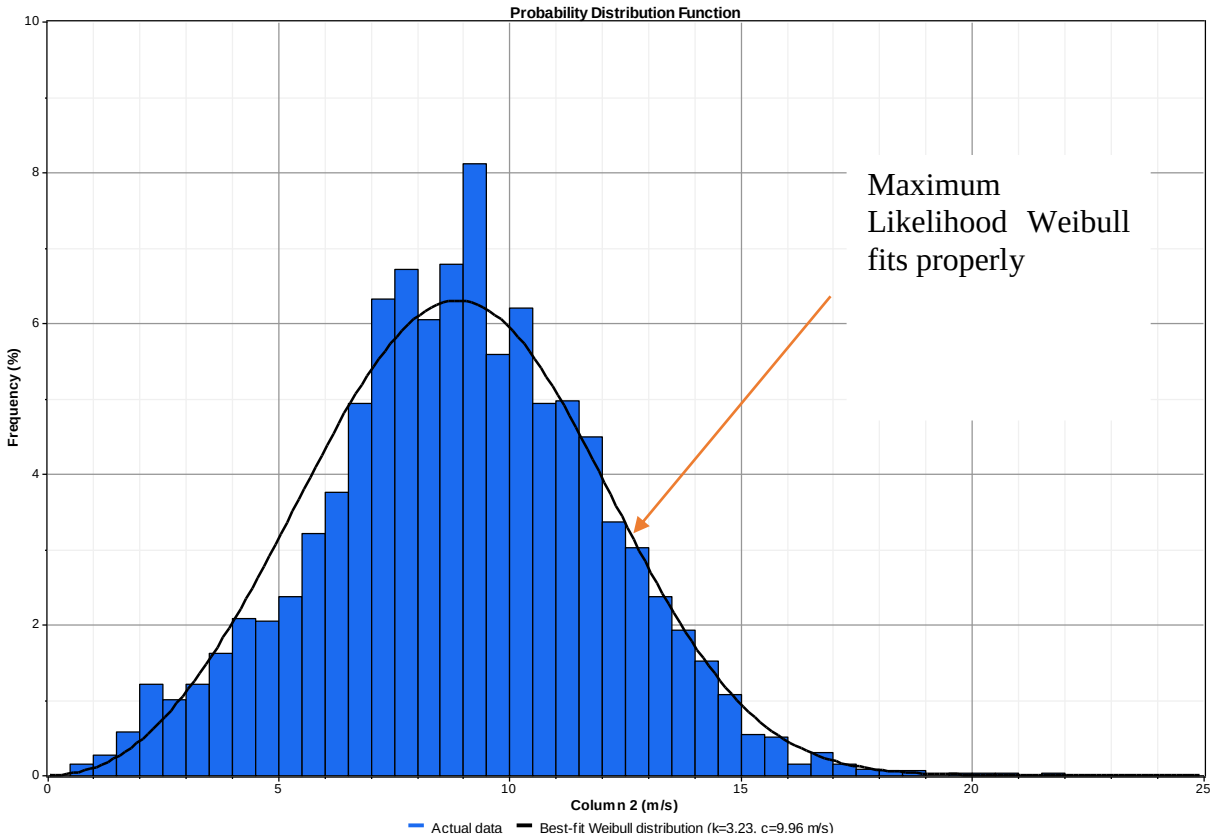

Figure 5.15 Probability Distribution for Kinangop from October 2011 to March 2012.

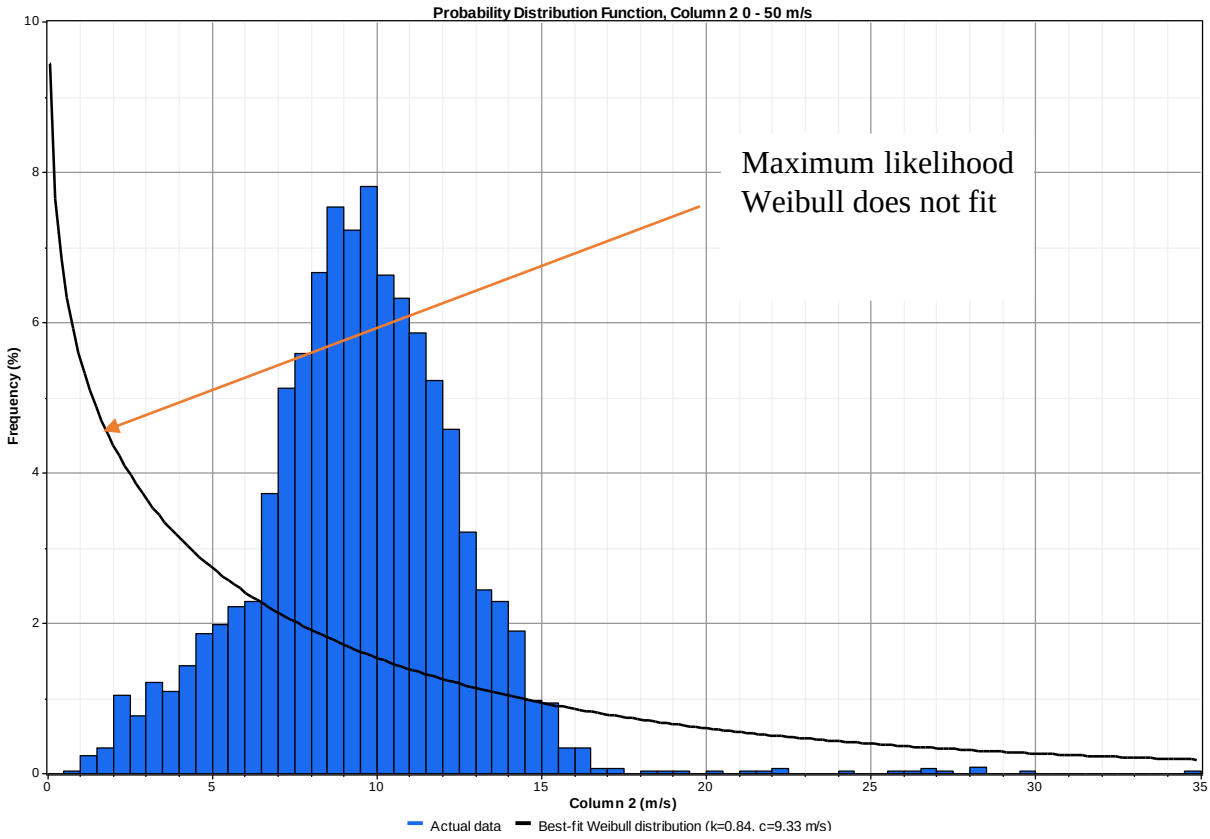

Figure 5.16 Probability Distribution for Ngong from October 2011 to March 2012.

5.6 Wind Power Production.

The wind farm model (seen Figure 3.1) was used to generate wind production data for analysis. These data were loaded with Microsoft Excel to generate respective wind power profiles. Figures 5.17 to 5.19 show the hourly productions for Ngong, Kinangop and Turkana from October 2011 to March 2012. The wind production patterns on the three sites are similar to their wind speed. However, the spikes and zeros seen in their respective wind speeds tend to disappear due to smoothing effect. The turbine outputs are not correlated therefore largely balance out each other. As a result, the maximum amplitudes of wind power fluctuations experienced in a site are reduced.

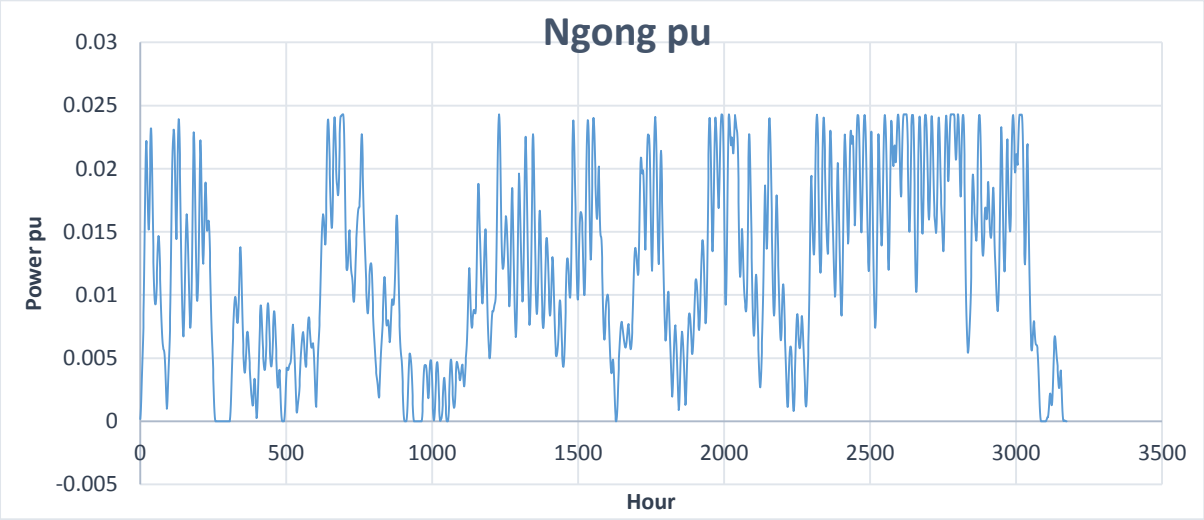

Figure 5.17 Wind power production for Ngong from October 2011 to March 2012.

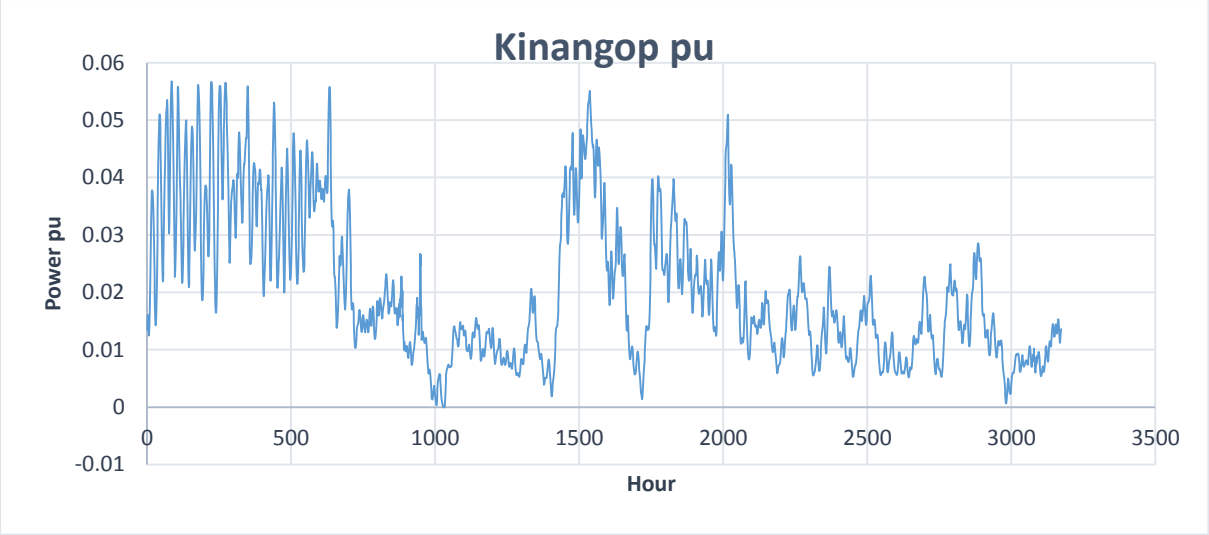

Figure 5.18 Wind power production for Kinangop from October 2011 to March 2012.

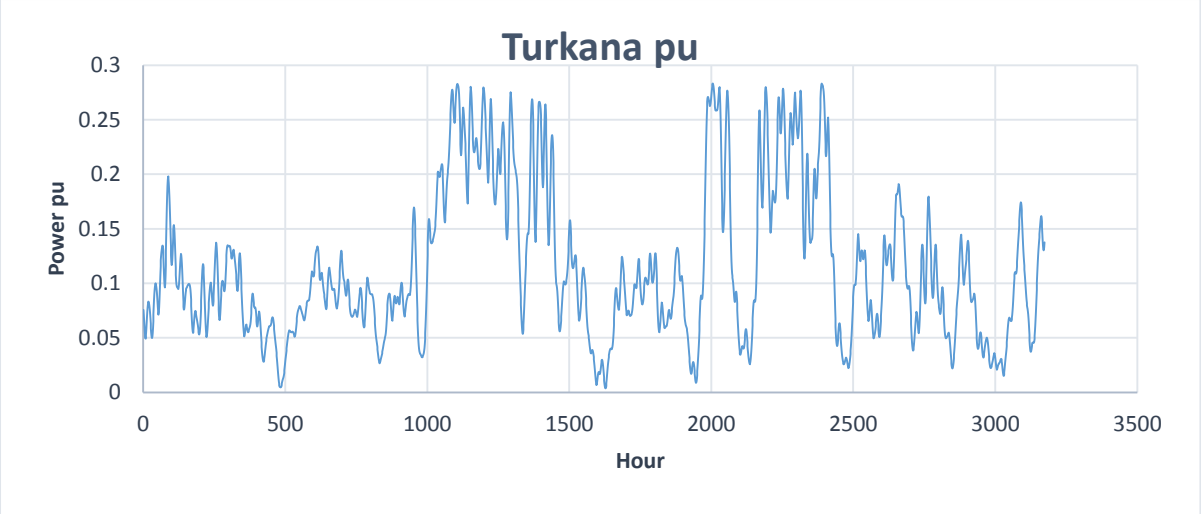

Figure 5.19 Wind power production for Turkana from October 2011 to March 2012.

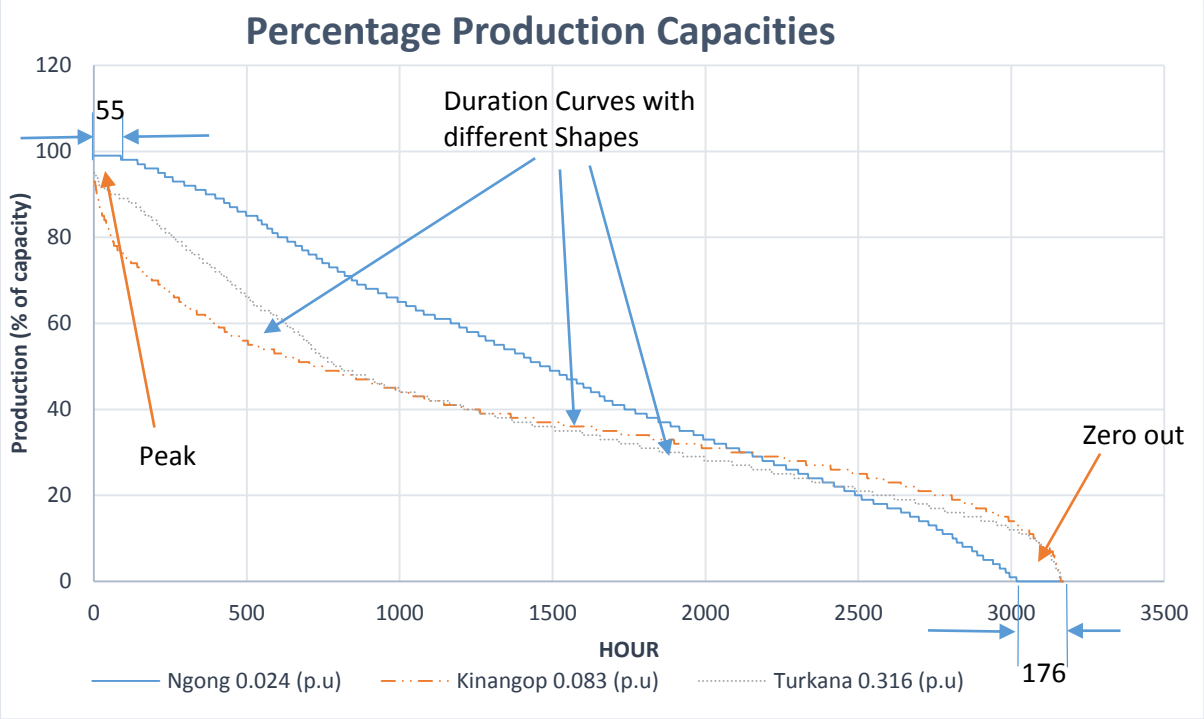

Figure 5.20 Duration plot for the percentage production capacities at different penetration levels from Oct 2011 to Nov 2012.

One method of representing the smoothing effect of aggregation on system scale is the load duration curve of wind farms, which gives the frequency distribution of the partial load states of generated wind power. Fig. 5.20 shows the wind-power production (percentage of peak load) for Ngong, Kinangop and Turkana. The solid line, the dash and the dash in the plot show the respectively duration curves for Ngong, Kinangop and Turkana. Each duration plot has been derived from the respective wind production plots rearranged chronologically from maximum to minimum. No single point on these duration curves represents a time instant; the difference between two points on the plot represents time duration. The turbines are likely to be shut down because of low or high wind speeds. A typical cut-off speed for modern turbines is 4 m/s. The turbine will shuts down and stops producing energy at speeds below the cut-off speed. The results to a phenomenal referred to as zero out, and is represented in Fig 5.20 by 0% in wind

production (percentage of capacity). Peak production, a phenomenal where all the turbines produce at their rated capacities is represented by 100% in wind production. The duration curves for Ngong depicts peaks for 55 hours and zeros for 176 hours. In contrast, the duration curve for Kinangop and Turkana show no peaks at all; zero's outs occur in single instances. Kinangop (0.058 Pu) and Turkana (0.292 Pu) have higher production capacities compared to of Ngong (0.024 Pu). The variations in Kinangop are the least, concentrated between 20 and 60%; Turkana is concentrated between 20 and 80%; and Ngong is evenly distributed from zero to 100%. Ngong has a small wind farm size compared to Kinangop and Turkana. This shows that the number of hours with zero out diminishes, while the maximum value of instantaneous aggregated power produced is decreasing when wind power aggregated over a large area.

5.7 Wind Power Variations

The wind-power variability may increase or reduce that of the whole system. Wind production data from underlying Figures 5.17 to 5.19 was used for assessing power variations i.e. the differences between consecutive time steps. The positive and negative power variations were further sorted in the order of reducing magnitude. The results were then plotted chronologically and sequentially as shown in Figures 5.21 to 5.23. The corresponding wind power variations and the standard deviation σ_w (determined as a percentage of the P_{nom}) are characterized by the statistics presented in Table 5.1. Where max up variations and max up, variation is the extent of the hourly wind variations; P_{nom} is the production capacity of the wind farm; and the wind standard deviation σ_w is the variability the site. As seen from these results, the respective values wind power fluctuations, for Ngong Kinangop and Turkana are 3.45, 2.47 and 1.7 percent of rated power. Ngong has penetration levels of 0.24 Pu; corresponding to 30 turbines, Kinangop has a penetration level of 0.058 corresponding to 70 turbines while Turkana with penetration levels of 0.292 Pu corresponding to 353 turbines. This indicates that as the number of turbines in a site increase the site wind variability reduces.

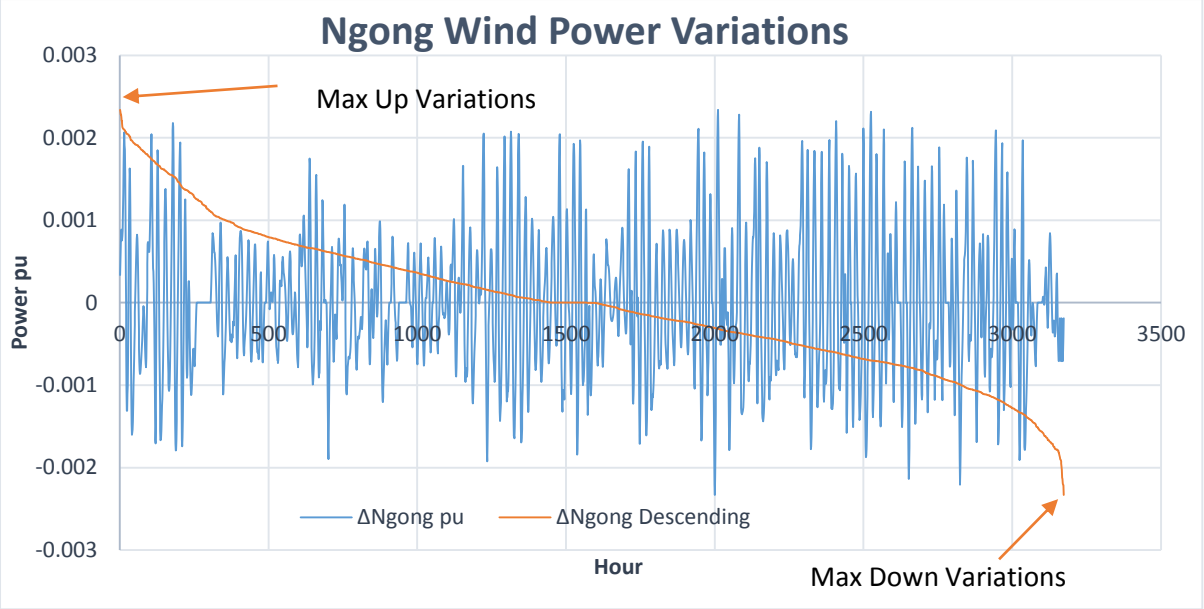

Figure 5.21 Hourly wind variations for Ngong from October 2011 to March 2012.

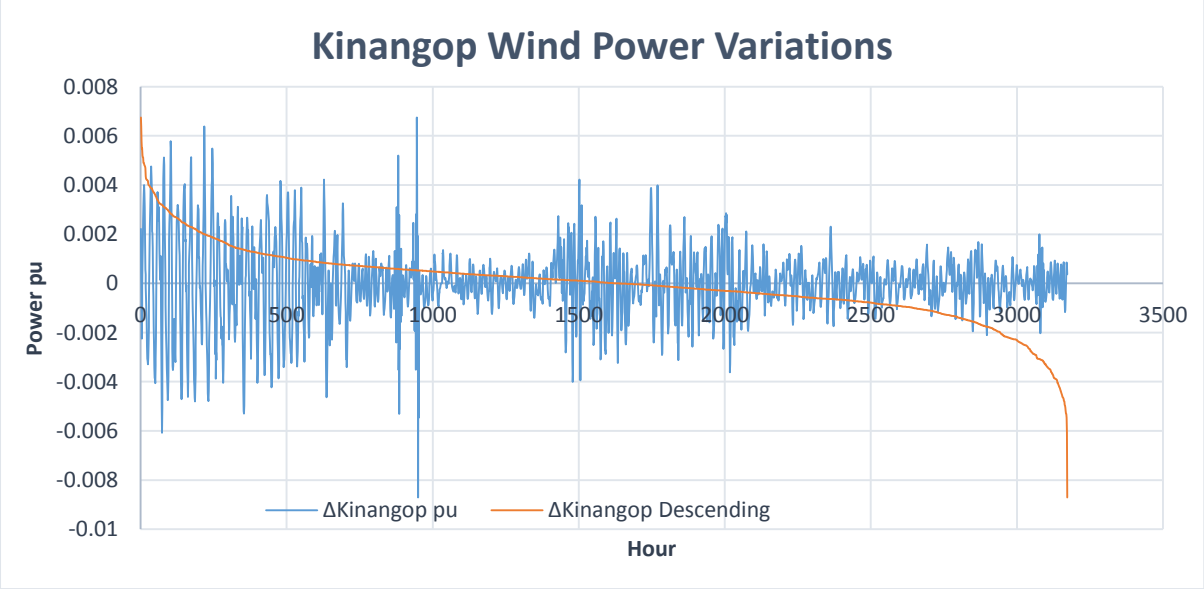

Figure 5.22 Hourly wind variations for Kinangop from October 2011 to March 2012.

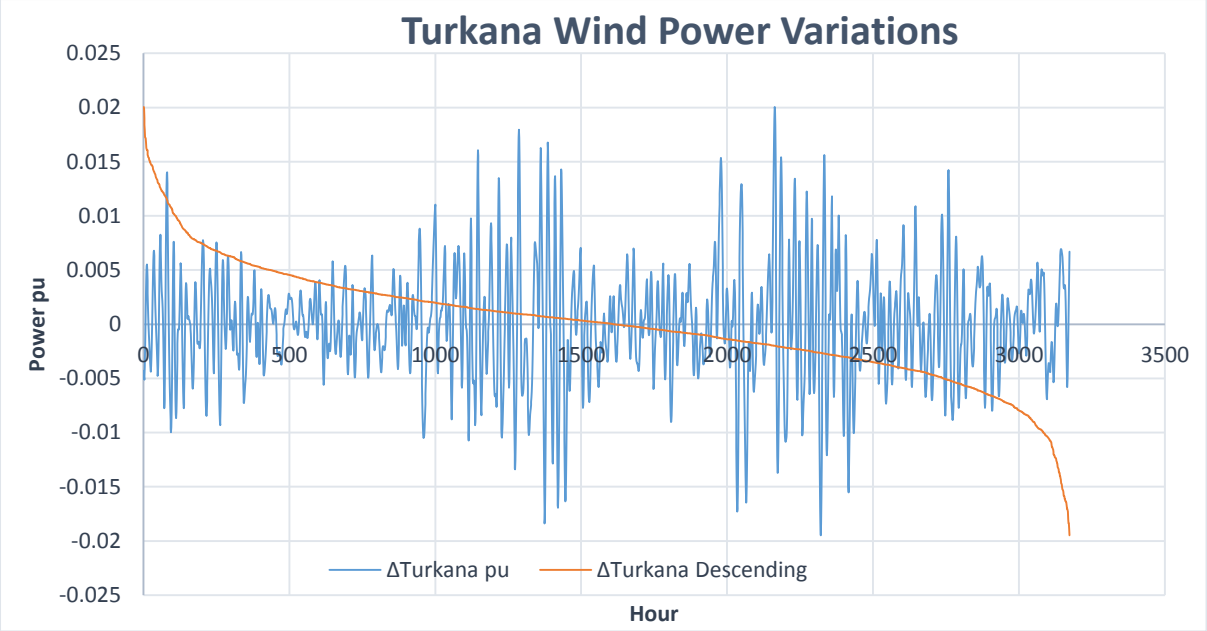

Figure 5.23 Hourly wind variations for Turkana from October 2011 to March 2012.

Table 5.1 Results for hourly wind variations for Ngong, Kinangop and Turkana from October 2011 to March 2012.

Statistics	Ngong	Kinangop	Turkana
P_{nom}	0.024 Pu	0.058 Pu	0.292 Pu
Wind Max-Up Variations	0.0023 Pu	0.0067 Pu	0.0201 Pu
Wind Max-Down Variations	-0.0023 Pu	-0.0136 Pu	-0.0194 Pu
Wind Standard Deviation σw (% P_{nom})	3.4536 Pu	2.4708 Pu	1.7493 Pu

5.8 Kenya Load Profile

Historical data (covering 30 minutes) from June 2008 to November 2008 was processed in excel to calculate the hourly average loads from October 2011 to March 2012. Fig. 5.24 shows the generated time series for the electricity consumption in Kenya from October 2011 to March 2012. The solid line shows the electricity consumption for Kenya and the dashed line shows the trend. Clearly, the pattern of electricity consumption in Kenya from October 2011 to March 2012 is consistent, varying from a minimum of 0.3560 Pu to a maximum of one Pu. The electricity consumption for Kenya increases annually at a rate of 0.26298 Pu. Fig. 5.25 shows the 24 hours extract of the electricity consumption divided into weekdays and weekend days. The dashed line shows the plot for Sunday (weekend) while the solid line shows the plot for Monday (weekday). The different characteristics of electric load by daily pattern are noticeable, with a higher on weekdays than weekend. The off-peak load hours start from 00:00 to 07:00hrs and 23:00hrs up to 24:00hrs while the hours in between peak hours. This shows that load peaks occur during the day whereas the off peaks during the night.

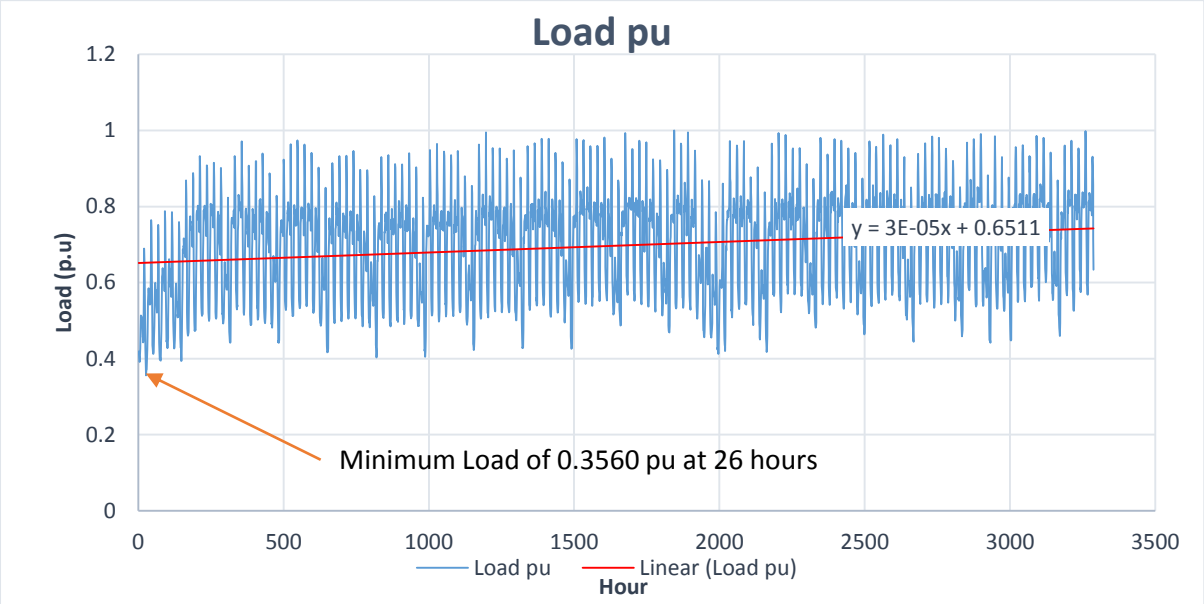

Figure 5.24 Hourly Load of Kenya from October 2011 to March 2012, chronologically and duration curve.

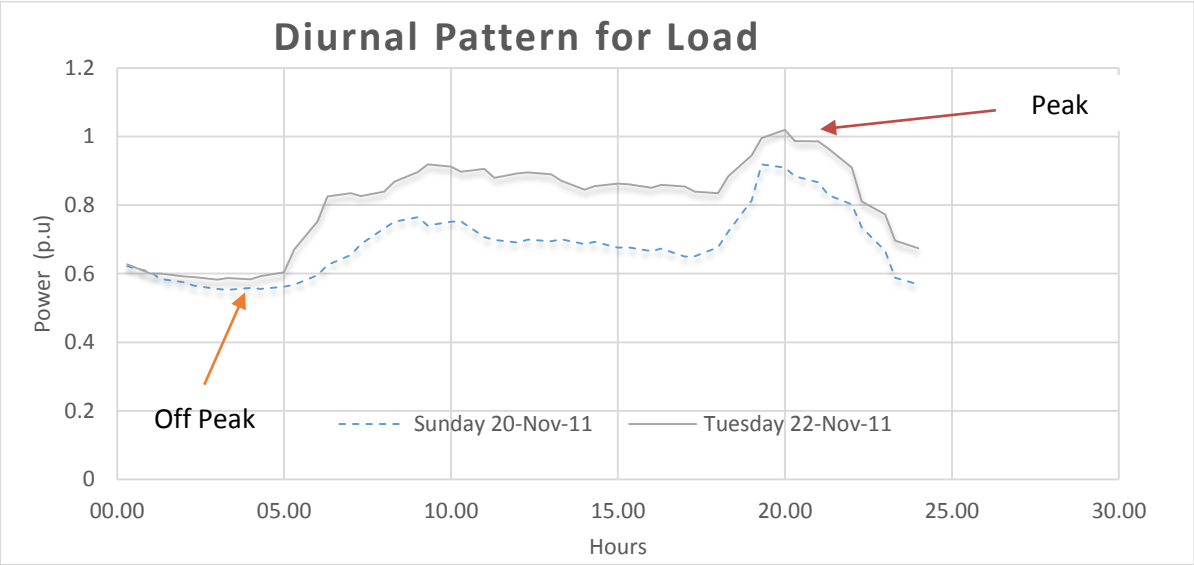

Figure 5.25 The comparison of Kenya's hourly load during the first week of June 2011

5.9 The Load Variations

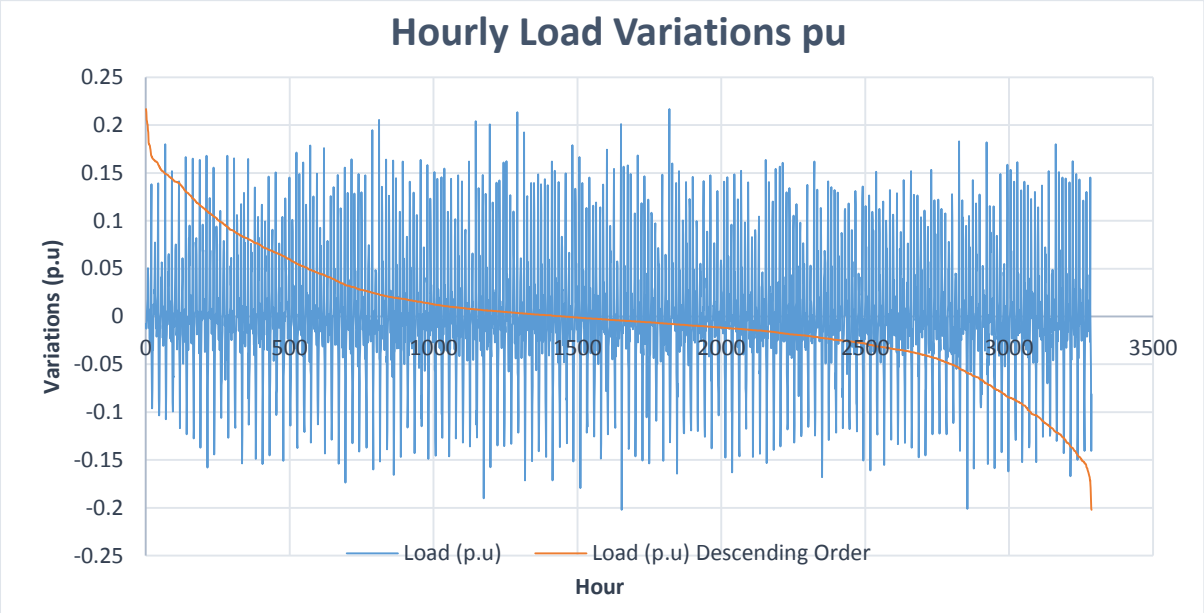

Figure 5.26 Hourly load variations in Kenya from October 2011 to March 2012.

Fig. 5.26 shows the hourly load variations for Kenya from October 2011 to March 2012. The load variations were assessed from the consecutive hourly difference in the actual the electricity consumption shown in Figure 5.24. The corresponding hourly load variations are characterized by the statistics presented in Table 5.2. On both the max up variation, the max down variations and the standard deviation, the extent and variability of load is obvious. Comparing Tables 5.1 and 5.2, clearly the system demand variations dominate and surpasses wind variability even as penetration levels reach 0.374 Pu.

Table 5.2 Results for hourly load variations for Kenya from October 2011 to March 2012.

Statistics	
Load Max-Up Variations	0.217 Pu
Load Max-Down Variations	0.202 Pu
Load Standard Deviation σl	6.216 Pu

5.10 The Net Load Variations

Wind power variations and load variations must be considered in combination create a counterbalance effect. The counterbalance between the two may reduce of increase the overall system variations. The coincidence of wind generation with the load and the coincident change in load are very important as their combination determines the rate of change of the operation reserve. Figure 5.27 shows duration curves for the net hourly variations individually sorted, based on five different scenarios. The gap between the duration curves for load and net load indicates the amount of operating reserve required for the curtailment of the net load variations. Comparing the gap the duration curves, there is no sufficient evidence that additional wind generation results in the need for additional operating reserve. The size of operating reserve required for Ngong phase I and II with Kinangop (0.083 Pu) exceeds that of Ngong phase I and II with Turkana (0.316 Pu) despite the contrast in wind penetration levels. The same result is also seen when comparing Ngong phase II and I (0.024 Pu) with Kinangop (0.083 Pu) or Ngong phase II and I (0.024 Pu) with Turkana (0.316 Pu).

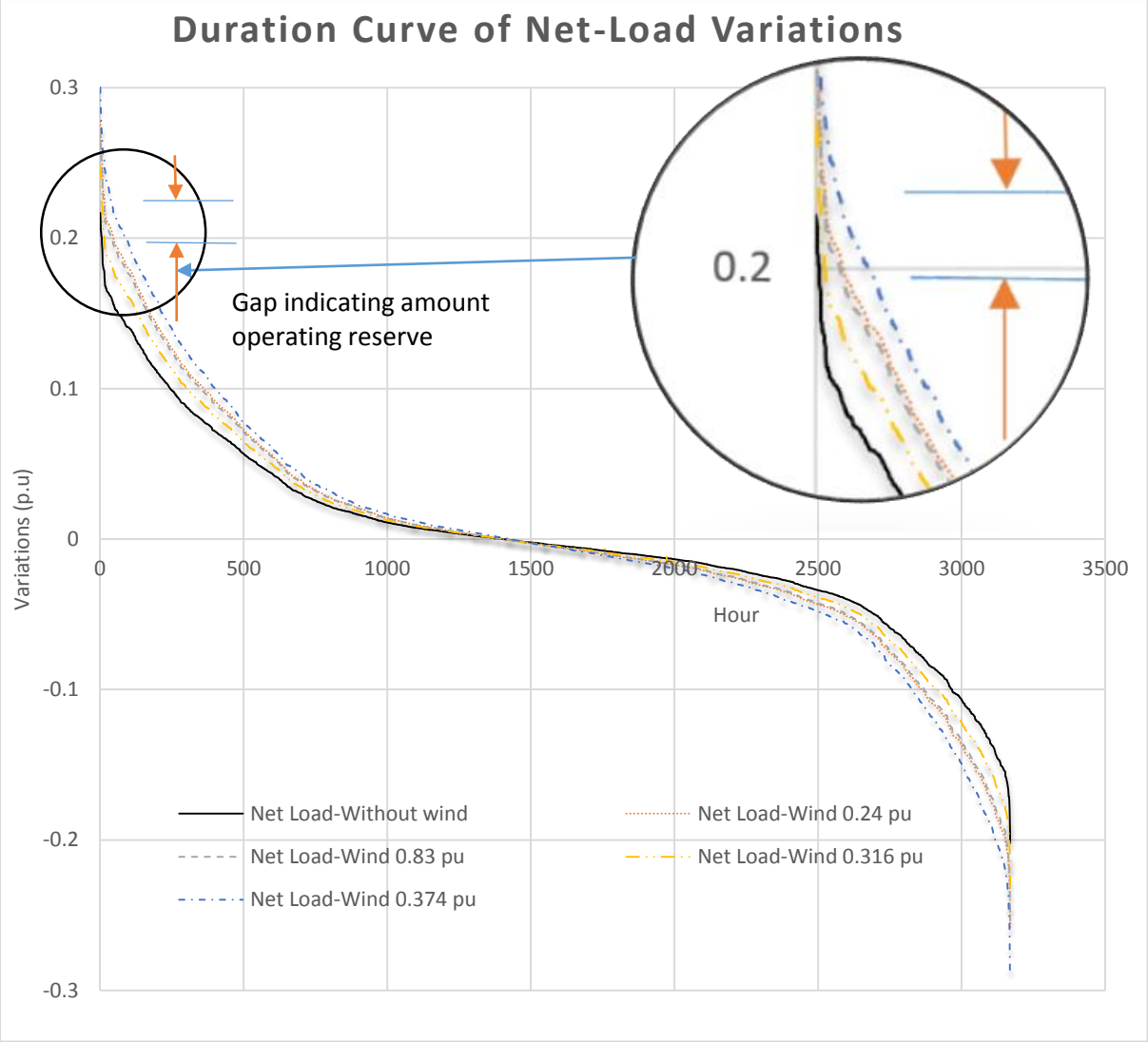

Figure 5.27 Duration curve of load variations (without wind power) and net load variations (load minus wind power).

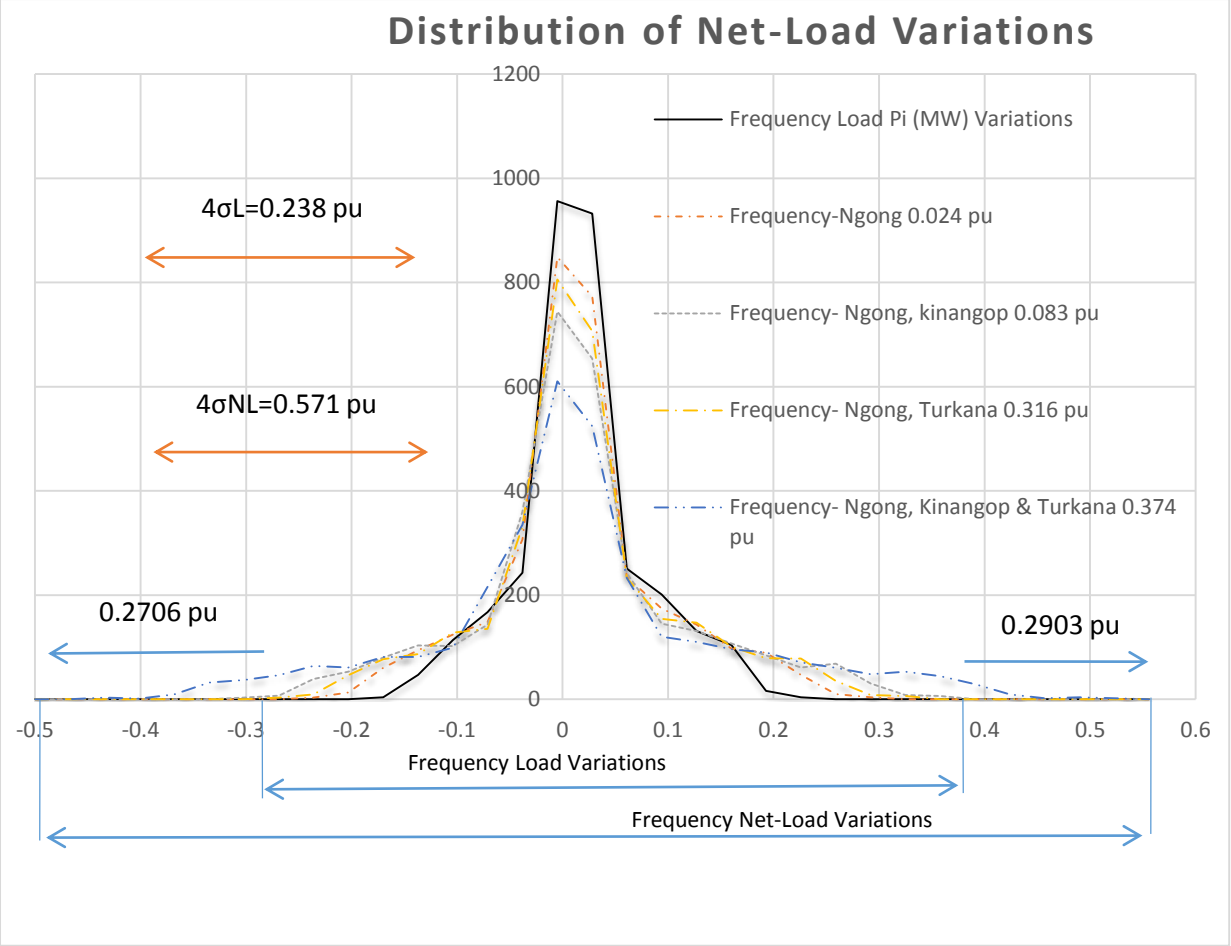

Figure 5.28 Frequency distribution for load at different penetration using distinct site data.

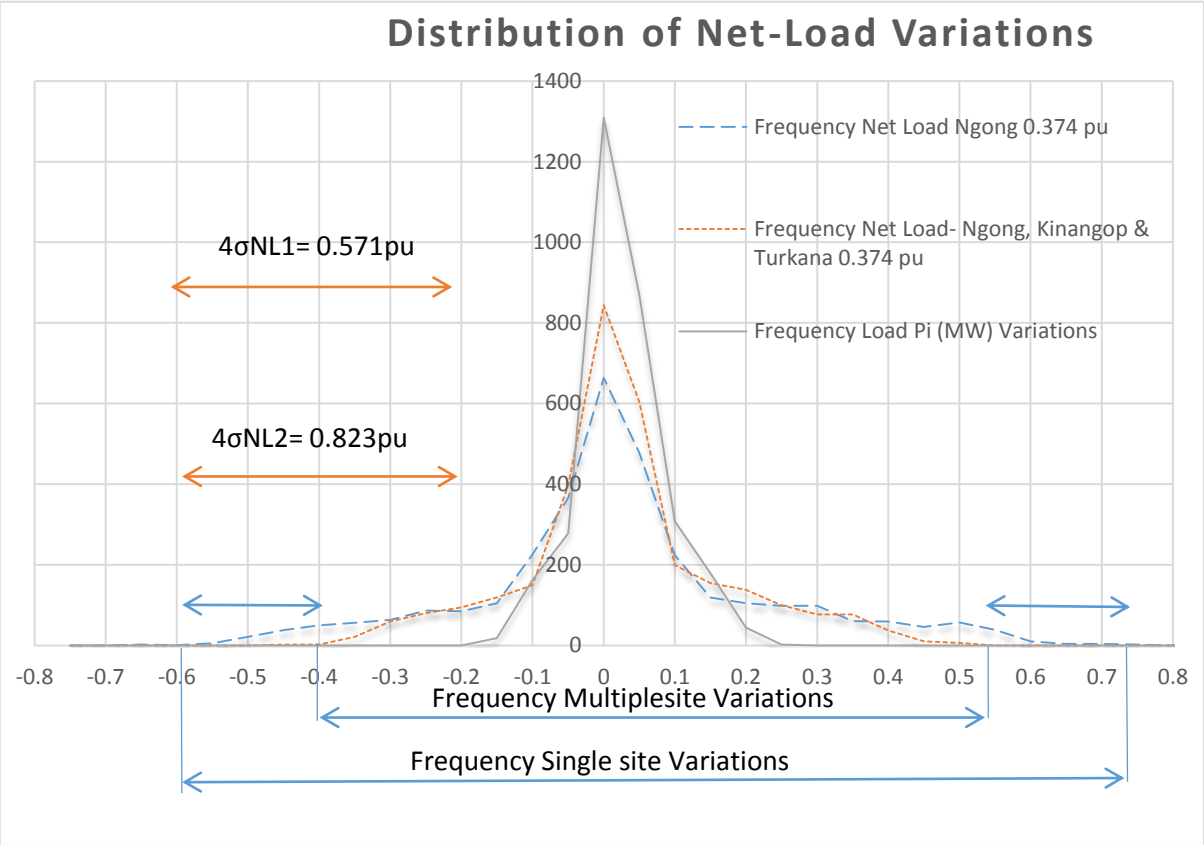

Figure 5.29 Frequency distribution for load at different penetration using different site data.

The frequency distribution of the system variations due to additional varying wind resources are presented in Fig. 5.28 and 5.29. The distributions were determined to a confidence level of 99.99 percent(4σ) of the hourly variations. The corresponding hourly load variations are characterized by the statistics presented in Table 5.3. The normalized distributions of Net hourly variations are shown in Appendix 3. The overall impact of Kenya's 2015 wind power expectations and the statistical nature of net load variations can be seen from these plots. The frequency distribution is generally normal with slight variance on the extremes. Note that the wider the distribution is the higher the variability in a site i.e. load only scenario has the lowest variability.

The relationship between the wind penetration levels and the frequency of the net variations is also not symmetrical. The standard deviation of the load only variations from October 2011 to March 2012 is 0.060 Pu. When Ngong phase I and II is added to the power system the standard deviation (σ) increases from 0.060 Pu to 0.080 Pu (an increase of 0.020 Pu). The standard deviation increases from 0.080 Pu to 0.102 Pu (an increase of 0.022 Pu) when Kinangop is added to the mix, consistent with the expectation based on 4σ. The standard deviation increases from 0.080 Pu to 0.091 Pu (an increase of 0.010 Pu) when Ngong phase I and II with Kinangop is replaced by Ngong phase I and II with Turkana, The standard deviations for Ngong phase I and II with Kinangop surpass Ngong phase I and II with Turkana by 0.011 Pu, despite having lower penetrations. These findings show the effect of the wind resource mix to the net variation and contradict the expectation based on 4σ. The coincidence between the maximum and the minimum output from individual sites has an impact to the aggregate output in which wind variability is derived. The correlation between Ngong and Kinangop surpass those of Ngong and Turkana despite its small wind farm size. The strong correlation between Ngong and Kinangop is a result of the near simultaneous occurrence of lower wind power fluctuations. Conversely, the weak correlation between Ngong and Turkana is attributed to the balance effect between the high fluctuations. The aggregation of Ngong phase I and II with Turkana by 0.011 Pu significantly reduces the possible imbalance within one hour. Hence, the impact of site correlations outstrips that of wind farm size.

The maximum net system variations distributions can be seen at the tails of the events. For load without wind scenario, the maximum variation from October 2011 to March 2012 is at 0.208 Pu. When Ngong phase II and I is added to the power system the standard deviation increases from 0.208 Pu to 0.0278 Pu (an increase of 0.070 Pu). When Kinangop is added to the mix, the

maximum variations in the system further increases from 0.278 Pu to 0.356 Pu (an increase of 0.078 Pu). This is consistent with the expectation based on 4σ. When the combination of Ngong phase I and II with Kinangop is replaced by that of Ngong phase I and II with Turkana the maximum variations increases by a lesser value of 0.278 Pu to 0.317 Pu (an increase of 0.039 Pu). The maximum variations for Ngong phase I and II with Kinangop surpass Ngong phase I and II with Turkana by 0.039 Pu, despite having lower penetrations contradicting the expectation based on 4σ. This can be attributed to the low correlation of production from different sites. The peaks in the power system reduce due to smoothing effect of wind power production from larger areas, thus lowering the net system variability.

Considering scenarios with the same wind penetration levels but with different wind mix, the variations for scenarios 5: combination of Ngong phase I and II with Kinangop and Turkana (0.374 Pu) is compared to that of scenario 6: Ngong wind farm up-scaled up to (0.374 Pu). The maximum variations differs by 0.821 Pu, yet both scenarios have penetration levels 0.374 Pu. This also contradicts the linearity in 4σ expectations and further demonstrate the impact of site interconnectivity into a power system. The wind resources in scenarios 5 a combination of three wind sites are well interconnected unlike scenario 6 that comprises of a single farm. Site interconnection causes smoothing effect resulting lesser need for operating reserves.

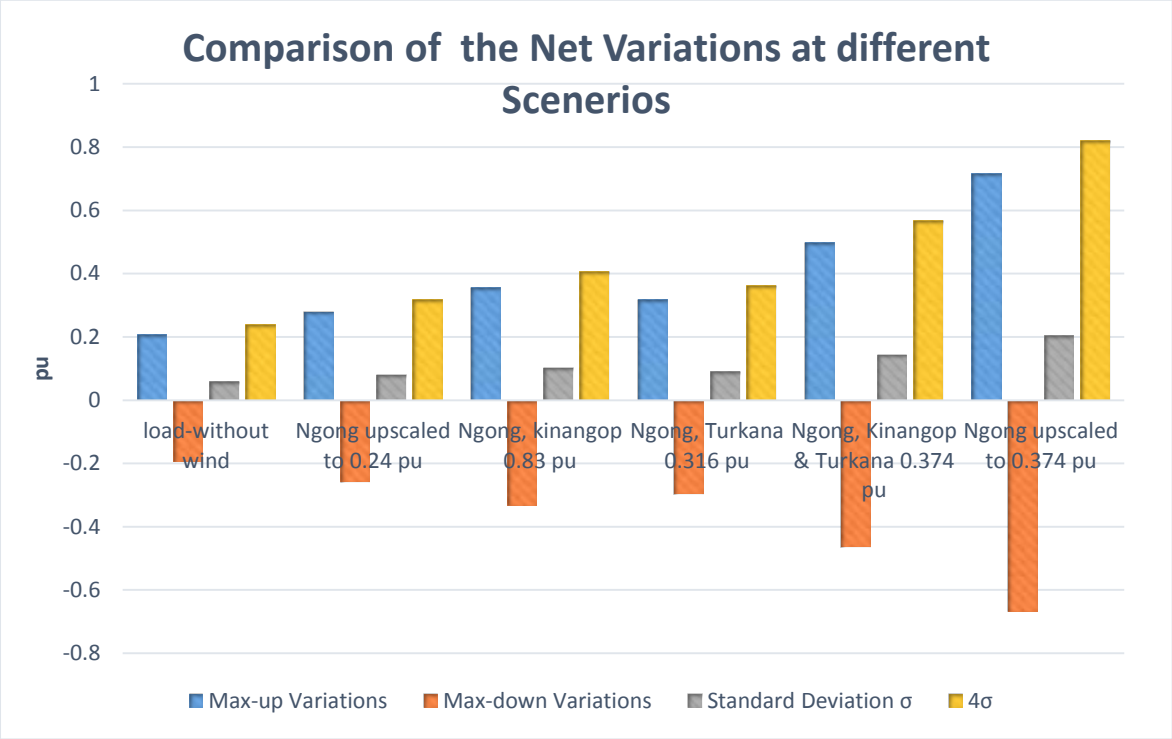

Figure 5.30 Net system variations at different penetration using different site data

Fig. 5.30 summarizes the details in Fig. 5.28 and Fig 5.29 the net system variability in six different from October 2011 to March 2012. Clearly, there is no proof of symmetry on the variations, maximum variations and standard deviations; the net system variations do not increase consistent with the penetration levels. These results can be attributed to wind generational diversity experienced within the system and the concentration of wind sites in designated areas. The distribution of wind sites in Kenya will have an impact when it comes to the size of the operating reserve. If more wind farms are located on sites with low wind variability like Kinangop than the net system variability will reduce. The size of the wind farm also has some impact when it comes to the size of the operating reserve. If large wind farms were located far apart as in the case of Kinangop and Turkana then the net system variability will reduce. On the contrary, if large wind farms are concentrated in a region the net system variability will increase.

Table 5.3 Results for net hourly variations for Kenya from October 2011 to March 2012.

Scenario	Max-up Variations (Pu)	Max-down Variations (Pu)	Standard Deviation σ (Pu)	4σ (Pu)	Load Following Reserve (MW)
Load-without wind	0.2077	-0.1938	0.0596	0.2382	244.6314
Ngong up scaled to 0.024 Pu	0.2778	-0.2589	0.0796	0.3185	327.0995
Ngong, Kinangop 0.083 Pu	0.3557	-0.3316	0.1016	0.4065	417.4755
Ngong, Turkana 0.316 Pu	0.3173	-0.2958	0.0905	0.3620	371.774
Ngong, Kinangop & Turkana 0.374 Pu	0.4980	-0.4643	0.1419	0.5674	582.7198
Ngong up scaled to 0.374 Pu	0.7163	-0.6677	0.2053	0.8214	843.5778

5.11 Load following requirements

The increase in hourly variations due to wind power can be taken as an estimate of the increase in load following requirement in the system. Fig. 5.27 shows the increase in load following requirement for wind power at different penetration levels. The linearized trend line in the plot shows the load following requirements for distinctive wind penetration levels. The load following reserve requirement for Kenya is estimated to increase at a rate of 29.6755 MW per percentage increase in wind penetration levels. However, the load following requirement at 31 percent penetration level is lesser than that at 9 percent. This shows the effect of regime and the geographical spread to hourly variations. At 31 percent, the correlation between the wind power generated in the two wind sites, Ngong and Turkana reduce the standard deviation between hence the Load following reserve requirement.

As seen in section 5.5 Kinangop and Turkana, have lower values of k signifying lesser wind variability. The low wind variability translates to low wind power variability. At 9 percent wind penetration level, Ngong is in the energy mix with Kinangop. Ngong has a high value of k signifying high wind variability. The low value of k has no significant effect to the overall system variability in this case because of low wind penetration levels. The wind penetration level for Kinangop exceeds that of Ngong by just 45 MW. At 31 percent wind penetration levels, one would expect total system failure. However, the low wind variability in Turkana at high penetration levels depicts itself as low power variability.

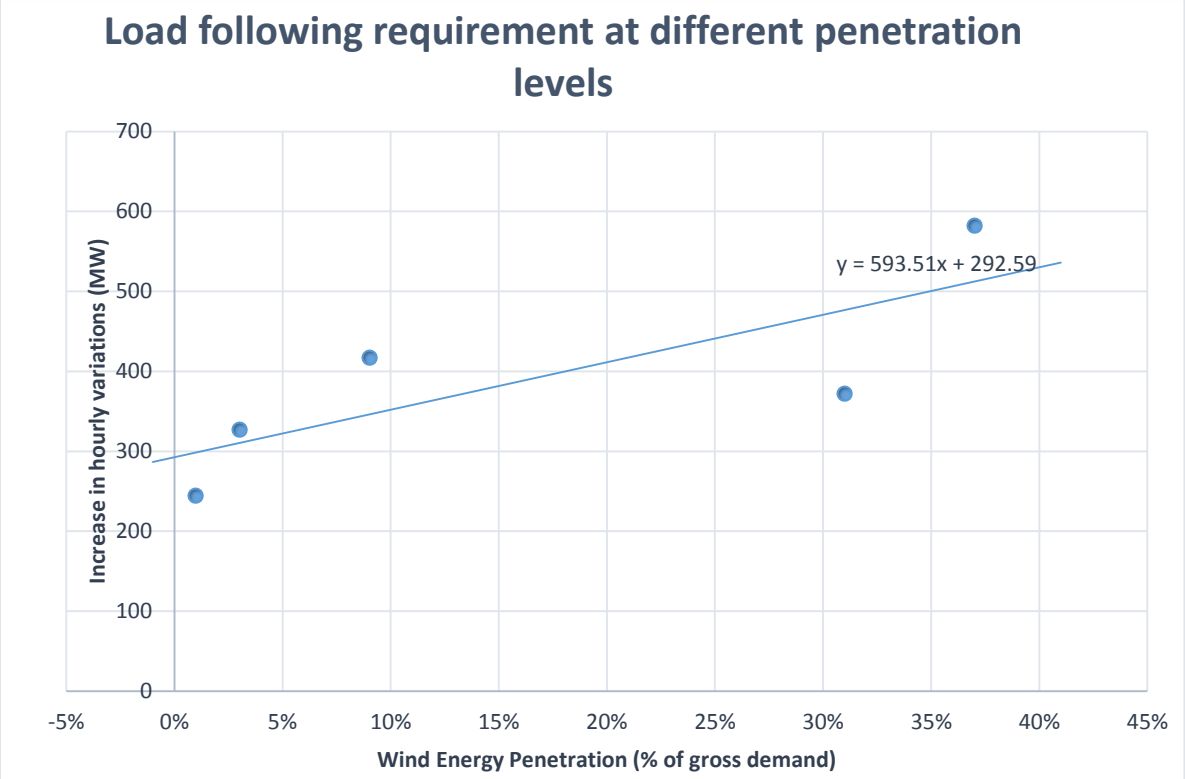

Figure 5.31 Increase in hourly load following requirement for wind power, calculated from the standard deviation.

Chapter 6 CONCLUSION AND RECOMMENDATIONS

6.1 Conclusion

The following conclusions can be drawn from this work;-

1. The general wind speed pattern in the three sites is predominantly random. Ngong exhibits high variability with high means of 11.5 m/s and high standard deviations of 6.92 m/s. Wind speeds for Ngong exhibits more zeros and spikes with seasonal properties, Kinangop exhibits lesser zeros and spikes with no seasonal properties while wind speeds for Turkana exhibits more spikes but with lesser zeros and no seasonal properties. The analysis of wind regime in Kinangop shows lesser variability compared to Ngong and Turkana by high means of 9.96 m/s and low standard deviations of 2.997 m/s. The analysis of wind regime for Turkana shows that high variability with high means of 9.43 m/s and low standard deviations of 3.09 m/s.
2. Ngong, Kinangop and Turkana exhibit high wind speeds during the night with low wind speeds during the day. The low wind variability translates to low wind power variability. However, wind power estimations for the sites exhibits the same pattern of intermittency but with lesser zeros and spikes. Wind variability in the three sites increases with the size of the wind farm. On the hand, the load pattern for Kenya also varies but consistently from peak to off peak. The weekend load varies in a similar manner as the weekday. However, weekdays load surpasses weekend loads.
3. The changes in net system variations contradicts the 4σ expectations. The findings showed no prove of symmetry on the variations, maximum variations and standard deviations consistent with the wind penetration. This is attributed to wind generational

diversity within Kenya. Sites concentration in areas with favourable wind regime has an impact on the net system variability. The load following reserve requirement for Kenya is estimated to increase at a rate of 29.6755 MW per percentage increase in wind penetration levels.

6.2 Recommendations

The following recommendations are made with reference to this study;-

1. Data for twelve months would be more appropriate for the analysis of monthly statistics and diurnal variations.
2. Analysis of wind regime in the sub hourly period would give critical information about the net system variability.
3. Unit commitment modelling will give more details how wind power behaves with other generation sources.

REFERENCES

Abeeku, B.-H., Darkwah, D., Obeng, G., & Kemausuor, F. (2008,). Renewable Energy Technology, Capacity and R&D in Africa. *International Conference on Renewable Energy in Africa.* Dakar, Senegal: The Energy Centre, KNUST Kumasi National University of Science and Technology.

Ackermann, T. (2005). *Wind power in power systems.* Southern Gate, Chichester,: John Wiley & Sons Inc.,.

Ahmad, S., Hussin, W., Bawadi, M., & Mohd, S. (1995). *Analysis of Wind Speed Variations and Estimation of Weibull Parameters for Wind Power Generation in Malavsia.* Pulau Pinang, Malaysia.

Allan, R. B. (1996). *Reliability Evaluation of Power Systems, 2nd ed.* New York: Plenum.

Archer, C. L., & Jacobson, M. Z. (2002.). The Spatial and Temporal Distributions of U.S. Winds and Windpower at 80 m Derived from Measurements.

Arizona Public Service Company. (2007). *Arizona Public Service, Wind Integration Cost Impact Study.* Arizona: Sustainable Energy Solutions Group at Northern Arizona University (NAU).

Arthur, O. (2011). *Hybrid Energy System for Off – Grid Rural Electrification.* Department of Wind Energy, Gotland University.

Asnani, G., & Kinuthia, J. .. (1979). *Diurnal variation of precipitation in East Africa.* Kenya Meteorological Department .

Axelsson., U., Murray., R., & Neimane., V. (2005). *Wind Power in Sweden- Impact on regulation and reserve requirement.* Stockholm: Elforsk Report 05:19.

B. Stott, 0. A. (Dec. 1987). Security Analysis and Optimization. *Proceedings of the IEEE, 75*(No. 12).

Bach, P. F. (September 2005). A power system with high penetration of renewables. *CIGRE Colloquium on Grid Integration of Renewables – Achievements and Challenges.* Dublin, Ireland.

Biswas, R. G. (February 2010). Wind data nalysis of Silchar (Assam, India) by Rayleigh's and Weibull methods. *2*(1).

Boehme, T., Wallace, Robin, A., & Harrison, G. P. (November 15, 2006.). Applying Time Series to Power Flow Analysis in Networks With High Wind Penetration. *0885-8950*.

Brandberg, M., & Broman, N. (2005). *Future trading with regulating power*. Vatenfall Utveckling: Uppsala University.

Brendan, F., Damain, F., & Leslie, B. (2007). *Wind Power Integration.* SixHills Way, Stevenage: Institution of Electrical Engineers.

Brun, C. E. (2009). *Economic and technical impacts of wind variability and intermittency on long-term generation expansion planning.* Massachusetts Institute of Technology.

Cabello, M., & Orza, J. (2010). Wind Speed Analysis in the province of Alicante, Spain. Potential for small-scale wind turbines. *Elsevier*, 1364-0321.

Calif, R., Emilion, R., Soubdhan, T., & Blonbou, R. (2005). *Wind speed PDF classification using Dirichlet mixtures.* Université des Antilles et de la; Université d'Orléans, France.

DFIC. (2007). *Renewable Energies Investment for East Africa Investment Framework.* 45130 Essen: East African Business Council.

Ding, Y., Wang, P., Goel, L., Loh, P. C., & Wu, Q. (MAY 2011). Long-Term Reserve Expansion of Power Systems With High Wind Power Penetration Using Universal Generating Function Methods. *VOL. 26*(NO. 2).

Doherty, R. (July 2005). *new methods for planning and operating modern electricity systems with significant wind generation.* University College Dublin.

Eerens, H., & Visser, E. d. (December 2008). *Wind-energy potential in Europe 2020-2030.* 3720 AH Bilthoven: The European Topic Centre on Air and Climate Change (ETC/ACC).

EnerNex Corporation. (January 2010). *Eastern Wind Intergration.* 1617 Cole Boulevard, Golden, Colorado 80401: The National Renewable Energy Laboratory, A national laboratory of the U.S. Department of Energy.

GoK. (2011). *SREP (Scaling-up renewable energy program).* Nairobi: Goverment of Kenya.

GWEC. (2013, February 25). *Global wind energy council*. Retrieved February 28, 2013, from http://www.gwec.net/

Halamay, D. A. (2010). Reserve Requirement Impacts of Large-Scale Intergration of Wind, Solar and Ocean Wave Power Generation. *IEEE*, 978-1-4244-6551-4/10.

Hashim, A. H. (September 2007). *Future Great Britain Generation System Reliability Evaluations in the Presence of Intermittent Renewables.* Glasgow: University of Strathclyde.

Holtinen, H. (2004). *The Impact of large scale wind power production on the Nordic electricity system.* Vuorimiehentie, Finland: VTT.

IAP. (2006). *Kenya: Integrated assessment of the Energy Policy;- With focus on the transport and household energy sectors.* Nairobi: UNEP.

Joseph , F. D., & David, W. K. (January/February 2005). The Costs of Wind's Variability: Is There a Threshold? *1040-6190*(2004.12.006).

Karekezi, S. K. (2005). *Sustainable Energy in Africa: Cogeneration and Geothermal in the East and Horn of Africa – Status and Prospects.* Nairobi: AFREPREN/FWD.

KenGen. (2011). *59th ANNUAL REPORT & FINANCIAL STATEMENTS.* Nairobi.

KIPRA. (2009). *Kenya Economic Report 2009.* Nairobi: Kenya Institure of Public Policy Research and Analysis.

Kirai P, S. B. (November 2009). Target Market analysis. *Kenya's Wind Energy Market*.

KPLC. (2011/2012). *Annual report & financial statements.* Nairobi: The Kenya Power & Lighting Company Limited.

Kuri, F. L. (2005). Generation Scheduling in a system with Wind. *IEEE/PES Transmission and Distribution, 0-7803-9114-4/05.* Conference & Exhibition: Asia and Pacific.

Lake Turkana Wind Power Project Kenya. (April 24th, 2009). *ENVIRONMENTAL AND SOCIAL IMPACT ASSESSMENT.* P-KE-FZ0-001.

Liik, O. V. (2005). *Optimization of electricity production capacity under uncertainity.* Tallinn 19086, Estonia: Tallinn University of Technology.

Lindenberg, J. (2011). *A verification study and trend analysis of.* 21502 Geesthacht: HZG.

Lindenberg, J. (2011-3). *A verification study and trend analysis of.* 21502 Geesthacht: HZG .

Lund, H. (2005). Large-scale integration of wind power into different energy systems. *Energy, 2402–12*(30).

Macro Planning Directorate. (September 2008). *A SUMMARY OF KEY INVESTMENT.* Nairobi, Kenya: National Development and Vision 2030.

Maisonneuve, N., & Gross, G. (2011). A Production Simulation Tool for Systems With Integrated Wind Energy Resources. *VOL. 26*(NO. 4).

Mary Black and Goran Strbac, M. I. (October 16, 2006.). Value of Bulk Energy Storage for Managing. *VOL. 22, NO. 1*.

Miguel, A., Ortega, V., & S.Kirschen, D. (2008). Estimating the Spinning Reserve Requirement in System with Significant Wind Power Generation Penetration. *IEEE*, TPWRS.2008.20047456.

Milligan, M. (2006). *Variance Estimates of Wind Plant Capacity Credit.* Denver: American Wind Energy Association.

Mukabana, J. R. (1992). *Numerical Simulation of the Influences of the Large-Scale Monsoon Flow on the Diurnal Weather Patterns over Kenya.* Fort Collins, Colorado: Department of Atmospheric Science Colorado State University.

Okeyo, A. (1987). *Towards the development of a forecasting numerical model for Kenya.* Nairobi: University of Nairobi.

Oludhe, C. (2008). Assessment and Utilization of Wind Power in Kenya – A Review. *2(1)*(39–52).

Papavasiliou, A., Oren, S. S., & O'Neill, R. P. (NOVEMBER 2011). Reserve Requirements for Wind Power Integration: A Scenario-Based Stochastic Programming Framework. *VOL. 26*(NO. 4).

Pereira, A. d. (June 2000). *Modular supervisory controller for hybrid power systems.* Roskilde: Risø National Laboratory.

Shuai Lu, Y. V. (2010). Prediction of Power System Balancing Requirement and Tail Event. *IEEE*, 978-1-4244-6547-7/10.

Sinden, G. (2005). Characteristics of the UK wind resource: Long-Term patterns and relationship to electricity demand. *Elsevier*, 0301-4215.

Söder, L., Hofmann, L., Nielsen, C. J., & Holttinen. (2006). A comparison of wind integration experiences in some high penetration areas. Espoo, Finland: Nordic Wind Power Conference.

Soens, J., Driesen, J., & Belmans, R. (7-8 April 2005). Estimation of Flactuaton of Wind Power Generatons in Belgium. *Fifth International Workshop on Large scale Intergration of Wind Power and Transmission Networks for Offshore Wind Farms.* Glasgow: ESAT-ELECTA.

Strbac, G., Shakoor, A., Black, M., Pudjianto, D., & Bopp. (2007). Impact of wind generation on the operation and development of the UK electricity systems. *Electrical Power Systems Research,, Vol. 77*(issue 9).

SWERA. (2008). *KENYA COUNTRY REPORT* . Nairobi: SOLAR AND WIND ENERGY RESOURCE.

T. Yong, R. E. (2009). Reserve Determination for System with Large Wind Generation. *IEEE*, 978-1-4244-4241-6/09.

Waewsak, J., Chancham, C., Landry, M., & Gagnon, Y. (2011). An Analysis of Wind Speed Distribution at Thasala, Nakhon Si Thammarat, Thailand. *51-55*(2).

Wang, Y. (15-18 May 2005). Flactuation and amping chaacteistics of Large Wind Power Plants. *Windpower 2005 (Windpower 05) Conference and Exhbition. CP-500-38057.13 p.* Denver, Colorado, Washington DC: NREL.

Wil L. Kling, M. G. (2008). Implementation of Wind Power in the Dutch. *IEEE*.

Yang, G. a. (2009). Renewable Energy Focus Handbook. *pg 43*.

Appendix 1

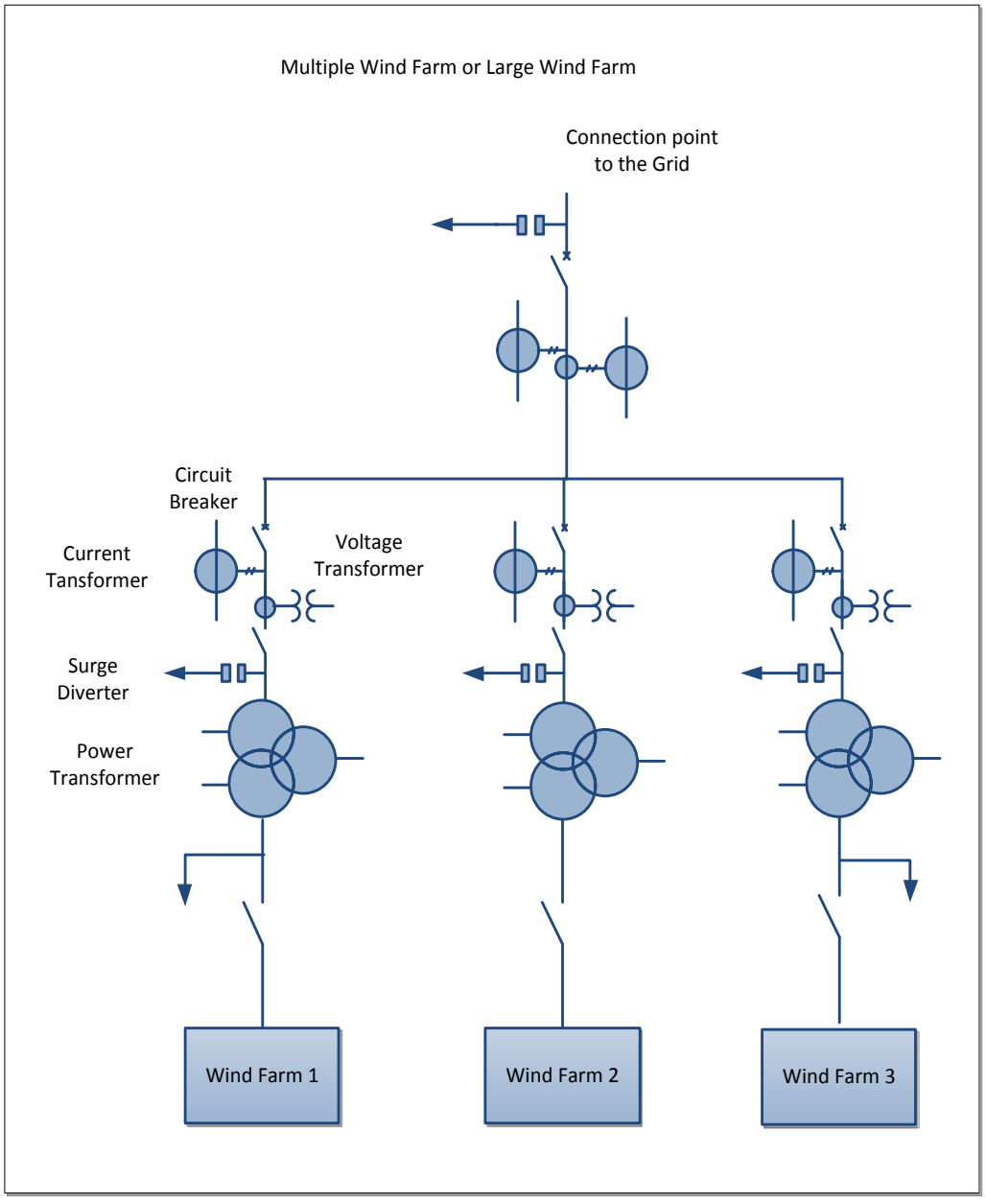

Fig. A.1 Large of Multiple wind Farms Connection to the Grid

Appendix 2

Table A.1 MATLAB/Simulink simulation input Parameters

Type	Unit	Turbine Data
Rotor diameter	[m]	52
Nominal Power	[kW]	850
No of blades	[No.]	3
Controller type	[Hz]	VMP-850-690-50
Frequency	[Hz]	50Hz +1/-3
Current (cos ϕ=1)	[A]	711
Current (cos ϕ=0.95)	[A]	749
Maximum Pitch Angle	[deg]	90
Pitch at low idling speed	[deg]	36
Generator Data		
Nominal speed	[m/s]	16
Cut in speed	[m/s]	4
Cut out speed	[m/s]	25
No of Poles	[No.]	4
Stator Resistance (Rs)	[Ω]	0.0029
Stator Leakage Resistance (LIs)	[Ω]	0.0417
Rotor Resistance (Rr)	[Ω]	0.0031
Rotor Leakage Reactance (LIr)	[Ω]	0.0425

Table A.2 Actual Turbine parameter

Type	Unit	Ver. 1	Ver. 1	Ver. 3	Ver. 5	Ver. 1 50Hz	Ver. 1 60Hz
Rated voltage	[V]	690	690	690	690	690	690
Rated frequency	[Hz]	50	50	50	50	50	50
Rated power	[kW]	800	800	800	800	800	800
Rated power factor (Inductive)	Cos phi	0.9	0.895	0.895	0.92	0.91	0.92
Rated stator current	[A]	742	756	756	729	736	730
Rated rotor current	[A]	268	256	256	254	254	247
In-rush current ratio	[Iblocked/ In]	9.6	7.3	7.3	9.1	7.0	5.9
Rated slip	[%]	-0.6	-0.6	-0.6	-0.53	-0.6	-0.56
Rated torque (T_N)	[kNm]	5.2	5.2	5.2	5.3	5.2	5.3
Starting torque (T_S)	[kNm]	2.2	4.0	4.0	9.0	1.64	0.93
Break down torque (T_{max}) as generator	[kNm]	17.0	15.3	15.3	16.0	19.0	12.1
Break down torque (T_{max}) as motor	[kNm]	15.0	13.5	13.5	15.0	17.4	11.1

Consumed active power	[kW]	9.8	11.8	11.8	11	8.1	7.7
Consumed reactive power	[kVAr]	239	257	257	215	221	155
Rotational loss	[kW]	2.1	1.5	1.5	2.5	3.0	3.9
Copper losses	[kW]	0.4	0.4	0.4	0.3	0.4	0.2
Iron losses	[kW]	7.5	9.9	9.9	8.2	5.7	3.6
Stator current	[A]	200	216	216	180	185	130
Power factor (Inductive)	P.U.	0.041	0.046	0.046	0.05	0.04	0.05
Stator current at rated voltage	[A]	7150	5500	5500	6600	5165	4330
Power factor		0.09	0.19	0.19	0.24	0.10	0.08
Voltage on open rotor terminals	[V]	1811	1820	1820	1820	1849	1850
Voltage ration Stator/Rotor	[U open rotor / Un]	2.62	2.64	2.64	2.64	2.68	2.68
Stator resistance R_1	[Ω]	0.0029	0.0028	0.003033	0.00337	0.004367	0.00495
Stator leakage reactance X_1	[Ω]	0.0417	0.05	0.05	0.0432	0.02803	0.0390
Iron loss resistance R_{FE}	[Ω]	0.070	0.06208	0.07095	0.0944	0.03767	0.065
Magnetizing	[Ω]	1.97	1.77624	1.7984	2.194	1.967	2.94

reactance X_m							
Rotor leakage reactance X_2	[Ω]	0.0425	0.054515	0.054019	0.0477	0.0481	0.060
Rotor resistance R'_2	[Ω]	0.0031	0.00365	0.003293	0.00303	0.003367	0.0034
Voltage (phase – star							
point) $U_N/\sqrt{3}$	[V]	398.4	398.4	398.4	398.4	398.4	398.4
Frequency	[Hz]	50	50	50	50	50	60

Appendix 3

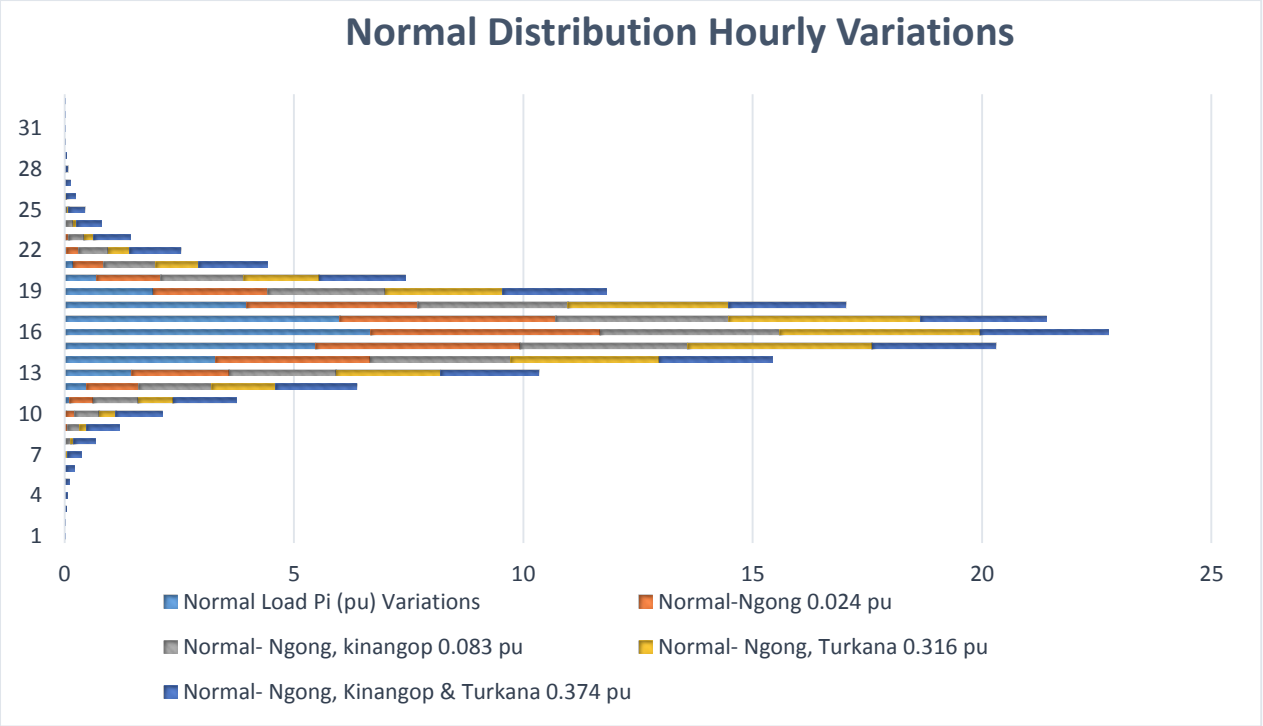

Fig. A.3.1 Normal Distribution of Net hourly variations from October 2011 to March 2012.

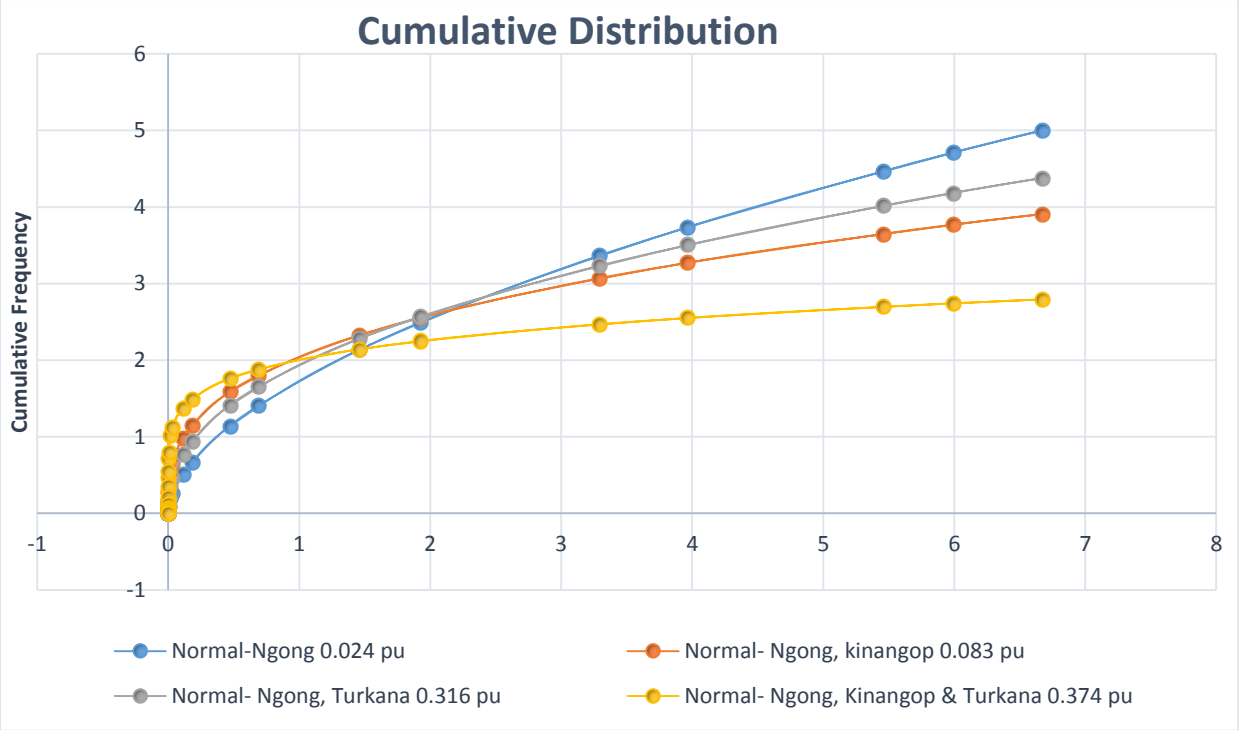

Fig. A.3.2 Normal Distribution of Net hourly variations from October 2011 to March 2012.

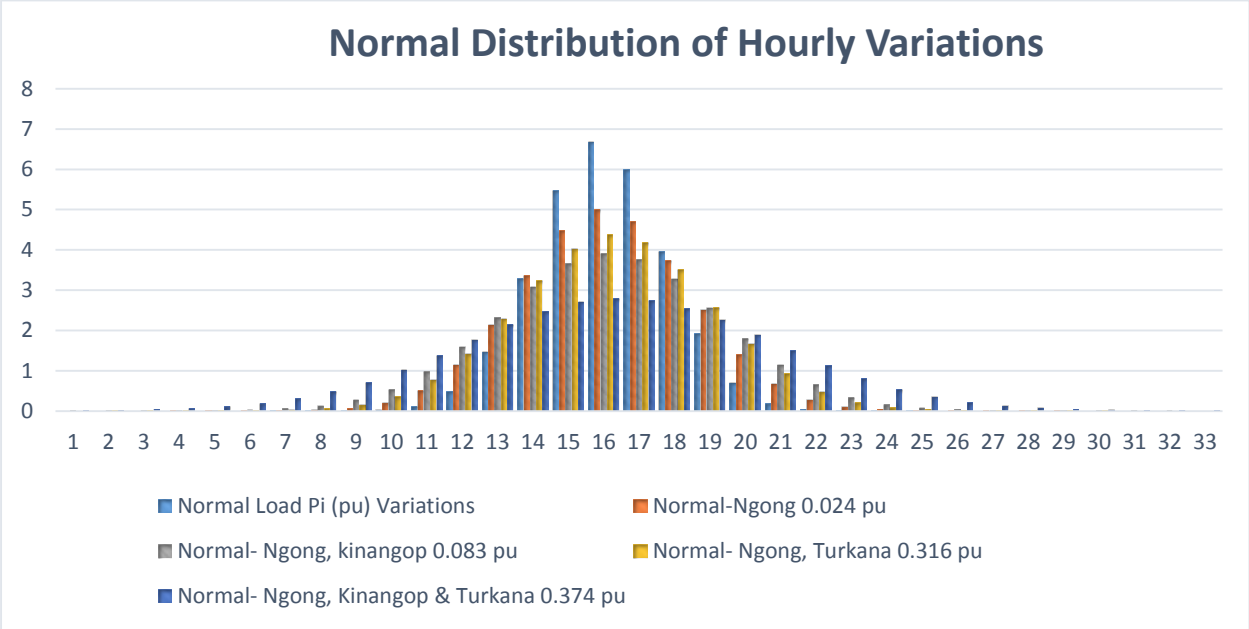

Fig. A.3.1 Normal Distribution of Net hourly variations from October 2011 to March 2012.